Study on interaction between bacteria and hematite under seawater condition for the elution of iron

A dissertation submitted in partial fulfillment of the requirements for the degree of Doctorate of Engineering

by

APICHAYA ANEKSAMPANT

Laboratory of Biotechnology for Resources Engineering,

Division of Sustainable Resources Engineering,

Graduate School of Engineering,

Hokkaido University, Japan

March 2019

Acknowledgement

Firstly, I would like to express my deepest gratitude to my supervisor Associate Prof. Kazunori NAKASHIMA for the continuous support and push me throughout my Ph.D. study, for his patience, motivation, and inspiration in my research. His patient guidance helped me in all the time of my research and during writing of this thesis. Without his advice, support and most of all, patience, this work would not have been possible. Besides my supervisor, I would like to express my sincere gratitude to my co-supervisors: Prof. Satoru KAWASAKI for his kind support and opportunity for me being in this research group. I would like to express my deeply gratitude in the research to my previous supervisor Associate Prof. Masami FUKISHIMA for his inspiration.

In addition, I would like to express my sincere gratitude to Assistant Prof. Masaji KATO for his kindness in cooperation.

My sincere thanks also go to my lab mates, Mr. Yoshiaki Iwata and Mr. Wilson Mwandira for their generosity. Their patience and support in overcoming numerous obstacles I faced during my research works is highly appreciated. I would also like to give my special thanks to Mrs. Hitomi for her patience and support during the time I have been working on this doctoral degree program.

I would like to thank all the other laboratories members for their welcome and support me as throughout both good and bad time I faced during my study. I am truly thankful to bring many activities we shared together. I hope them all the best.

I would like to thank to all of my international friends here also, without them I could not enjoy my life abroad that much. Especially, my Thai community that support me all along way in term of both mentally and physically issues.

Last but not the least, I would like to thank my parents and to my brother for the best family one could ask for. Without their support I could not overcome and finish my degree. Thank you for their faith and never give up in me.

Table of contents

CHAPTER 1 INTRODUCTION

1.1 Background

In recent decades, the development from the rural area into urban has been expanded. This has led to rapid growth of the population and longer life span of people all over the world. The increase in population requires more construction of residential areas. The expanse of the construction causes deforestation and the need for water supply requires dam construction. These human modifications affect the ocean community. In many coastal countries, the problem is severed as seaweed has drastically reduced. The decrease in amount of seaweed has become serious in most coastal area worldwide. In order to maintain the biodiversity, seaweed recovery must be restored. One of the ways to restore seaweed is to supply eluted iron into seawater. However, the oxic seawater condition is not suitable for iron dissolution. To overcome the challenge of seaweed reduction for the sustainable environment, we investigated on the supply of dissolved iron into seawater to encourage recovery and restoration techniques under three themes:

(i) microbial influence in hematite elution into seawater mediated via dissolved organic matter,

(ii) bacterial leaching of iron from hematite: direct or indirect interaction; and

(iii) performance improvement for bacteria adsorption onto hematite surface.

1.2 Literature review

1.2.1 Barren ground situation and restoration

The barren ground in coastal area is a phenomenon where seaweed beds are decreased or extinct, and coralline algae which contained calcium carbonate in their component become to cover the rock surface (Fig.1-1, Iwai et. al, 2013).

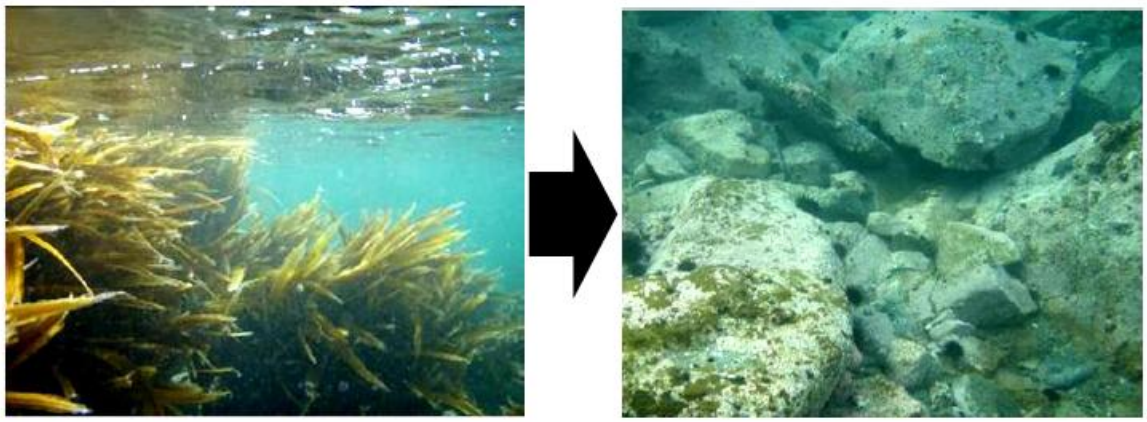

Fig. 1-1 Seaweed beds (left) vs Barren ground (right) (Iwai et. al, 2013)

Seaweed is the name of "algae", in general, which include macroscopic marine green, red and brown algae. Seaweed is vitally important to marine biodiversity and for human use. The decrease of seaweed not only impact the environmental but also the economical and ecological point too. As shown in Fig. 1-2 (Iwai et al., 2013),

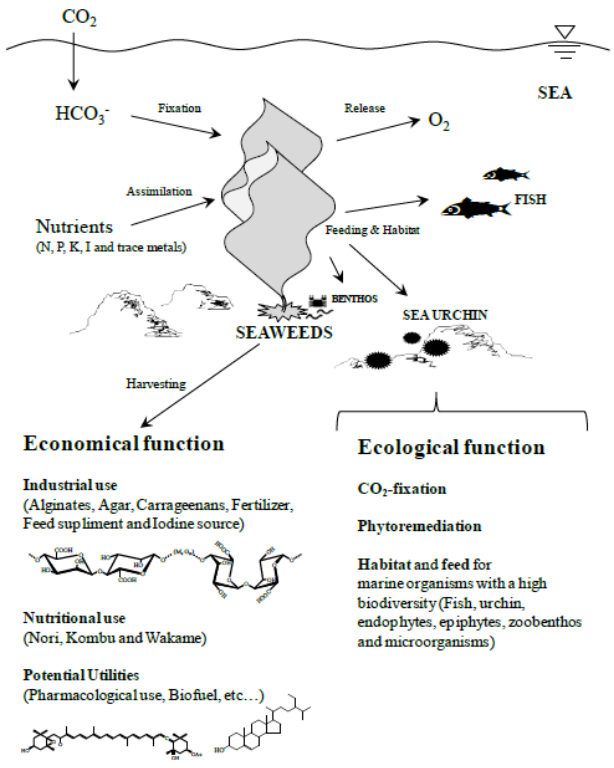

Fig. 1-2 Roles of seaweeds (Iwai et al., 2013)

Seaweed has been widely used in a variety of industrial products and effect to the marine environment (Lobban et al., 2000 and Hoppe et al., 1969). The seaweed beds act as shelter for coastal biodiversity (Lobban et al., 2000 and Kraan et al., 2013). Seaweed depletion has been well known as one of the most important coastal environmental problem in East Asia, Canada and Australia (Fujita, 2010; Chapman, 1981; Graham, 2010; Yao et al., 2010; Okuda, 2008; Millar, 2003 and Mann, 1997). For instant, more than 90% of Tokyo Bay was claimed and it led to the loss of seaweed beds. The barren ground of coastal areas due to various environmental factor could recognized as a serious coastal problem, that called "Isoyake" in Japanese since the 1800s (Fujita, 2010 and Okuda, 2008). The reason for barren ground has been mainly considered at marine biological damage and aquatic environmental change (Fujita, 2010; Matsunaga et al., 1994 and Matsunaga et al., 1999). In addition, lack of essential minerals micronutrients especially Fe might lead to the poorly growth of seaweed (Fujita, 2010, Matsunaga et al.,

1994 and Matsunaga et al., 1999). The development of rural area and the rapid growth of city lead to varieties of environmental issues such as deforestation and mineral supply limitation. Matsunaga et al., 1998 reported that dam construction and other urban development prevent the input of dissolved iron from rivers to coastal areas (Fig.1-3).

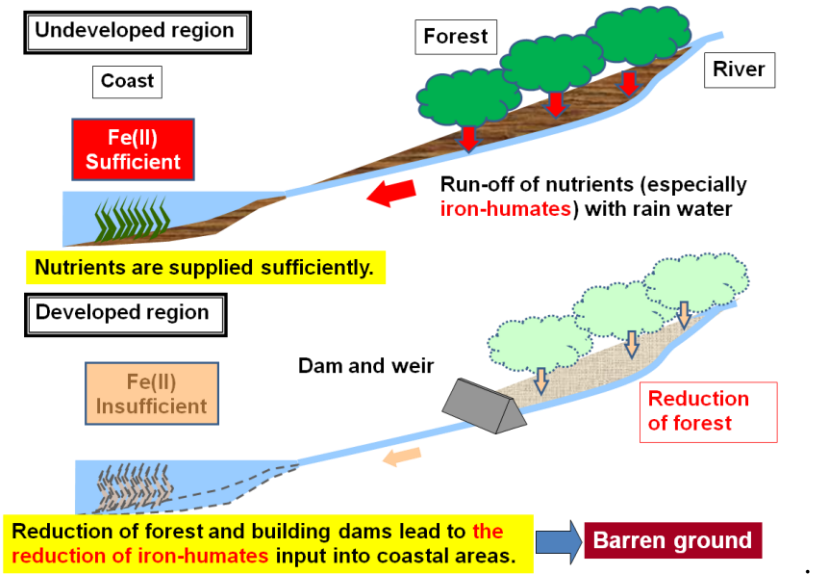

Fig 1-3 Why does the barren ground occur? (Matsunaga et al., 1998).

The restoration of seaweed beds in barren coasts had been developed using fertilization technique to supply dissolved iron into seawater of barren areas. The fertilizer is composed of a mixture of steel slag served as iron source and compost that served as source of humic substances (Fig. 1-4) was applied in coastal area at the Shaguma coast, Mashike (Hokkaido, Japan) (Yamamoto et al., 2010a).

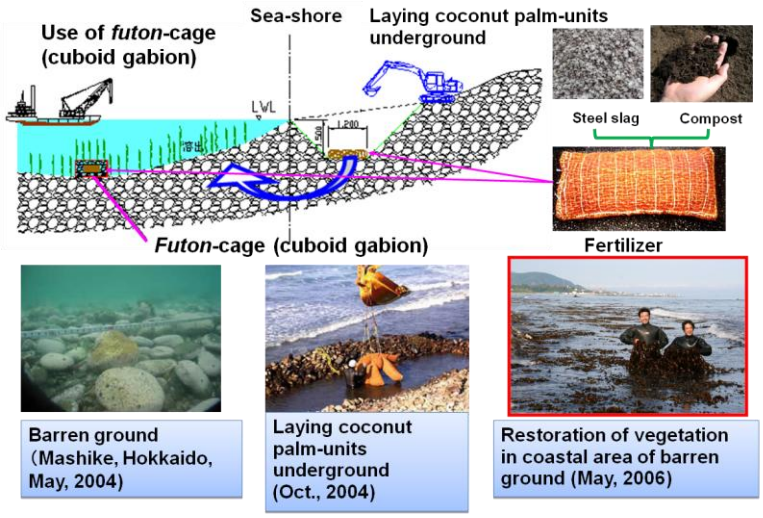

Fig. 1-4 Method for burying the fertilizer (Yamamoto et al., 2010a).

The condition of seawater is one of the most challenging condition to supply dissolved iron in stabilized form. However, the application of eluted iron into seawater is crucial in seaweed growth as we mentioned earlier as it is a necessary nutrient in its reproductive growth. The Eh-pH diagram as show in Fig. 1-5 (Brookins, 1987), shows the suitable pH of iron elution. Under oxic conditions (around $Eh = 0$) in coastal seawater, eluted Fe(II) can easily be oxidized to Fe(III) and form solid hydroxides (Fig.1-5)

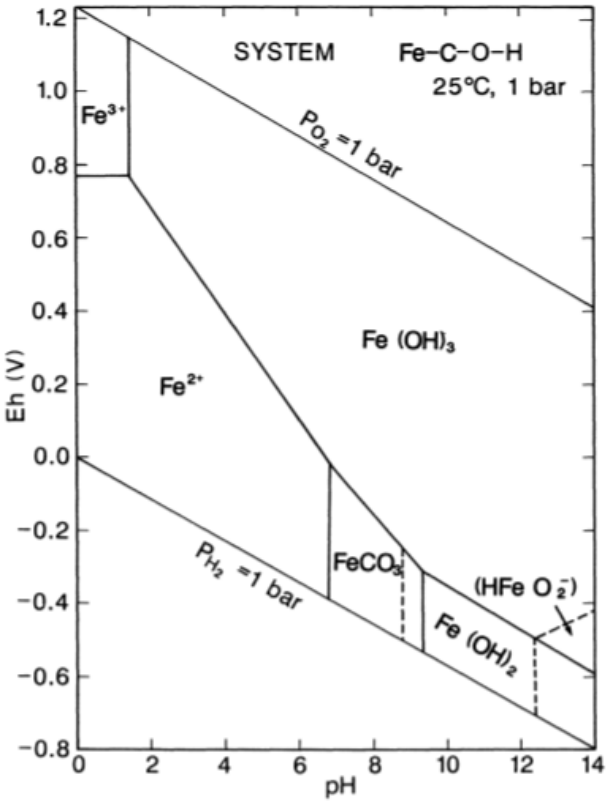

Fig. 1-5 Eh-pH diagram for part of the system Fe-O-H (Brookins, 1987).

Humic substances serve as chelator of iron to stabilize the dissolved iron species under oxic conditions (Yamamoto et al., 2010b). In addition, humic substances contain quinone/hydroquinone redox couple, suggesting that the reductive dissolution of iron from the surfaces of iron oxide is possible (Nishimoto et al., 2013).

Fujisawa et al. (2012) reported that the degradation of humic acid in fertilizer could be attributed to microbial activities. The elution of iron was promoted in the presence of humic substances. Such processes may be related to continuous elution of iron via microbial processes. This evidence leads to our study in chapter 2 and chapter 3.

1.2.2 Bacterial cell interaction with hematite

The bacteria cell interaction with metal oxide has been widely investigated in the recent past. This interaction could be used in many biotechnological applications. The extracellular electron transfer is one of the pathways to transfer electron between bacteria cell and the multivalent metal ions (Shi, et al., 2016). Microorganisms that have extracellular electron transfer capability have been harnessed for various biotechnological applications. For example, stimulation of the activity of indigenous *Geobacter* spp. helps immobilize uranium at contaminated sites (Anderson et al., 2003). The electron interaction between bacteria cells and minerals has been demonstrated in Fig. 1-6 (Shi, et al., 2016). Microorganisms use minerals that contain metal ions as terminal electron acceptors for respiration (Fig.1-6a), electron and/or energy sources for growth (Fig.1-6b), electrical conductors that facilitate electron transfer between microbial cells of the same and different species (Fig.1-6c) and electron-storage materials, or batteries, to support microbial metabolism (Fig.16d).

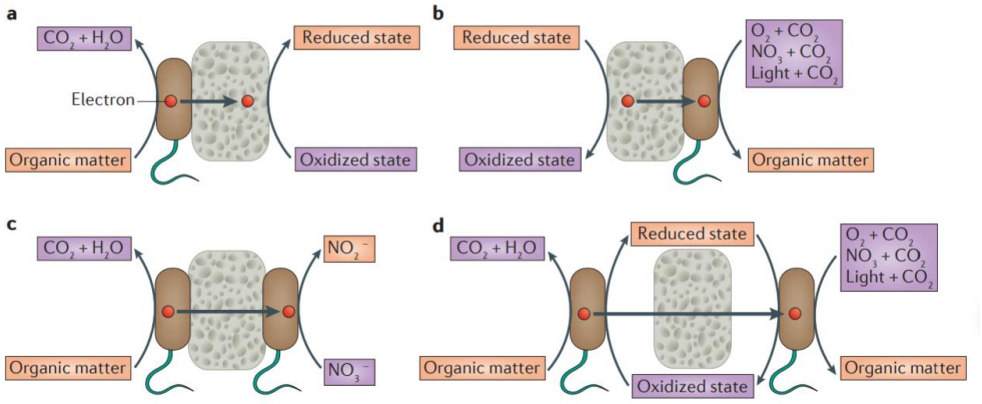

Fig. 1-6 Electron transport between microorganisms and minerals (Shi, et al., 2016)

In our study, we focused on the electron transfer from bacteria cells to hematite surface. Direct electron transfer between the microbial cells should be one of the evidences provided in our investigation. Some microorganisms can exchange electrons to minerals (Kato et al., 2012a; Byrne et al., 2015; Zhao et al., 2015; Liu et al., 2015; Kato et al., 2012b and Cruz Viggi et al., 2014). Kato et al.(2012) reported

interspecies electron transfer between bacteria cell and conductive minerals. This also shows the possibilities of hematite which is a semiconductive material that could interchange electron with bacteria cell directly. These reviews are useful for us to interpret the result data we reported in chapter 3.

We also focused on gram positive bacteria which we used in our study. Pankratova et al.(2018) reported the study on electron transfer of gram-positive bacteria and illustrated the electron transfer pathway in Fig.1-7. Figure 1-7 (Pankratova et al., 2018), illustrated the electron transport to outside of the cells via cytochrome c pathway. This could confirm that bacteria direct interaction to hematite surface would lead to the reduction of hematite.

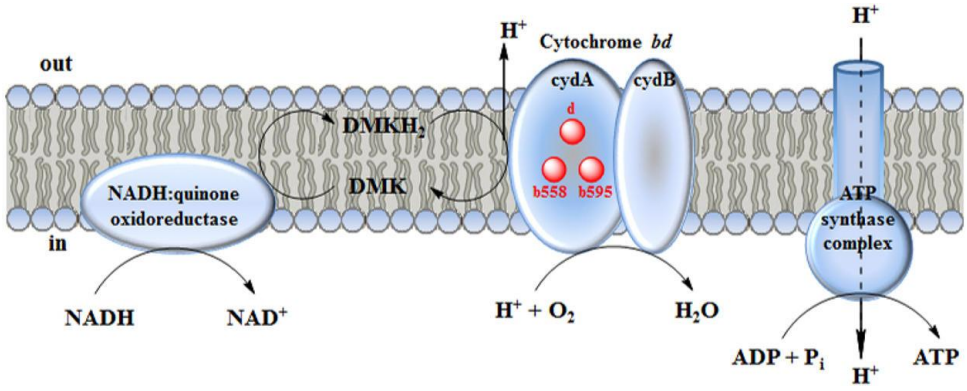

Fig. 1-7 Schematic representation of the aerobic respiratory chain of *E. faecalis* as assembled in the cytoplasmic membrane (Pankratova et al., 2018).

1.2.3 Solid material binding peptide

Related to our investigation, the binding between bacteria cell and hematite surface might be useful in variety of applications. Care et al.(2015) reviewed about the solid-binding peptide as tools for nanobiotechnology. Solid-binding peptide or SBPs are short amino acid sequences that display binding affinity for the surfaces of solid materials. They offer simple and versatile bioconjugation methods that can increase biocompatibility and direct immobilization onto solid supports without impeding their

functionality (Sengupta et al., 2008). SBPs have been used various application as illustrated in Fig. 1-8 (Care et al., 2015).

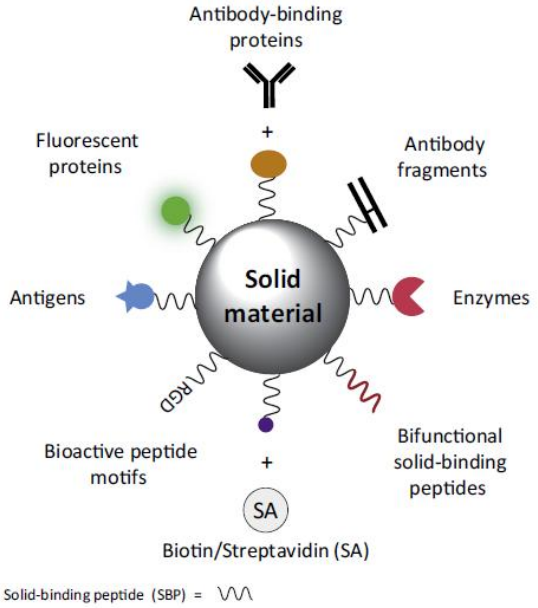

Fig. 1-8 Illustration of possible use of SBPs as molecular linker and many functions (Care et al., 2015).

The attachment of enzymes to magnetic nanomaterials allows their straightforward recovery and reuse in multiple reactions, maximizing their economic value (Puri et al., 2013). Peptides that bind to iron oxide have been used to facilitate the immobilization of a bioremediation-related enzyme (Brown et al., 1992). Tsai et al. (2015) investigated bacteria surface display of the metal binding peptides as whole cell biocatalysts. This study allowed the cells contained gold-binding peptide and the whole cells could act as catalysts to reduce the 4-nitroaniline. The examination leads us to the variety of using modified bacteria in the environmental application.

1.3 Scope of this thesis

The scope of this thesis is the investigation of laboratory scale effect of isolated bacteria and bacterial influence on iron elution. The thesis consisted of two major sections, with different sub sections as follows.

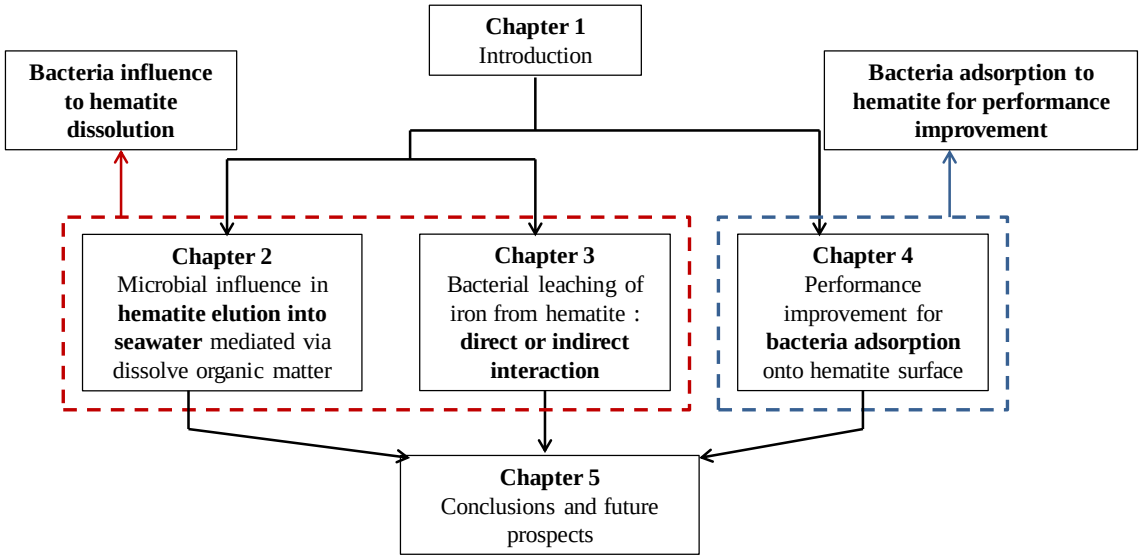

Fig. 1-9 Scope of this thesis

In chapter 1, the background of this current research, literature review related to the current research, objectives and the originality of the research are described. Bacteria influence on the iron elution in seawater condition is reported in Chapter2. We proposed the possible mechanism of bacterial influence to hematite surface suggest that direct interaction between bacterial cells to hematite leads to the elution of iron is described in Chapter3. In Chapter 4, we investigated genetically-modified bacteria as model of bacteria for iron elution. We observed the capability of bacteria containing iron binding peptide behavior onto hematite surface. Further investigation was done using bacteria containing iron binding peptide applied to iron elution into seawater based on the mechanism reported in Chapter3. Finally, Chapter 5 provided overall the conclusions for Chapter 2, 3 and 4 and area for further studies.

1.4 Originality and usefulness of the study

We proposed that bacteria have an effect on iron elution into seawater. Many studies have proposed iron dissolution in acidic condition, however, there are very few researches focused on iron dissolution in alkaline condition, especially into seawater. As mentioned earlier in section 1.2.1 and 1.2.2 in this Chapter, iron supplied to seawater is one of the most challenging for seaweed recovery. Bacteria in the fertilizer support iron dissolution process. To understand the mechanism, we isolated and identified the bacteria from the fertilizer. The elution of iron into seawater influenced by isolated bacteria was investigated and shown significantly effect on dissolution of iron in seawater condition as detail provided in Chapter 2. This investigation showed possible application by using environmentally friendly bacteria to support iron supply into marine environment.

To understand interaction between bacterial cells and hematite surface to the iron elution. We proposed the possible mechanism of bacterial influence on iron elution is reported in Chapter 3. The importance of interaction between bacterial cell and hematite surface led us to investigate the interaction between the cells and hematite. Chapter 4 investigated the using geneticcally-modified bacteria as a model for iron elution. Iron binding peptide was introduced to the outer membrane of the bacterial model. The genetic-modified bacteria were used as whole cell to investigate the adsorption onto hematite surface. After the adsorptions were observed, we determined iron dissolution. We found the possible application to enhance the iron dissolution efficient by using the genetic modification technique as an environmental and sustainable tool for to supply iron into seawater.

Reference

[1] H. Iwai, M. Fukushima and M. Yamamoto. Determination of labile Fe(II) species complexed with seawater extractable organic matter under seawater conditions based on the kinetics of ligand-exchange reactions with ferrozine. *Analytical Science, The Japan Society for Analytical Chemistry*, 29, 723-728, 2013.

[2] C.S. Lobban and P.J. Harrison, "Seaweed ecology and physiology", Cambridge University Press, Cambridge, 2000.

[3] H.A. Hoppe and O.J. Schmid, Commertial products. In T. Levring, H. A. Hoppe and O.J. Schmid (eds.), Marine Algae: A Survey or Research and Utilization, Cram, de Gruyter and Co., Hamburg, 1969, 288-368.

[4] S. Kraan, Mass-cultivation of carbohydrate rich macroalgae, a possible solution for sustainable biofuel production, Mitig. Adapt. Strateg. Glob. Change. 18 (2013) 27-46.

[5] D. Fujita, Current status and problems of isoyake in Japan, Bull. Fish. Res. Agen. 32 (2010) 33-42..

[6] A.R.O. Chapman, Stability of sea urchin dominated barren grounds following destructive grazing of kelp in St. Margaret's Bay, Eastern Canada, Mar. Biol. 62 (1981) 307-311.

[7] M.H. Graham, Comparisons between East-Asian isoyake and deforestation in global kelp systems, Bull. Fish. Res. Agen. 32 (2010) 47-50.

[8] J. Yao, H. Jiang, and D. Duan, Artificial enhancement of sea-forest for reducing the Isoyake degree along the north coast of China, Bull. Fish. Res. Agen. 32 (2010) 19-24.

[9] K. Okuda, Coastal environment and seaweed-bed ecology in Japan, Kuroshio Science 2 (2008) 15-20.

[10] A.J.K. Millar, The world's first recorded extinction of a seaweed, Proceedings of the 17th International Seaweed Symposium in 2003, Oxford University Press, Oxford, 313-318.

[11] K.H. Mann, Destruction of kelp-beds by sea-urchins: A cyclical phenomenon or irreversible degradation?, Helgol. Wiss. Meeresunters. 30 (1977) 455-467.

[12] K. Matsunaga, Y. Suzuki, K. Kuma, and I. Kudo, Diffusion of Fe(II) from an iron propagation cage and its effect on tissue iron and pigments of macroalgae on the cage, J. Appl. Phycol. 6 (1994) 397-403.

[13] K. Matsunaga, T. Kawaguchi, Y. Suzuki, and G. Nigi, The role of terrestrial humic substances on the shift of kelp community to crustose coralline algae community of the southern Hokkaido Island in the Japan Sea, J. Exp. Mar. Biol. Ecol. 241 (1999) 193-205.

[14] M. Yamamoto, M. Fukushima, E. Kiso, T. Kato, M. Shibuya, S. Horiya, A. Nishida, K. Otsuka and T. Komai. Application of iron humates to barren ground in a coastal area for restoring seaweed beds. *Journal of Chemical Engineering of Japan*, 43, 627-634, 2010.

[15] D.G.Brookins, Eh-pH diagram for Geochemistry, Springer-Verlag Berlin Heidelberg 1988, 75

[16] M. Yamamoto, A. Nishida, K. Otsuka and T. Komai and M. Fukushima. Evaluation of the binding of iron (II) to humic substances derived from a compost sample by colorimetric method using ferrozine. *Bioresource Technology*, 101, 4456-4460, 2010.

[17] R. Nishimoto, S. Fukuchi, G. Qi, M. Fukushima and T. Sato. Effects of surface Fe(III) oxides in a steel slag on the formation of humic-like dark-colored polymers by the polycondensation of humic precursors. *Colloids and Surfaces A : Physicochemical and Engineering Aspects*, 418, 117-123, 2013.

[18] L. Shi, H. Dong, G. Reguera, H. Beyenal A. Li J. Liu, H.Q. Yu and J.K. Fredrikson. Extracellular electron transfer mechanisms between microorganisms and minerals. Nature review, Microbiology, 14, 651-662, 2016.

[19] Anderson, R. T. et al. Stimulating the in situ activity of Geobacter species to remove uranium from the groundwater of a uranium-contaminated aquifer. Appl. Environ. Microbiol. 69, 5884–5891 ,2003

[20] Kato, S., Hashimoto, K. & Watanabe, K. Microbial interspecies electron transfer via electric currents through conductive minerals. Proc. Natl Acad. Sci. USA 109, 10042–10046 ,2012.

[21] Byrne, J. M. et al. Redox cycling of Fe(ii) and Fe(iii) in magnetite by Fe-metabolizing bacteria. Science 347, 1473–1476, 2015

[22] Zhao, L. et al. Biological redox cycling of iron in nontronite and its potential application in nitrate removal. Environ. Sci. Technol. 49, 5493–5501, 2015

[23] Liu, F. et al. Magnetite compensates for the lack of a pilin-associated c-type cytochrome in extracellular electron exchange. Environ. Microbiol. 17, 648–655, 2015

[24] Kato, S., Hashimoto, K. & Watanabe, K. Methanogenesis facilitated by electric syntrophy via (semi)conductive iron-oxide minerals. Environ. Microbiol. 14, 1646–1654, 2012

[25] Cruz Viggi, C. et al. Magnetite particles triggering a faster and more robust syntrophic pathway of methanogenic propionate degradation. Environ. Sci. Technol. 48, 7536–7543, 2014

[26] G. Pankratova, D. Leech, L. Gorton and L. Hederstedt, Extracellular Electron Transfer by the Gram-Positive Bacterium *Enterococcus faecalis*, Biochemistry. 57, 4597-4603, 2018.

[27] Sengupta, A.. A genetic approach for controlling the binding and orientation of proteins on nanoparticles. Langmuir 24, 2000–2008 , 2008

[28] Puri, M., Enzyme immobilization on nanomaterials for biofuel production. Trends Biotechnol. 31, 215–216, 2013

[29] Brown, S.Engineered iron oxide-adhesion mutants of the *Escherichia coli* phage lambda receptor. Proc. Natl. Acad. Sci. U.S.A. 89, 8651–8655, 1992

[30] D.Y. Tsai, Y.J. Tsai, C.H. Yen, C.Y Ouyang and Y.C. Yeh. Bacterial surface display of metal binding peptides as whole-cell biocatalysts for 4-nitroaniline reduction, RSC advances communication, 5, 87998-88001, 2015.

CHAPTER 2 MICROBIAL INFLUENCE IN HEMATITE ELUTION INTO SEAWATER MEDIATED VIA DISSOLVED ORGANIC MATTER

2.1 Introduction

Seaweed depletion is a common occurrence in barren grounds along the coasts of Japan and throughout the world. Barren ground is ground devoid of seaweed beds in coastal areas present and this seriously affects coastal ecosystems as well as fisheries. There are many factors that have been cited for causing of barren ground. Firstly, it has been reported that one of the possible factors for barren ground development is lack of dissolved iron, which is required for the reproductive growth of seaweeds as shown in Fig. 2-1(Fujita et al., 2002). Secondly, another study in the Kesennuma Bay reported that riverine iron and nutrients inputs are additional factors in phytoplankton growth (Matsunaga et al., 1999). Therefore, dam construction and other urban development prevent the input of dissolved iron from rivers to coastal areas hence the development of barren area.

Thirdly, is the pH of seawater. Generally, the pH of seawater ranges from 7.8 to 8.2, therefore, iron cannot be dissolved in such weak alkaline condition because of the formation of hydroxide colloids (Kuma et al., 1998; Boye et al., 2001). This pH condition is not suitable for iron to be supplied in eluted form.

Finally, natural organic matter such as humic substances have the potential to be effective in maintaining soluble Fe(II) levels at concentration of several-hundred nanometers in estuarine and coastal areas, however they are prevented to enter the system due to human development upstream (Rose et al., 2006).

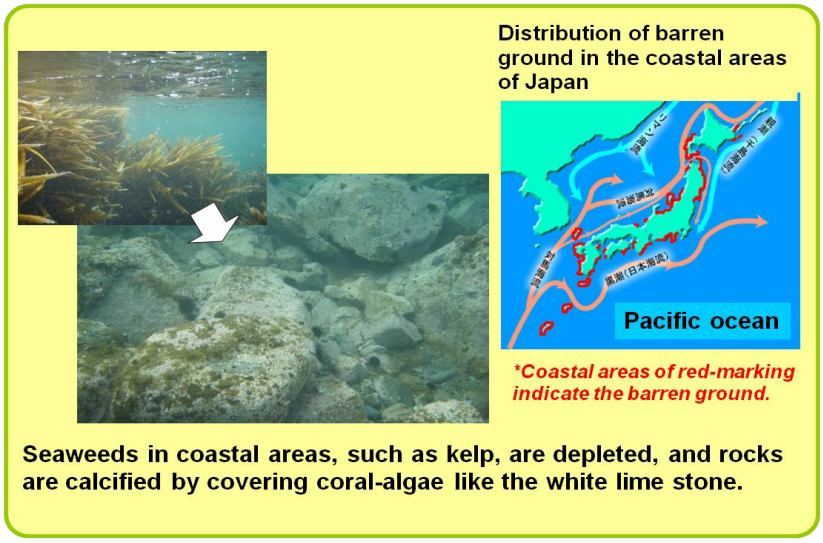

Fig. 2-1What is barren ground? (Fujita et al., 2002)

The restoration of seaweed beds in barren coasts had been developed by using fertilization technique to supply dissolved iron into the seawater of barren coastal areas. The composition of the fertilizer is a mixture of steel slag (serves as source of iron) and compost (serve as source of humic substances). The fertilizer was applied at Shaguma coast area, Mashike, Hokkaido, Japan (Yamamoto et al., 2010a). The fertilizer was placed at the bottom of the sea at approximately 2-3 m of the depth. This was done so that the fertilizers may contact relatively oxic condition of seawater because oxygen is important for the dissolution of iron. Additionally, the use of compost as a source of humic substances can serve as chelator of iron to stabilize the dissolved iron species under oxic conditions (Yamamoto et al., 2010b). As shown in Fig. 2-2, the chemical structure of humic substances contain acidic funtional groups such as carboxylic and phenolic hydroxyl groups which serve as binding sites for iron (Puchalski et al., 1992; Gagosian et al., 1977). Furthermore, humic substances contain quinone/hydroquinone redox couple, which, suggest that they are capable promoting reductive dissolution of iron from the surfaces of iron oxide (Nishimoto et al., 2013).

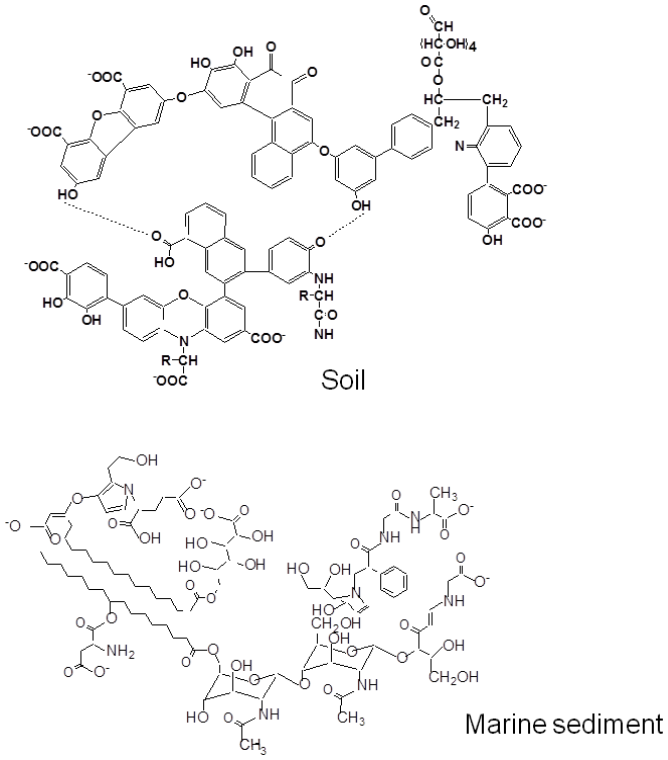

Fig. 2-2 Structural model of humic substances (Puchalski et al., 1992; Gagosian et al., 1977).

According to the results from restoration sites, seaweed beds were successfully recovered within three-year. It has been proven therefore that the fertilizer can significantly restore seaweed beds in barren ground (Yamamoto et al., 2010a). This content of humic acid was decreased from 2.2% to 0.5% during the 2-month incubation studied (Fujisawa et al., 2012). Therefore, elution of organic matter was rapidly digested and most of organic matter was lost within 2 months, while the iron was continuously eluted until the end of 6-month incubation. This phenomenon could not be explained because of the complexation of iron with organic matter. A study by Fujisawa et al. (2012) reported that biomarker fatty acids were detected in humic fractions from the fertilizer after a 6-month fertilization in seawater by a pyrolysis-GC/MS technique. This suggested that the degradation of humic acid in fertilizer could be attributed to microbial activites. Such processes may be related to continuous elution of iron via microbial activities.

To confirm this hypothesis of microbial activities in iron elution, we investigated and elucidated the effect of microbial activities on iron elution using artificial seawater. The model fertilization test was performed using water tank at Mashike coast, Hokkaido Japan (Fujisawa et al., 2012). Then bacterial cultures from fertilizer were isolated and identified. The test for iron elution was performed for a month to elucidate the effect of bacterial activity on iron elution to seawater using hematite as an iron oxide model (Royer et al., 2002; Bose et al., 2009). Anthraquinone-2,7-disolfonate (AQDS, Fig.2-3) was employed as dissolved organic matter model, since AQDS has been regarded as a monolog of humic matter (Royer et al., 2002). The eluted iron was determined in comparison in the absence and presence of both microorganism and AQDS.

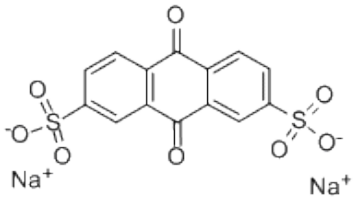

Fig. 2-3 Chemical structure of anthraquinone-2,7-disolfonate (AQDS).

2.2 Objectives

The aim of the Chapter 2 was to isolate and identify the bacteria from the steel slag-compost fertilizer. Then elution test using isolated bacteria were monitored in period of one month. We observed total dissolved iron concentration, ferrous ion concentration, organic acids production, as main focus. The chemical profile of pH, oxidation-reduction potential and temperature were also observed. The surface properties of hematite after treatment with bacteria were investigated using XRD, XPS, FE-SEM and ATR-FTIR.

2.3 Materials and Method

2.3.1 Field Experiment

The compost was prepared from a conifer wood bark according to literature (Fukushima et al., 2009). A basic oxygen furnace slag treated with CO_2 were used in this study to prevent increasing pH due to the hydration of CaO when slag was in contact with water (Rose et al., 2006). Mixture of compost and steel slag were prepared using the following weight/weight ratios:

(i) Compost alone without slag (slag/compost = 0g/394g);

(ii) Slag alone (slag/compost = 1000g/0g);

(iii) Slag/compost = 500g/147g;

(iv) Slag/compost = 333g/263g and

(v) Original seawater (as a blank).

Each mixture was packed in nylon-net bags, and then placed in 300L water tanks in the Shaguma coast in Hokkaido, Japan (N 43°89'36", E 141°60'46") as shown in Fig. 2-4.

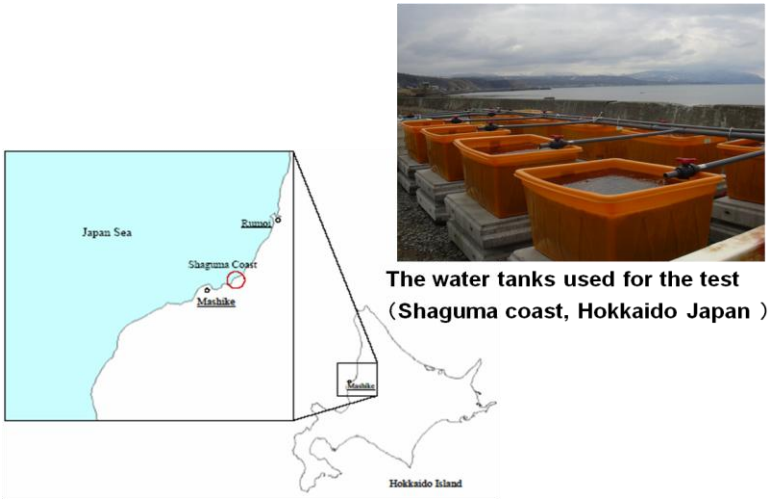

Fig. 2-4 Location for water tanks containing fertilizer test (Fujisawa et al., 2012).

Seawater was introduced into the tanks and could drain out at a flow rate of 4.1 L min^{-1}. A volume of 200 L of seawater was constantly maintained in the 300 L tanks. Fertilization period was divided into 2 phases. The first was from June 2014 to December 2014 whereas the second phase was from July 2015 to January 2016. After each fertilization period, one bags of fertilizer was sampled for isolation and identification of microorganisms at the interval of 2, 4 and 6 months from beginning of incubation. Additionally, temperature, pH ORP and salinity were measured when sampling the fertilizer. (Table 2-1).

2.3.2 Isolation and identification of bacteria from fertilizer

The fertilizer at slag/compost ratio = 500g/147g after a 6-month incubation was collected for isolation. The 0.1 mL volume of the sample was taken and inoculated onto a modified Postgate's B medium (Ghazy et al., 2011) to enrich the targeted bacteria before the plated-isolation. The enrichment was shaken at 120 rpm. The Postgate's B medium was composed of (in g L^{-1}): mixture of distilled water/artificial seawater = 1:1 (V/V)): KH_2PO_4 (Wako Pure Chemical Industries Ltd., Tokyo, Japan) 0.5; NH_4Cl (Wako Pure Chemical Industries Ltd., Tokyo, Japan) 1.0; Na_2SO_4 (Wako Pure Chemical Industries Ltd., Tokyo, Japan) 1.0; $CaCl_2.2H_2O$ (Nacalai Tesque, Tokyo, Japan) 0.1; $MgSO_4.7H_2O$ (Nacalai Tesque, Tokyo, Japan) 2.0; Sodium lactate (60-70%) (Nacalai Tesque, Tokyo, Japan) 5mL; Yeast extract (Nacalai Tesque, Tokyo, Japan) 1.0; L-ascorbic acid (Wako Pure Chemical Industries Ltd., Tokyo, Japan) 0.1; $FeSO_4.7H_2O$ (Wako Pure Chemical Industries Ltd., Tokyo, Japan) 0.5; NaCl (Nacalai Tesque, Tokyo, Japan) 26; pH 8.0±0.2; autoclaved at 121°C, 20 minutes (Bose et al., 2009). The artificial seawater composition was prepared by dissolving the following salts (g) in 1 L of distilled water: NaCl 28; $MgSO_4.7H_2O$ 7.0; $MgCl_2.6H_2O$ (Nacalai Tesque, Tokyo, Japan) 4.0; $CaCl_2.2H_2O$ 1.47; KCl (Wako Pure Chemical Industries Ltd., Tokyo, Japan) 0.7, pH 8.0±0.2 (Iwai et al., 2013).

After 5 days of inoculation, the enriched bacterial culture was diluted 10-times with ultra-pure water and a 0.1 mL aliquot was then plated by a spread plate method. The composition of PCA medium

was (in g L^{-1} of distilled water): peptone bacteriological (Becton, Dickinson & Company, USA) 5.0; proteose peptone (Becton, Dickinson & Company, USA) 5.0; L-cycteine (Nacalai Tesque, Tokyo, Japan) 0.25, NaCl 5.0; ammonium iron (III) citrate (Nacalai Tesque, Tokyo, Japan) 1.0; K_2HPO_4 (Nacalai Tesque, Tokyo, Japan) 0.3; agar (Nacalai Tesque, Tokyo, Japan) 15.0; pH 7.4±0.2; autoclaved at 121°C, 20 minutes then poured into Petri plates in triplicate ((Stillnovic and Hrenovic, 2009). These triplicates were incubated at 20.0±0.5 °C in an incubator (LTI-700, EYELA, Tokyo, Japan).

After 7 days of incubation, colonies that appeared in orange-peach-pale color were isolated and then directly picked up separately into 1.8 mL a vial (1.5 × 5 cm) containing glycerol (50%, V/V) to stock as shown in Fig. 2-6. Identification of each isolated colony was performed by Techno-Suruga Laboratory (Shizuoka, Japan).

2.3.3 Iron elution test

(a) Bacterial culture conditions

Stocks of identified colonies (*E. oxidotolerans* T-2-2) were enriched again with Postgate's B medium (Ghazy et al., 2011) at 20.0±0.5 °C while shaking at 120 rpm for 5 days to obtain cell density of 10^8 cell mL^{-1} (Royer et al., 2002).

Iron elution tests were performed in a Postgate's B medium, which was prepared and autoclaved at 121°C for 20 minutes in sterile 250 mL culture flasks. The composition of inoculated microorganisms, medium, hematite (Wako Pure Chemical Industries Ltd., Tokyo, Japan) and AQDS (Tokyo Chemical Industry, Tokyo, Japan) are summarized in Table 2-2. S1 and S2 were control cases that, contained *E.oxidotolerans* T-2-2 and hematite only respectively.

Table 2-2 Composition for iron elution test

Composition	S1	S2	S3	S4	S5
Postgate's B (mL)	200	200	200	200	200
E. oxidotolerans T-2-2 (mL)	1.0	-	1.0	1.0	1.0
Hematite (g)	-	1.0	1.0	-	1.0
AQDS (50μM)	-	-	-	1.0	1.0

2.3.4 Characterization of cultivation sample

(a) Monitoring of cultivation sample

Culture solutions were daily monitored for pH, oxidation-reduction potential (ORP) and temperature (pH-meter HM-31P, using pH and ORP probe). All measurements were conducted in a sterilized chamber (CCV clean bench, Hitachi, Japan).

2.3.5 Iron elution test

(a) Analyses of iron in the culture solution

To determine the amount of iron in culture solutions, samples were periodically collected at day 0, 5, 9, 14, 21, 28 and 30 of incubation. 1.2 mL of culture solutions were transferred to centrifugal tube (2mL) then centrifuged at 6500 rpm for 10 minutes. After the filtering using a 0.45 μm membrane filter, 1 mL filtrate was transferred to a polyethylene tube and diluted to 10 mL with 0.01 M aqueous HCl to preserve Fe in the solution. Total iron concentration was analyzed using an Inductively Coupled Plasma-Atomic Emission Spectrometer; ICP-AES (ICPE-9000, Shimadzu, Japan) (Nishimoto et al., 2013).

A colorimetric method using the complex formation of ferrozine-Fe(II) was used for the analysis of Fe(II) species in culture solution (Iwai et al., 2013). The stock solutions for Fe^{2+} standard (0.01M) was

prepared by dissolving $Fe(SO_4)_2(NH_4)2.6H_2O$ in 0.01 M aqueous HCl. The 50 mM ferrozine solution was prepared by dissolving in ultra-pure water. A 1 mL aliquot of the culture solution was transferred to a centrifugal tube then centrifuged at 6500 rpm for 10 minutes. A 800 µL aliquot of the supernatant was mixed with 4150 µL of ultra-pure water and then the 50 µL aliquot of ferrozine solution was added, 5 minutes was allowed for reaction. Sample solutions were placed into the 1×1 cm quartz cell. The absorbance at 562 nm was monitored using a V-630 type UV-vis spectrometer connected to PAC-743 type temperature controller with a Peltier device (Japan Spectroscopic Co., Ltd., Tokyo, Japan). The absorbance was reading at intervals of 1s (Iwai et al., 2013).

(b) Total organic carbon (TOC)

The 2 mL of culture solution was transferred to a centrifugal tube then centrifuged at 6500 rpm for 10 minutes. A 1.5 mL aliquot of the supernatant transferred into a TOC vial and diluted with ultra-pure water to final volume of 20 mL. The concentration of total organic carbon (TOC) of cultured solutions was analyzed by means of TOC-V CSH-type analyzer (Shimadzu, Japan).

(c) Molecular weight analysis by HPSEC

Prior to analysis, a 0.01 M phosphate buffer (pH7) containing 25% acetonitrile was prepared. A 500 µL aliquot of culture solution was transferred to the centrifugal tube mixing with 500 µL of 0.01 M phosphate buffer. Samples were allowed to precipitate overnight to remove $CaHPO_4$ that is formed by Ca^{2+} in seawater and then centrifuged at 6500 rpm for 10 minutes. Aliquots of supernatant were transferred into HPLC vials.

The molecular weights of culture solutions were determined by size exclusion chromatography using a TSK-Gel α-M column (7.8 mm i.d. × 300mm, void volume of 6.33 mL, Tosoh Co. Ltd. (Fujisawa et al., 2012). Polystyrene sulfonic acid sodium salts (Fulka, molecular weight of 0.208, 1.4, 4.3, 6.8, 17, 32, 49, 77, 150, 350, 990 kDa) were used as standard materials for calibrating the molecular weights. A 20 µL aliquot of an aqueous culture solution was injected into a PU-2080 type HPLC system (Japan

Spectroscopic Co. Ltd., Japan). The mobile phase consisted of a mixture of 0.01 M phosphate buffer (pH 7.0) and acetonitrile (75/25, v/v), and the flow rate was set at 0.75 mL min $^{-1}$. The column temperature was maintained at 40°C, and a UV-2075 type UV-vis detector was used for detection of molecular weights in the cultured solution at wavelength of 260 nm. Weight average (M_w) and number average (M_n) molecular weights were calculated using the equation below:

$$M_w = \frac{\Sigma(M_i h_i)}{\Sigma h_i} \quad (1)$$

$$M_n = \frac{\Sigma(h_i)}{\Sigma(\frac{h_i}{M_i})} \quad (2)$$

where the M_i is the molecular weight for the i-th molecule, and the h_i is the peak height of the i-th molecule (Fujisawa et al., 2012).

(d) UV-vis absorption spectra

Aliquot left from 2.4.3 was taken 100 µL into 4900 µL of ultra-pure water. UV-vis absorption spectra were recorded at 200-800 nm using a V-630 type UV-vis spectrophotometer.

(e) Organic acid analysis by Ion chromatography

A 1 mL aliquot of culture solution was transferred to the centrifugal tube then centrifuged at 6500 rpm for 10 minutes. The supernatant of aliquot was filtered through 0.45 µM membrane filter and then transferred to the HPLC vial. Mixture of oxalic, citric, lactic and acetic acid (at 1, 2, and 3 ppm) were used as standard organic acids. A 50 µL aliquot of an aqueous culture solution was injected into an IC20-type Ion Chromatograph (DIONEX). The regenerate was 1.5 mM Tetrabutyl ammonium hydroxide (TBAOH) and eluent was 1mM of Heptafluorobutyric acid. The flow rate was set at 0.80 mL min $^{-1}$, background conductivity was in the range of 45 - 50 µS, backpressure at 550-600 psi. The column for the separation of organic acids was an IonPac® ICE-AS6 (DIONEX, California, USA).

(f) Hematite particle size

Particle size distribution of hematite was determined to know the size distribution with Microtrac Size Analyzer (MT3300SX, Microtrac Inc., USA) instrument. The powdered hematite was dispersed in distilled water prior to analyze. Figure 2-5 shows the size distribution of hematite particle used in this study. The accumulation shows that most of hematite particle size less than 10 µM. The highest accumulation is around 5µM.

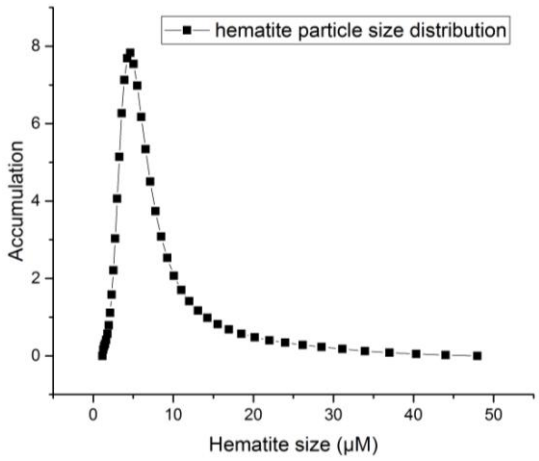

Fig. 2-5 Hematite particle size distribution

(g) Surface analysis of hematite

Hematite slurry cultured for 30 days of incubation was transferred into a visking tube (MWCO: 12000 - 14000 Da, Japan Medical Science, Japan) and dialyzed against ultrapure water. After dialyzed, the slurry was freeze-dried to obtain the powdered sample. The X-ray photoelectron spectroscopy (XPS) of the powdered hematite samples before and after the incubation were measured using JPS-9200 XPS instrument (JEOL, Japan). A monochromatic A MgK_{α} x-ray source was used for all samples, with pressures in the analysis chamber of 10^{-6} - 10^{-7} Pa. The condition used for all the survey scans were as follows: energy range 1250 - 250 eV, pass energy 50eV, step size 1 eV and sweep time 300 s (Grosvenor et al., 2004).

The powdered hematite samples were introduced to Pt ion for 60 second with JS-1100E ion sputtering device (JEOL Ltd., Japan) before Field Emission Scanning Electron Microscope (FE-SEM) investigation. For the surface observation, JSM-6500F (JEOL Ltd., Japan) was operated with accelerating voltage at 10 kV for treated samples and at 5 kV for untreated sample due to the resolution result of the image. The magnification varied from 10,000 to 100,000 times.

The Fourier transform infrared (FTIR) spectroscopy, 6200HFV (Jasco, Japan) equipped with Attenuated Total Reflectance (ATR) extension (ATR-pro one, Jasco, Japan) with view-through diamond prism was introduced to observe the hematite surface alteration. Spectra were obtained via spectra manager program (Jasco, Japan).

2.4 Results and discussion

2.4.1 Chemical profile of seawater during fertilization period

Temperature, pH, ORP and salinity were measured at the interval time of sampling at 2, 4 and 6 months. As shows in Table 2-1.

Table 2-1 Water temperature (a), pH (b), ORP (c) and salinity (d) monitoring at sampling time at 2, 4 and 6 months of incubation.

(a) Water temperature (°C)

Sample	Start (2014/6/5)	2-month (2014/8/9)	4-month (2014/10/2)	6-month (2014/12/2)
i	18.4	27	18.2	4.1
ii	18	27	18.1	4.1
iii	18.7	27.7	18.2	2.5

iv	18.4	27.3	18.1	4
V	18.6	25.5	18.1	7

(b) pH

Sample	**Start (2014/6/5)**	**2-month (2014/8/9)**	**4-month (2014/10/2)**	**6-month (2014/12/2)**
i	8.93	8.59	8.09	8.11
ii	8.96	8.61	8.11	8.13
iii	8.95	8.64	8.13	8.12
iv	8.94	8.62	8.17	8.15
V	8.95	8.54	8.1	8.1

(c) ORP (mV)

Sample	**Start (2014/6/5)**	**2-month (2014/8/9)**	**4-month (2014/10/2)**	**6-month (2014/12/2)**
i	-56	-57	-77	-45
ii	-35	-59	-80	-55
iii	-26	-64	-81	-59
iv	-25	-64	-84	-66
V	-25	-62	-87	-71

(d) Salinity (%)

Sample	Start (2014/6/5)	2-month (2014/8/9)	4-month (2014/10/2)	6-month (2014/12/2)
i	3.05	2.66	3.14	3.23
ii	3.03	2.66	3.12	3.26
iii	3.02	2.68	3.15	3.28
iv	3.04	2.71	3.14	3.26
V	3.04	2.67	3.15	3.24

2.4.2 Identification and characterization of isolated bacteria

The isolation of bacteria from fertilizer was successful in fertilizer containing slag/compost ratio of 500g/147g after a 6-month incubation period. After 5 days of inoculation in PCA agar, orange-color colonies appeared, and more than 10 orange-color colonies were observed at 7-day of inoculation (Fig. 2-6).

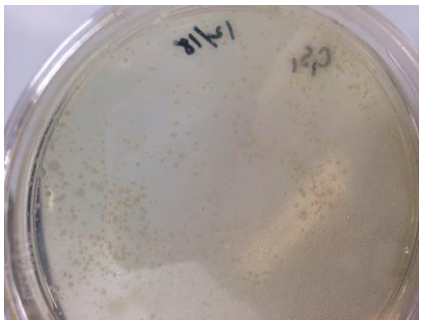

Fig. 2-6 The appearance of colonies in orange on plate which were isolated for identification.

The isolated colony was identified as *Exiguobacterium oxidotolerans* T-2-2 with its phylogenetic tree shown in Fig. 2-7. This novel species has been previously isolated from drain fish processing plant

(Vishnivetskaya et al., 2009). The isolated species can grow in 0-12% NaCl and range of preferable pH of 7-10 (Bharti et al., 2013).

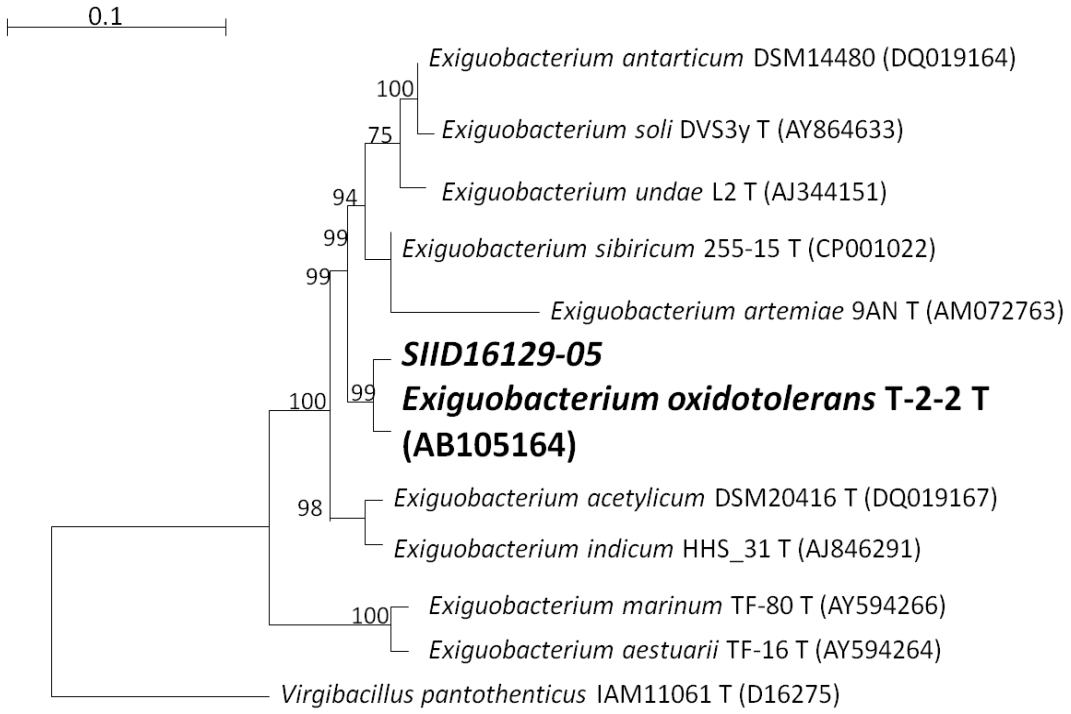

Fig. 2-7 Phylogenetic tree derived from 16S rRNA gene sequence data of *SIID16129-05*(isolated bacteria from fertilizer). 99% related to *Exiguobacterium oxidotolerans* T-2-2 and other *Exiguobacterium* species and some other related organisms using the neighbour-joining method. Numbers indicate bootstrap values, 0.1 K_{nuc} units.

The cells were found to be gram-positive, facultatively aerobic, and motile rods with peritrichous flagella. It has also reported that the colonies color is orange to yellow (Yumoto et al., 2004). Its cell extract exhibited 567 times higher in catalase activity compared to *Eschrichia coli* cell extract (Takebe et al., 2007). The major cellular fatty acids are *iso*-$C_{13:0}$, *anteiso*-$C_{13:0}$, *iso*-$C_{15:0}$, *iso*-$C_{16:0}$, *iso*-$C_{17:0}$, *anteiso*-$C_{17:0}$, *iso*-$C_{17:1}$ (Kulshreshtha et al., 2012). These results are consistent with biomarker fatty acids, which were found in the fertilizer containing slag after 4 and 6 months of incubation in the water tanks at the

Mashike coast (Fujisawa et al., 2012). This is also consistent with the composition of *Exiguobacterium oxidotolerans* T-2-2 activities in the fertilizer in this study shown by the data indicated in bold in Table 2-3.

Table 2-3 Biomarker fatty acids peaks areas (%) for *iso*-$C_{15:0}$, *iso*-$C_{17:0}$ and *anteiso*-$C_{17:0}$ founded in fertilizer contained slag/compost ratio = (i) 2:1 and (ii) 3:1 from previous study (Fujisawa et al, 2012).

R_t[a] (min)	Assigned pyrolysate compound (methyl ester derivatives)	Compost (initial)	(i)			(ii)		
			2	4	6	2	4	6
25.73	*iso*-$C_{15:0}$ carboxylic acid	n.d.[b]	1.50	0.93	**1.06**	1.35	0.93	0.53
29.64	*iso*-$C_{17:0}$ carboxylic acid	0.51	0.52	0.51	**2.68**	0.43	0.45	**10.7**
30.05	*anteiso*-$C_{15:0}$ carboxylic acid	0.51	0.66	0.50	n.d.[b]	n.d.[b]	n.d.[b]	0.56

[a] Retention times.

[b]Not-detected.

It also has been reported that *Exiguobacterium sp.* could be employed to neutral alkaline conditions by producing some organic acids supplied into wastewater (Kulshreshtha et al., 2012). This might be advantage for leaching iron into seawater, since *Exiguobacterium sp.* may produce organic acid and neutral seawater conditions for the elution of iron. As earlier mentioned, this isolated species is salt tolerant bacteria, which has capability for removing heavy metals such as Cr(VI) via the reduction (Okeke 2008; Pattanapipitpaisal et al., 2002). This idea could be adapted into our study to dissolve iron from the iron oxide.

2.4.3 Characterization of culture solution

Cultivated solution were daily monitored, in terms of temperature, pH and oxidation-reduction potential (ORP). Temperature during incubation was mostly stable nearly 20±0.3 °C (Fig. 2-8(a)), which was temperature set in an incubator. At the beginning of incubation, all samples stay at pH around 7.5±0.3, since media were adjusted to be nearly seawater conditions. After 2 days of incubation in samples containing *E. oxidotolerans* T-2-2, pH values mostly decreased to lower than 7 and then stabilized to 7 or lower during incubation period (Fig.2-8(b)). Compared with the uninoculated sample for the control, which contained only hematite and medium, pH was almost stable at 7.5±0.3 during incubation period (Fig.2-8(b)). ORPs also indicated in most likely trends with pH. In the presence of E. *oxidotolerans* T-2-2, ORPs mostly decreased to between -100 to -300 mV during incubation period. In case of *E. oxidotolerans* T-2-2 with hematite and *E. oxidotolerans* T-2-2 in the presence of both AQDS and hematite, the ORPs reached at the lowest value after 9 days of incubation and then slightly increased to constant values around -300 mV and -400 mV. However, the control sample containing hematite alone, the ORP values were almost stable nearly 0±40 mV (Fig. 2-8(c)). The decrease in ORP values in the presence of *E. oxidotolerans* T-2-2 suggests the microbial activities in seawater matrices.

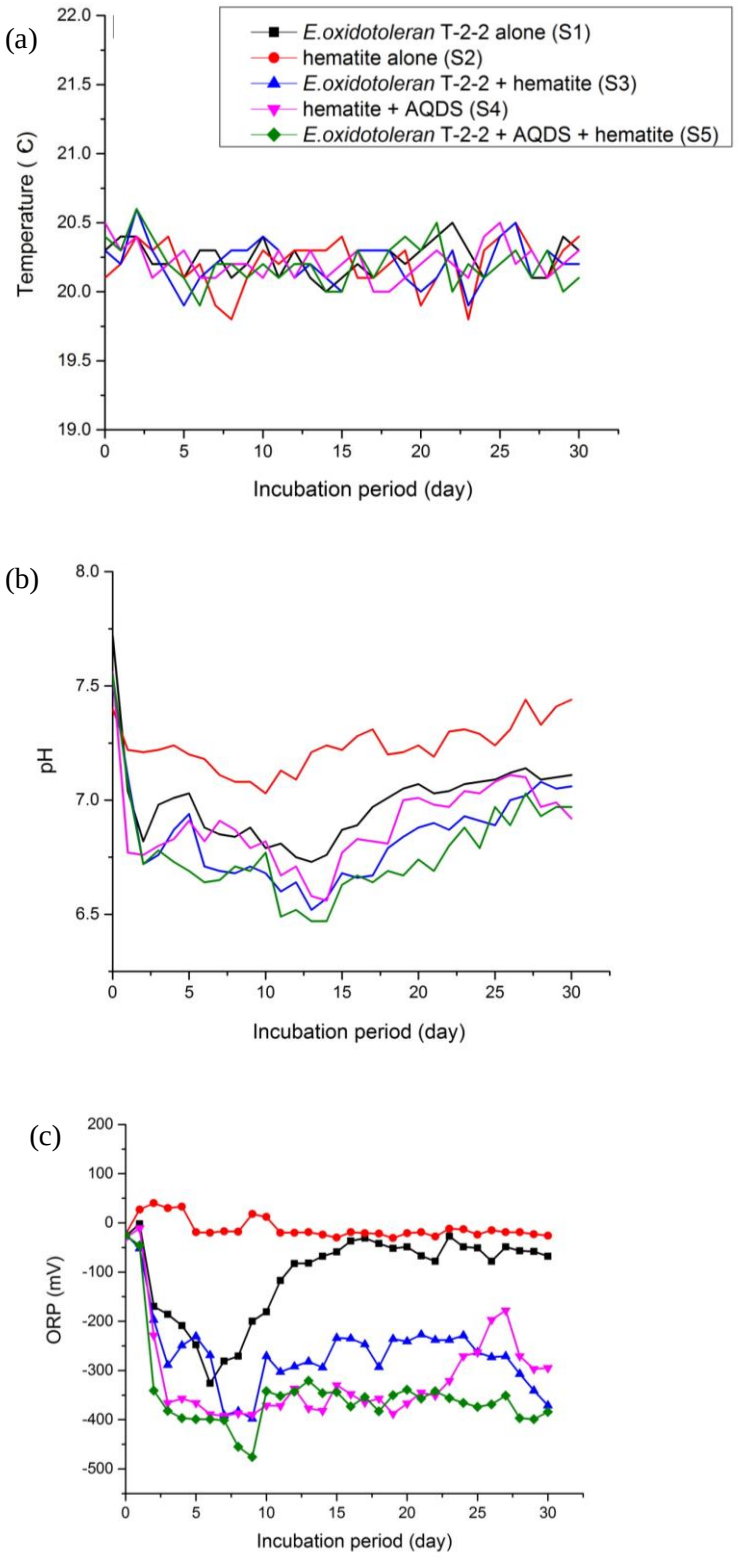

Fig. 2-8. Monitoring of the water temperature (a), pH (b) and ORP (c) in culture solution during 30-day of incubation.

2.4.4 Elution kinetics of Fe

The elution kinetics of total iron in the culture solutions shown in Fig. 2-9(a). The highest concentration of elution for total iron was observed after 9 days incubation at 38 mg L^{-1} and 22.3 mg L^{-1} in presence of AQDS and *E. oxidotolerans* T-2-2 (S5) and *E. oxidotolerans* T-2-2 only (S3), respectively. The S5 sample contained AQDS, and iron elution rapidly increased and reached the highest, while the iron concentration was suddenly decreased to lower than the S3 sample, which contained *E. oxidotolerans* T-2-2 and hematite after 2 weeks until the end of incubation period. Comparison to the uninoculated sample containing hematite only (S2), trace amount of iron was detected slightly around 0.3 ± 0.05 mg L^{-1}, which mostly came from composition in medium. Confirmation iron detected in S1 sample around 0.2 ± 0.05 mg L^{-1}.

Figure 2-9(b) shows the elution kinetics of Fe(II) species among total iron, which were determined by a colorimetric method using ferrozine. Fe(II) species may form Fe(II)-complex with dissolved organic matter (AQDS) (Royer et al., 2002). The elution of Fe(II) increased to the highest concentration after 9 days of incubation for S5 at 4.08 mg L^{-1} and S3 at 2.7 mg L^{-1}, being consistent with the results in Fig. 2-9(a). After a 2-week of incubation, Fe(II) was undetected and then detected again after the 3-week until the end of incubation. For the case of S1, S2 and S4, there were no detection of Fe(II) species in culture solution during incubation period. The highest levels of Fe(II) species that were detected after the 9-day incubation in S3 and S5 samples can be attributed to the minimum values for ORPs (Fig. 2-8(c)).However, among the dissolved species of iron, the rate of Fe(II) species was minor. The incubation was carried out under oxic conditions and the eluted Fe(II) from hematite (Fe_2O_3) might be oxidized immediately.

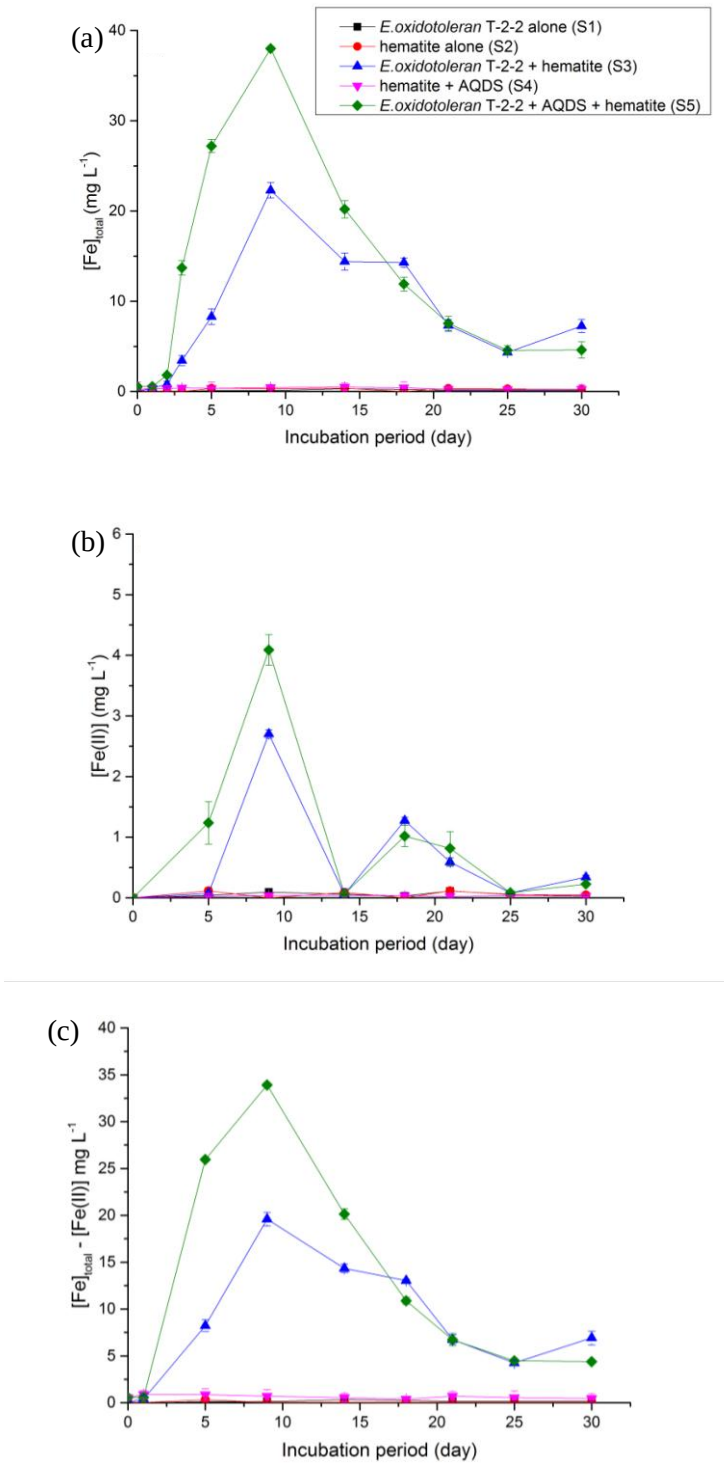

Fig. 2-9 Elution kinetics of iron in the culture solution during 30-day incubation (a) Total iron concentration, (b) Fe(II) species concentration and (c) Fe(III) species concentration.

Figure 2-9(c) shows the variations in the concentration of Fe(III), which were calculated by subtracting the concentration of Fe(II) from total Fe. As expected, the eluted Fe(III) from hematite in S5 and S3 reached the highest concentration after 9 days of incubation at 33.91 mg $L^{-1}$and 19.59 mg L^{-1} , respectively. After the 2-week of incubation, the eluted Fe(III) gradually decreased to around 4-6 mg L^{-1}. However, S3 showed slightly higher in eluted iron at the end of incubation at 6.91 mg L^{-1} compared to eluted iron of S5 at 4.37 mg L^{-1}. In control samples (S1, S2 and S4), almost nearly 0 mg L^{-1} of eluted iron were detected. These results indicate that bacteria in the fertilizer enhanced the elution of iron.

In the growth of macroalgae, trace levels of dissolved iron (several-ten to several-hundred nM) are required (Sunda et al., 2001; Lobban and Harrison 1994). Algae can uptake both Fe(III) and Fe(II) species via secretions like siderophore and receptor proteins on the surfaces of algae (Naito et al., 2008; Schneider et al., 1981). In the model experiments for the cultivation of algae, iron-EDTA chelate was employed (Hassler and Twiss 2006). For example, Suzuki et.al.(1995) reported that iron uptake to macroalga (*Laminaria japonica*) was facilitated in the presence of Fe(III)-EDTA complex. Iwai et.al.(2015) examined Fe (II) complexes with dissolved organic matter from compost to oogenesis on gametophytes of brown macroalga (*Saccharina japonica*), and the effects of Fe(II) complexes on oogenesis was observed. In these reports, iron hydroxide colloids cannot be taken by macroalgae, and the promotion of growth and gametophyte maturation were not observed. Thus, producing the dissolved species of iron via microbial processes is significant for supplying iron to seawater. However, Fe(II) and Fe(III) should be present as any complex species, to maintain the dissolved species in seawater.

For the culture system in the present study, lactic acid is presented and could serve as chelator of iron. However, this acid may decrease or convert to other acids via microbial processes. Thus, behaviors of total organic carbon were investigated in next section.

2.4.5 Total organic carbon contents

Figure 2-10 shows the variations in the levels of total organic carbon (TOC) in culture solution. TOC values for the culture solution containing *E. oxidotolerans* T-2-2 decreased within 5 days and likely to stabilize until the end of incubation period. This might be due to bacterial metabolism consuming organic compounds as carbon sources to produces metabolites, such as small molecule of organic acids (Kulshreshtha et al., 2012). However, decomposition to low-molecular-weight organic acids cannot lead to the decrease of TOC. One of reason for the TOC decrease is that organic acids are mineralized to CO_2 and/or CH_4 via the microbial processes. Alternatively, the decline of TOC levels might effect to the adsorption of AQDS to hematite and/or consumption of AQDS after metabolites reach at lower limit. This result can confirmed with UV-vis absorption data in section 2.4. and ion chromatography data in section 2.4. The uninoculated sample showed stabilize level of TOC during incubation period.

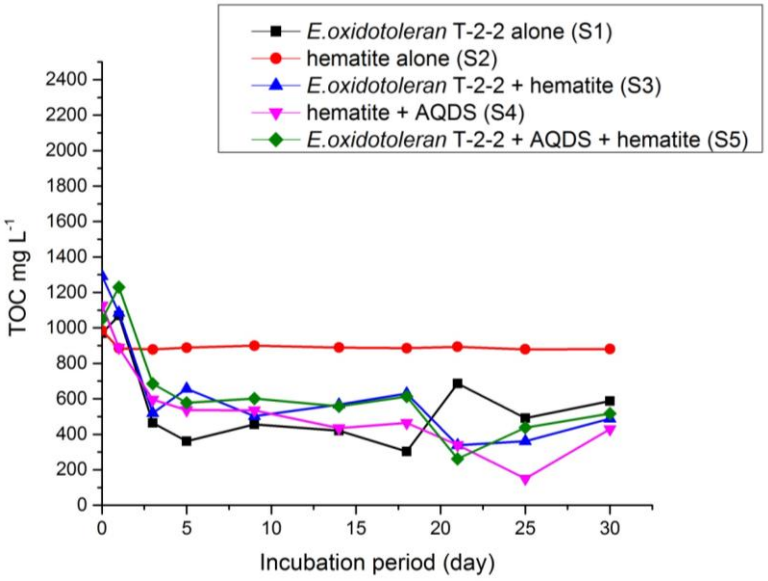

Fig. 2-10 Total organic carbon level during 30-day of incubation.

Another possible reason for the decrease of TOC was the adsorption of organic matter, such as microorganisms, yeast and AQDS. In the absence of *E. oxidotolerans* T-2-2 (S2), levels of TOC were not

so varied during incubation period. Thus, adsorption to yeast and other organic components in the culture media cannot be considered. The point of zero charge hematite has been reported to be in the range of 7.1-9.4 (Cromieres et al., 2002). Thus, hematite surfaces can indicate the positive charges. In addition, it has been reported that microorganism (*Bacillus polymyxa*), can be adsorbed to hematite surfaces in the higher ionic strength (Shashikala et al., 2002). This suggest that anionic organic species, such as proteins (bacteria and yeast), and AQDS can adsorbed to hematite surfaces under seawater conditions via electrostatic interactions. The total organic carbon data could be one of the evidences to confirm whether the decrease of TOC in the presence of *E. oxidotolerans* T-2-2 are due to the mineralization of organic matter via microbial activities and/or the adsorption of organic matter to hematite surfaces.

2.4.6 Molecular weight distributions

Figure 2-11 shows chromatograms of HPSEC at the detection wavelength of 260 nm (Fig. 2-11 (a)-(e)). Dissolution of organic matter in culture solution showed high-molecular weight compounds (around 1000 Da). This concentration suggested as component of medium (Fig. 2-12). The higher molecular weight fractions were decomposed within 5 days of incubation and low-molecular weight, which is considered as small organic acid from yeast (around 100-200 Da), was detected until 9 days of incubation for S1 and S3 (Fig. 2-11(a) and 2-11(c)). These results suggest that *E. oxidotolerans* T-2-2 slowly consumes yeast as organic carbon source. In the presence of AQDS (Fig. 2-11(d) and (e)), two peaks appeared at around 1000 Da and 100 Da. Because formula weight of AQDS is known to be 412.3 (g mol^{-1}), the peak of lower molecular weight was identified as AQDS monomer. It is reported that AQDS can bind to proteins via hydrophobic interactions (Maeda et al., 2010). Thus, the peak of the higher molecular weight may indicate the proteins-AQDS complexes. This was elucidated by comparing the chromatogram for AQDS alone with AQDS and Postgate's B medium (Fig. 2-12). These results show that some decomposition of AQDS occurs after 20 days of incubation, because of the consumption by microbial processes. However, large molecular weight fraction was not altered, suggesting that such

species of AQDS is not bioavailable. In comparison to S2 that contained only medium and hematite, chromatogram was almost constant during the incubation period (Fig. 2-13(b)).

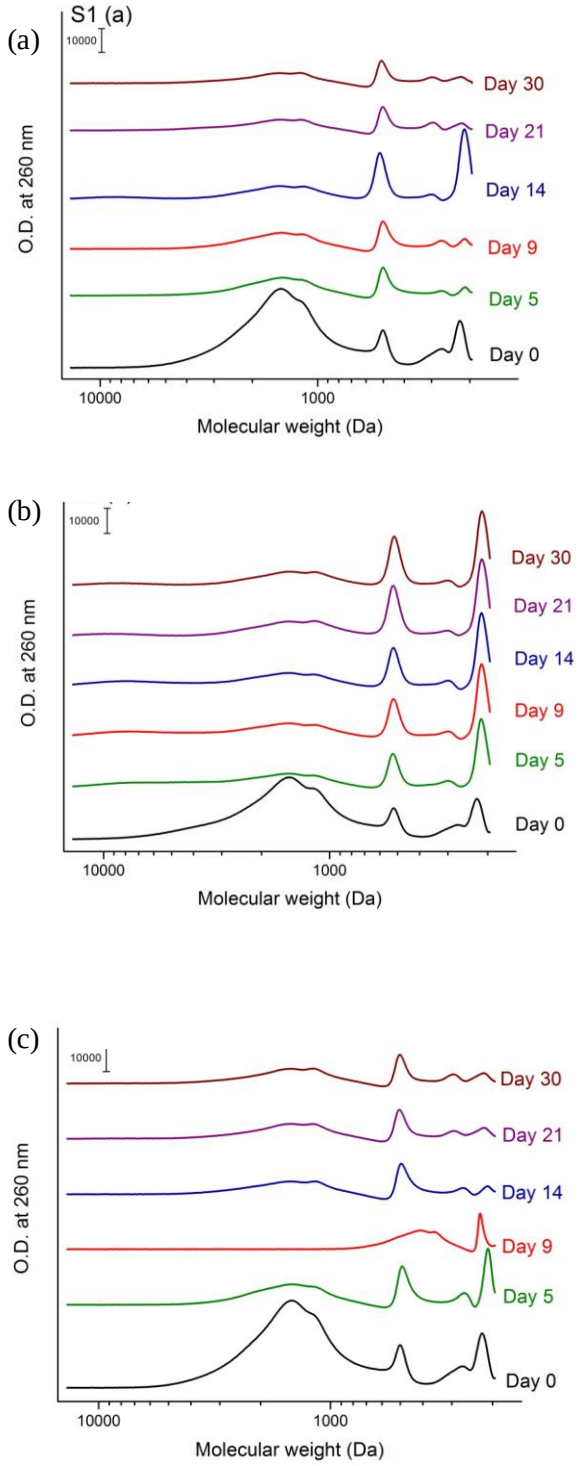

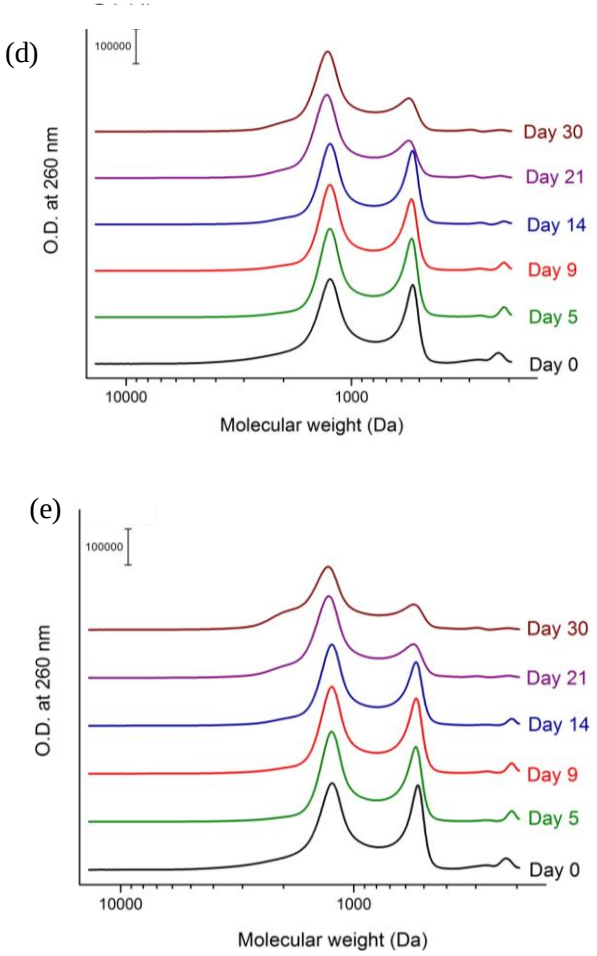

Fig. 2-11 HPSEC chromatogram of (a) S1: *E. oxidotolerans* T-2-2 alone; (b) S2 : hematite alone; (c) S3 : *E. oxidotolerans* T-2-2 with hematite; (d) S4 : Hematite with AQDS and (e) S5 : *E. oxidotolerans* T-2-2 with AQDS and hematite.

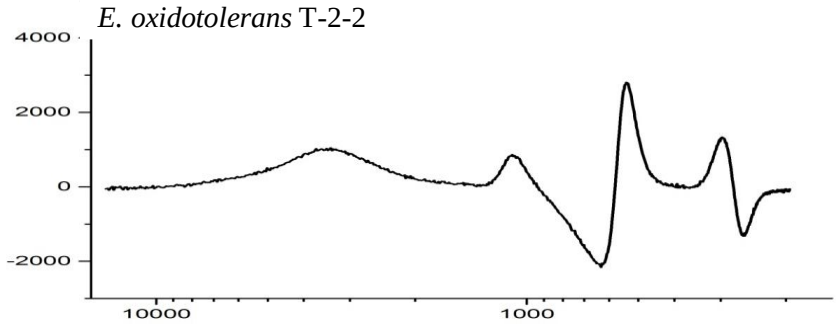

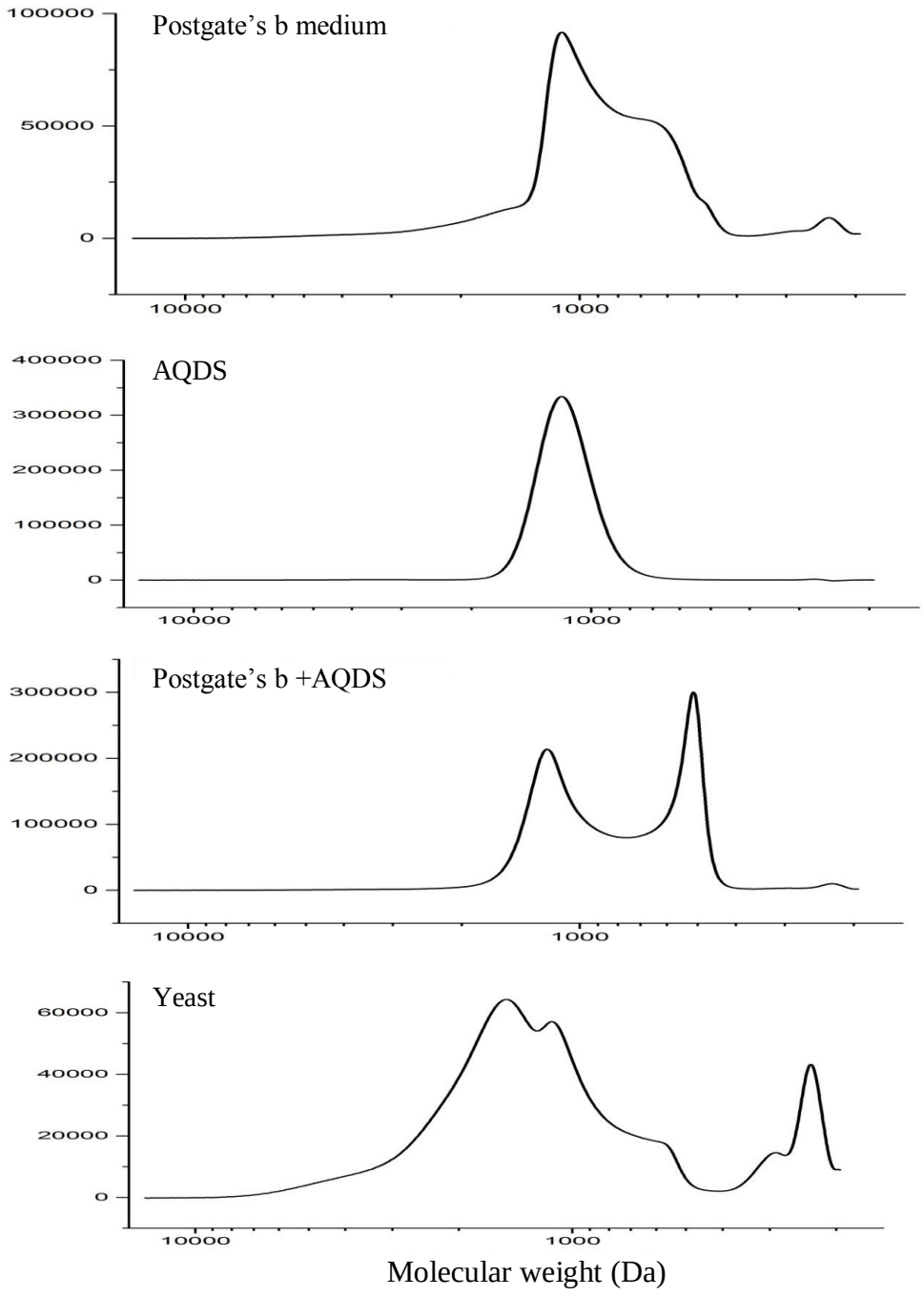

Fig. 2-12 HPSEC chromatogram of individual *E. oxidotolerans* T-2-2; Postgate's B medium; AQDS; AQDS with Postgate's B and yeast.

Weight average (M_w) and number average (M_n) also shown in Fig. 2-12(a) and 3-8(b).

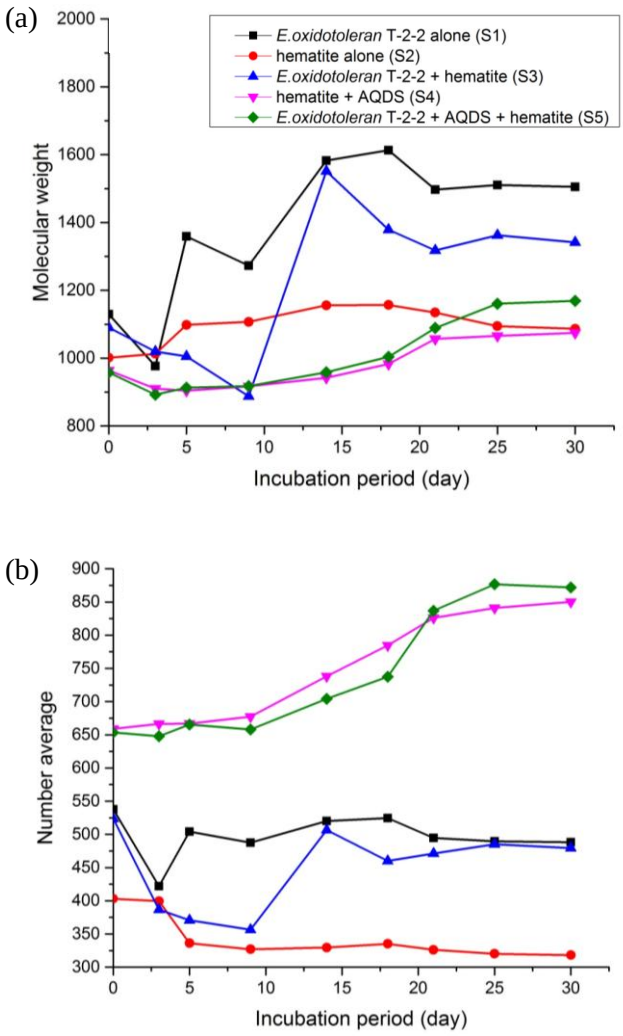

Fig. 2-13 Variations in weight average (a) and number average (b) molecular weights.

2.4.7 UV-vis absorption spectra of culture solution

Figure 2-14 shows the ratio of absorbance at 260 nm for day i (i= i-th day, A_i) today 0 (initial day of incubation, A_0) (A_i/A_0). The variations in the A_i/A_0 ratio for the decrease of absorbance at 260 nm were observed in the presence of *E. oxidotolerans* T-2-2 compared to the case for uninoculated sample.

Absorbance at 260 nm indicates the $n \rightarrow \pi^*$ electron transition for nitrogen auxochromes like proteins and $\pi \rightarrow \pi^*$ transition of C=C bond for AQDS.

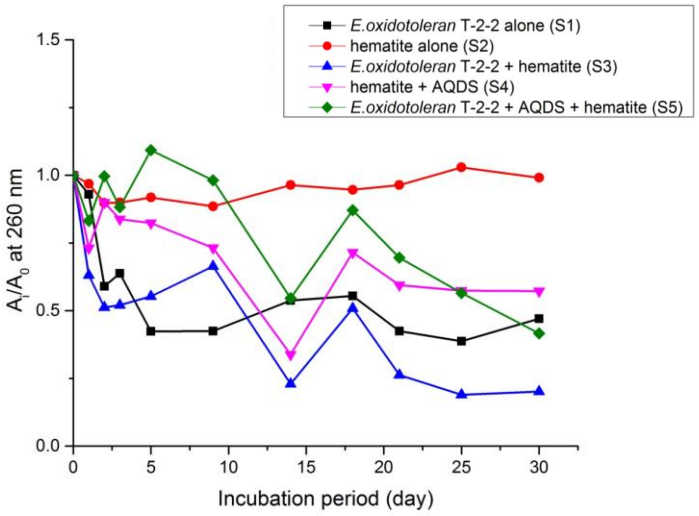

Fig. 2-14 A_i/A_0 absorbance at 260 nm.

Absorption spectra of each culture solution in the range of 200 - 800 nm are shown in Fig. 2-15(a) -(e). In the absence of AQDS (Fig. 2-15(a) and (c)), a broad peak appeared at around 230 nm. This can be identified as protein components in Postgate's B medium. However, in the presence of AQDS (Fig. 2-15 (d) and (e)), this peak became sharp and absorbance increased. This can be due to the absorption of AQDS. The peak from AQDS decreased after 14 days of incubation (Fig. 2-15 (d) and (e)), being consistent with the trends in chromatograms of HPSEC (Fig. 2-11 (d) and (e)). These results can be attributed to adsorption of AQDS to the hematite surfaces and/or consumption via the microbial processes. For the UV region of the spectra below 230 nm in the presence of AQDS (Fig. 2-15 (d) and (e)), absorbance values did not decrease with an increase in incubation period. This suggests that organic compounds from the degradations of AQDS or other organic matter in culture solution are formed because of microbial processes.

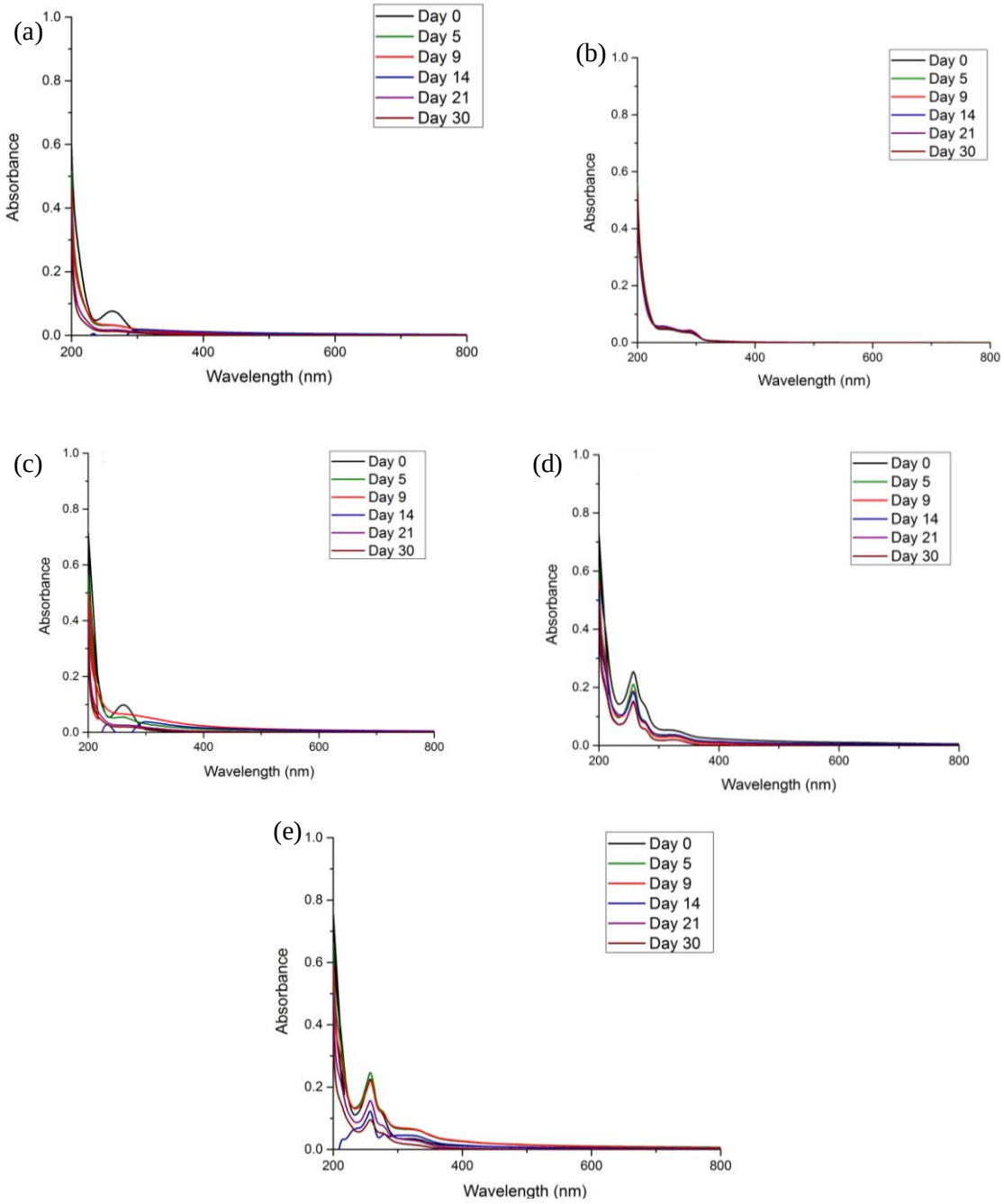

Fig. 2-15 Absorption spectra in the wavelength range of at 200 -800 nm for culture solutions of (a) S1: *E. oxidotolerans* T-2-2 alone; (b) S2: hematite alone; (c) S3: *E. oxidotolerans* T-2-2 with hematite; (d) S4: Hematite with AQDS and (e) S5: *E. oxidotolerans* T-2-2 with AQDS and hematite.

2.4.8 Organic acids production

In general, low-molecular-weight organic acids are formed as metabolite in the microbial processes. Such acids may serve as chelators of iron to maintain its dissolved form. However, the identified microorganism, *E. oxidotolerans* T-2-2, is novel bacterium that is isolated from the compost under seawater conditions, and metabolites are unknown. Thus, oxalic acid, citric acid, lactic acid and acetic acid in the culture solutions were monitored by an ion chromatography, because these acids can form complexes with iron. Retention times of standard organic acids (in mixture) for ion chromatography are summarized in Table 2-4.

Table 2-4 Retention time for standard organic acid; oxalic, citric, lactic and acetic.

No	**Organic acid**	**RT (min)**
1	Oxalic acid	6.10
2	Citric acid	9.77
3	Lactic acid	15.08
4	Acetic acid	19.78

Figure 2-16(a) -(d) shows the variations in organic acid concentrations of culture solutions. Oxalic (Fig. 2-16(a)) and lactic acid (Fig. 2-16(c)), which can serve as metabolites for bacteria, were high concentration at the beginning of incubation and then decreased after 5 days. Thereafter, the level of these organic acids largely increased again at 9 days of incubation and decrease again to stable until the end of incubation, especially in hematite containing sample. Crapart et. al. (2007) reported that *Exiguobacterium sp*. can produce lactic acid during incubation, which is related to our result in the production of lactic acid after 9 days of incubation. Lactic acid and oxalic acid were consumed by E. *oxidotolerans* T-2-2 as metabolites after medium was almost consume within 5 days. Citric acid and acetic acid were also detected at the highest concentration after 9 days of incubation (Fig. 2-16(b) and 2-16(d)), and then

decrease to stabilize. However, for acetic acid production after 9 days of incubation may be attributed to the specific abilities of *Exiguobacterium sp*. to neutralize alkaline water by producing acetic and formic acid (Kulshreshtha et al., 2012).

These results showed that *E. oxidotolerans* T-2-2 in culture solution, especially in hematite containing samples, had high activities for 9 days of incubation since the highest levels of all organic acids were correlated to the highest elution of iron. These results support the elution of iron from hematite can be attributed to microbial activities in culture solutions.

For the control sample in the presence of hematite alone, levels of organic acids remained constant.

The levels of oxalic and lactic acids at the start of incubation were relatively high. To explain this, the chromatogram for the medium only was recorded, as shown in Fig. 2-17, indicating that oxalic and lactic acids are composed in the Postgate's B medium.

The trend that slight increases in citric and acetic acids at the end of incubations suggests that oxalic and lactic acids are formed as result of metabolism via microbial activity, followed by citric and acetic acids formation. The higher levels of oxalic and citric acids may contribute to the enhanced elution of iron via the dissolution of iron by complexation with Fe(III) on the surface of hematite (Oulkadi et al., 2014).

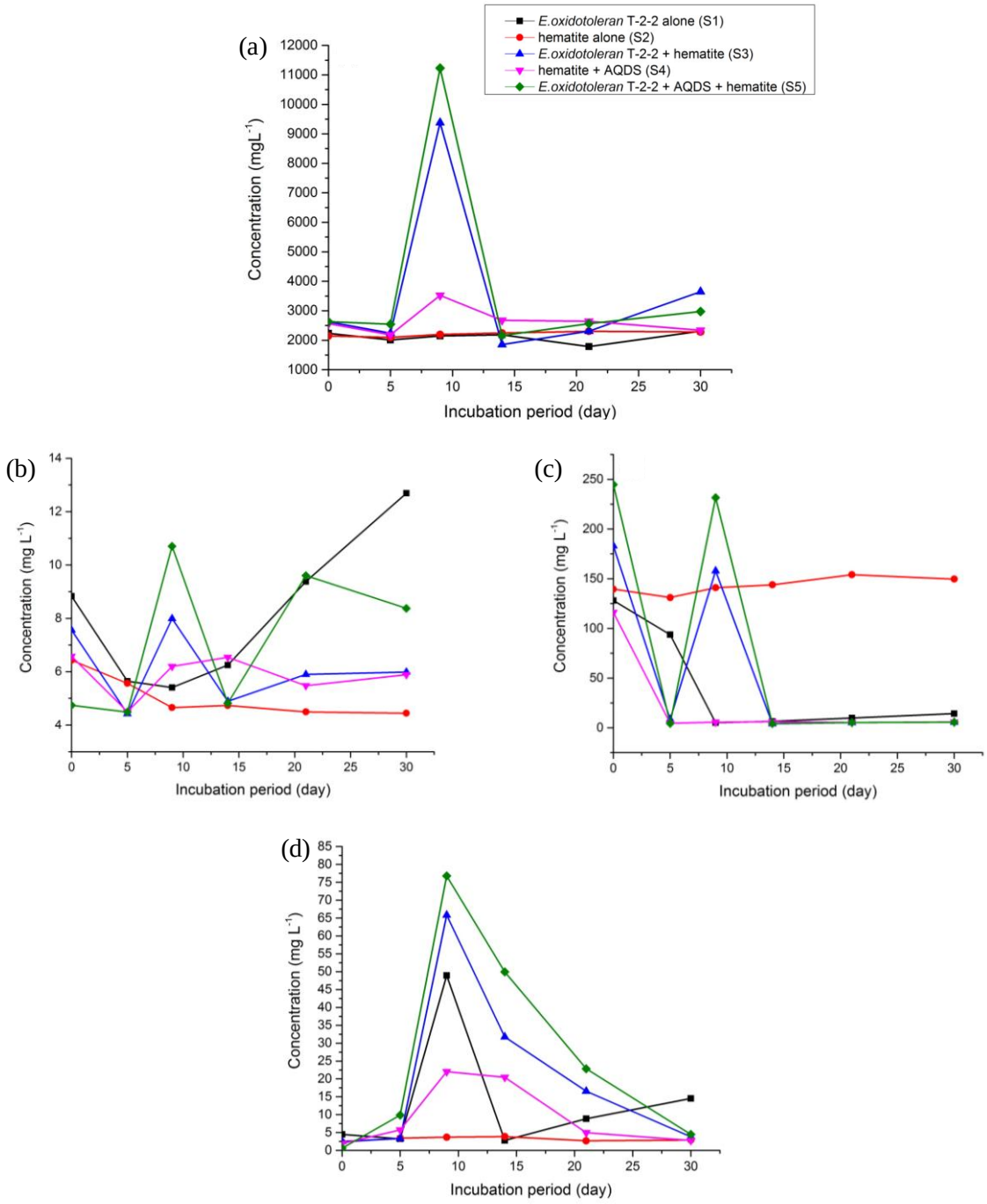

Fig. 2-16 Variations in the concentrations of oxalic acid (a); citric acid (b); lactic acid (c) and acetic acid (d) in culture solution during 30 days of incubation.

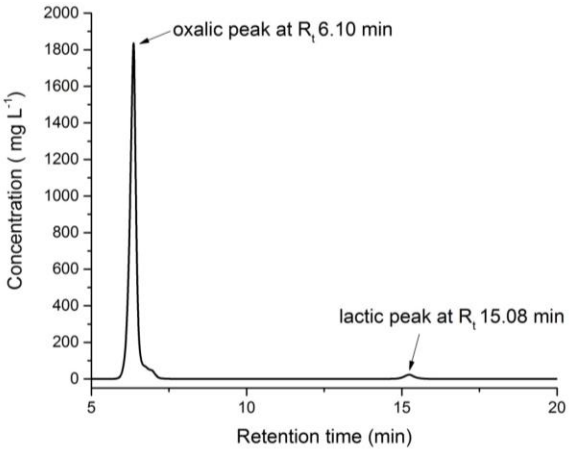

Fig. 2.17 Ion chromatogram of oxalic acid and lactic acid in medium

2.4.9 Surface analysis

XPS spectra of the samples are shown in Fig. 2-18. Figure 2-18(a) shows spectra of the high-spin $Fe^{3+}2p_{3/2}$ peak, in which no major differences were observed between treated and untreated hematite. However, in high-resolution of low- molecular masses in Fig.2-18(b) suggest a major difference between the untreated and treated hematite with and without AQDS. For the treated hematite, after 1 month of incubation, the intensity of the Fe^{3+} low-molecular mass peak markedly decreased, indicating that the Fe^{3+} species was eluted into the solution from the surfaces of hematite particles. The low molecular mass Fe^{3+} compounds could be attributed to eluted iron that was detecting during the incubation.

(a)

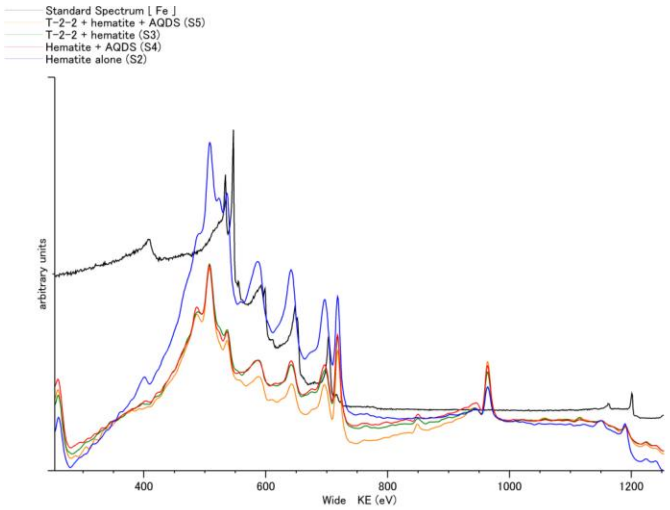

(b)

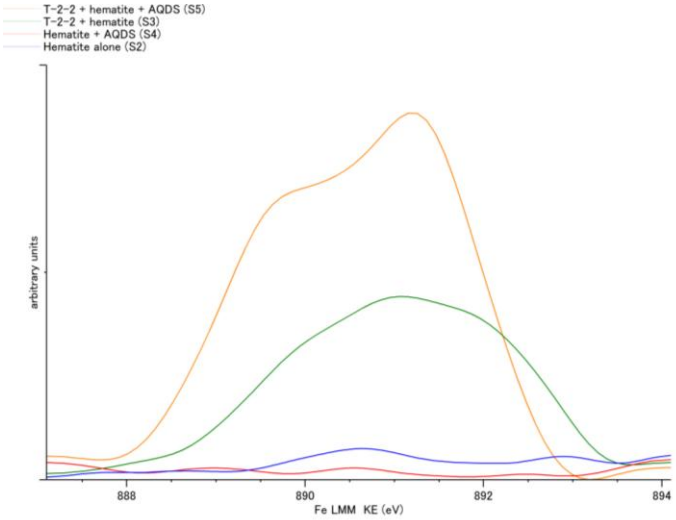

Fig. 2-18 XPS spectra of untreated and treated hematite after 30-day incubation (a) survey spectrum and (b) high resolution spectrum.

The surface visually observation using FE-SEM was used to investigate bacterial cells on hematite surface. Figure 2-19(a-d) show hematite surface after 30-day of incubation at the 10,000 magnifications. Since the size of hematite in the study was relatively the same as size of the bacteria cells. This was difficult to distinguish between the hematite particle and that of the cell of bacteria. However, the significant different between treated hematite compare to untreated hematite is the accumulation form

of the particles. Fig 2-19(a) and (b) show the hematite particle after incubated with T-2-2 and incubated with T-2-2 with AQDS respectively. The accumulation of hematite particle is less than the untreated (Fig. 2-19 (c) and (d)) hematite. Both untreated hematite (Fig. 2-19(c)) and hematite incubated with AQDS (Fig. 2-19(d)) show the fine accumulation of hematite particle. Especially in Fig.2-19c for the control, the magnetized interference strongly appeared 10kV of the observation, therefore the 5-kV field was introduced for this sample. The separation of hematite particle might distribute to the reduction of hematite by bacteria activities. In comparison, the medium without any inoculation could not change the magnetic properties of hematite (Roden et al., 2004). Therefore, the surface's property alteration is one of the evidences to confirm the reduction of hematite surface.

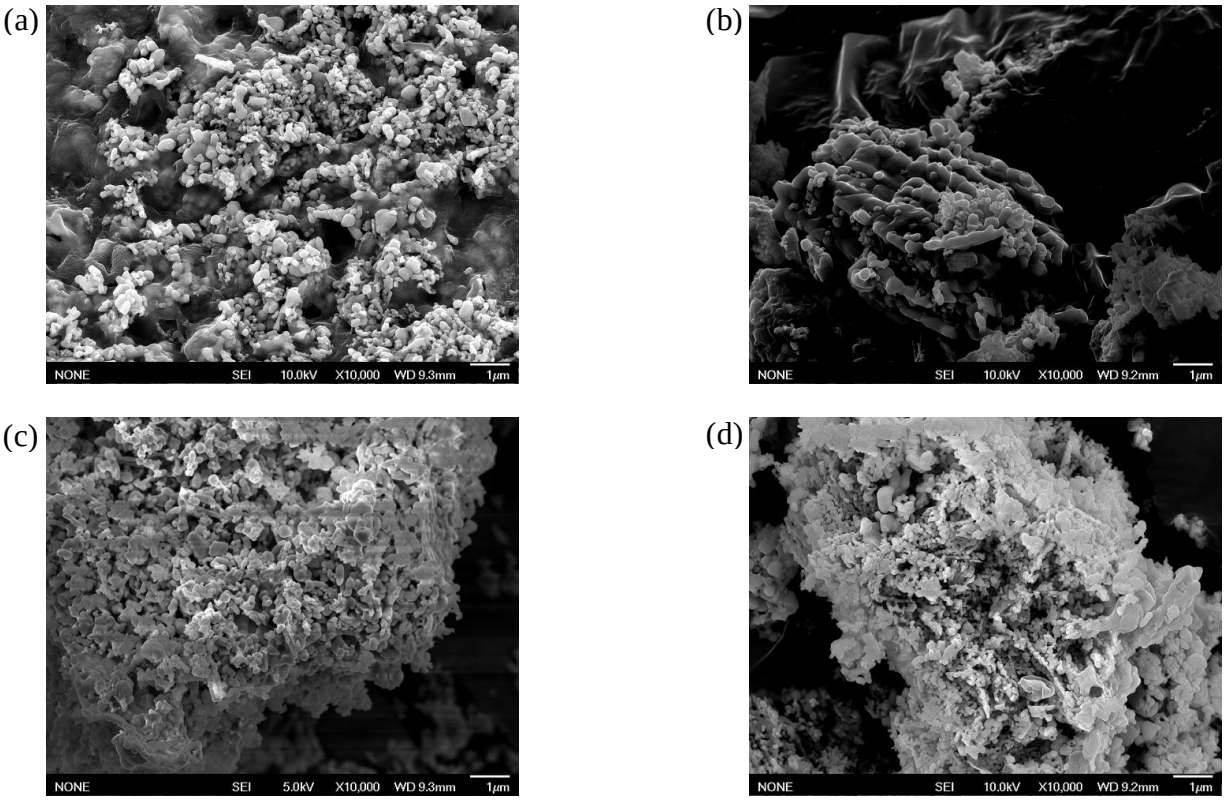

Fig. 2-19 FE-SEM image of hematite after 30 days of incubation (a) *E. oxidotolerans* with hematite, (b) *E. oxidotolerans* with hematite and AQDS, (c) untreated hematite and (d) hematite with AQDS

Figure 2-20(a) and (b) shows ATR-FTIR spectra of hematite comparison between untreated hematite with treated with bacteria for 30-day and hematite exposed in Postgate's B medium. The absorbance corresponded to bacteria cell interaction with iron should investigate in term amino acid functional group and phosphate group spectra from the bacterial cell. Figure 2-21(a) show the absorbance spectrum specify for appearance of amino acid functional group, the group frequency 1680-1590 (cm^{-1}) indicated the functional group for primary amine (NH bend) and group frequency 1650-1500 (cm^{-1}) for secondary amine (NH-bend), the functional group absorbance only detect in bacteria treated hematite sample (Coates, 2000). The group frequency at 1210-1150 (cm^{-1}) for tertiary amine (CN stretch) also appeared in medium containing sample, suggested this absorbance should come from the component of the medium (Fig. 2-20(b)). The bacteria treated sample shows the phospholipids IR band assignment appear at group frequency 1653-1639 (cm^{-1}) for C-N bending (Fig.2-20(a)) (Cagnasso et al. 2009). The frequency appears at 1223 (cm^{-1}) indicate for PO_2^- asymmetric stretching vibration, 1247 (cm^{-1}) for P-OH bending vibration and 1116 (cm^{-1}) for P=O vibration (Elzinga et al., 2007) in treated sample. Broad peak identical to formation vibration of P-OFe also appeared in treated sample at group frequency around 997-972 (cm^{-1}), this could be one of the evidences for the cell attachment at the hematite surface.

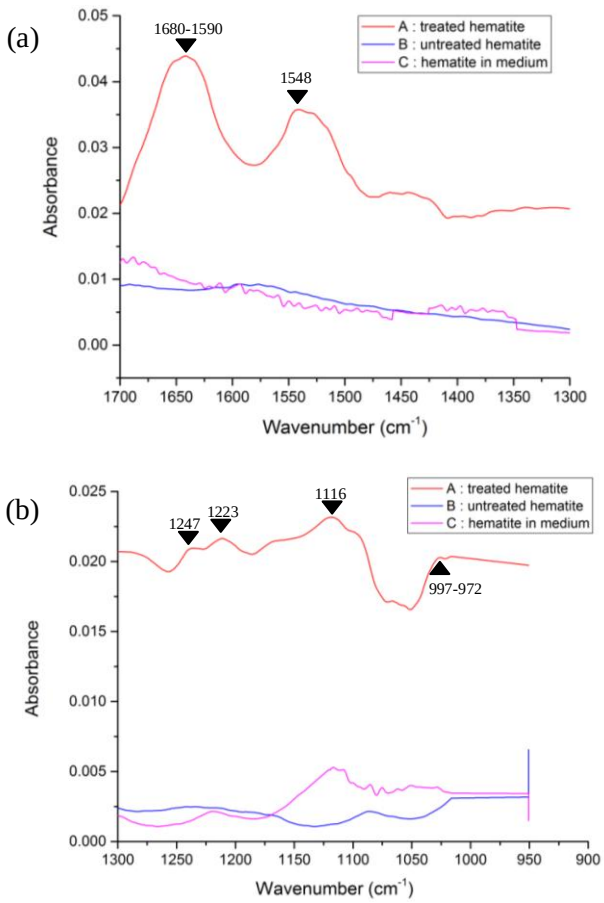

Fig. 2-20 FTIR spectra of hematite surface (a) at group frequency 1700-1300 (cm^{-1}) for amino acid functional group and (b) at 1300-950 (cm^{-1}) for FE-phosphate formation

2.5 Conclusion

Isolated microorganism from the fertilizer was identified as an alkaliphile *Exiguobacterium oxidotolerans* T-2-2. This species has abilities in adaptation into extreme nature, neutral alkaline conditions, to produce low molecular weight acids.

The elution test was conducted under seawater conditions by comparing with control samples. During the incubation period in the presence of both *E. oxidotolerans* T-2-2 and hematite, the eluted iron was detected and reached at the highest concentration at 9-day of incubation. AQDS can serve as

mediator and sample containing AQDS with *E. oxidotolerans* T-2-2 and hematite showed rapidly elution of iron at the highest concentration. To confirm the microbial activities, uninoculated control was observed and elution of iron was almost undetected. This can be attributed to the fact that *E. oxidotolerans* T-2-2 activities in the fertilizer enhanced the elution of iron.

Variations in total organic carbon (TOC) also confirmed that microbial activities in the system contributed to the elution. In all samples containing *E. oxidotolerans* T-2-2 showed the declination of TOC after 5 days of incubation. Molecular weight distribution of culture solution showed that bacteria were consumed organic compound from composition of medium within 9 days confirmed with the UV-vis absorption spectra. The wavelength region around 230 nm of organic components in medium culture gradually decreased during incubation indicated for the consumption of organic compounds by microorganisms, compared to the uninoculated sample.

Ion chromatography analysis for organic acids production also showed that the highest activities in the production of oxalic and lactic acids after consuming these acids was reached at 9-day of incubation and then *E. oxidotolerans* T-2-2 produced some low-molecular weight organic acids, such as citric and acetic acids, which were detected until the end of incubation. The highest concentration of eluted iron and the highest concentration of oxalic and lactic acids production were correlated at the 9-day of incubation. As well as the result of oxidation-reduction potential that reached the lowest at the 9-day of incubation. These results indicate that microbial processes can contribute to the iron elution under seawater conditions.

Surface analysis data also shown the decrease intensity of Fe^{3+} in bacteria containing sample. This evidence could assume that Fe^{3+} was eluted from the hematite surface into medium solution. The FTIR spectra also show the evidence of formation at the hematite surface via the observation of P-FeO vibration that appeared in treated hematite sample. The bacteria cell composition also detected at the hematite surface.

References

[1] D.Fujita, T. Hori, M. Ohno and T. Horiguchi eds. Barren ground current state of phycology in the 21st century. *Japanese Society of Phycology*, Yamagata, Japan, 2002.

[2] K. Matsunaga, T. Kawaguchi, Y. Suzuki and G. Nigi. The role of terrestrial humic substances on the shift of kelp community to crustose coralline algae community of the southern Hokkaido island in the Japan sea. *Journal of Experimental Marine Biology and Ecology*, 241, 193-205, 1999.

[3] K. Matsunaga, J. Nishioka, K. Kuma , K. Toya and Y. Suzuki. Riverine input of bioavailable iron supporting phytoplankton growth in Kesennuma Bay (Japan). *Water Research*, 11, 3436-3442, 1998.

[4] K. Kuma, A. Katsumoto, H. Kawakami, F. Takatori, and K. Matsunaga. Spatial variability of Fe (III) hydroxide solubility in the water column of Northern North Pacific ocean. *Deep Sea Research Part I*, 45, 91-113, 1998.

[5] M. Boye, C.M.G. van der Berg, J.T.M. de Jong, H. Leach, P. Croot and H.J.W. de Baar. Organic complexation of iron in the Southern ocean. *Deep Sea Research Part I*, 48, 1477-1497, 2001.

[6] A.L. Rose, T.D. Waite. Role of superoxide in the photochemical reduction of iron in seawater. *Geochimica et Cosmochimica Acta*, 70, 3869-3882, 2006.

[7] M. Yamamoto, M. Fukushima, E. Kiso, T. Kato, M. Shibuya, S. Horiya, A. Nishida, K. Otsuka and T. Komai. Application of iron humates to barren ground in a coastal area for restoring seaweed beds. *Journal of Chemical Engineering of Japan*, 43, 627-634, 2010.

[8] M. Yamamoto, A. Nishida, K. Otsuka and T. Komai and M. Fukushima. Evaluation of the binding of iron (II) to humic substances derived from a compost sample by colorimetric method using ferrozine. *Bioresource Technology*, 101, 4456-4460, 2010.

[9] M.M. Puchalski, M.J. Morra and R.V.Wandruszka. Fluorescence quenching of synthetic organic compounds by humic materials, *Environmental Science and Technology*, 26, 1787-1792, 1992.

[10] R.B. Gagosian and D.H. Stuermer. The cycling of biogenic compound and their diagenetically transformed products in seawater. *Marine Chemistry*, 5, 605-632, 1977.

[11] R. Nishimoto, S. Fukuchi, G. Qi, M. Fukushima and T. Sato. Effects of surface Fe(III) oxides in a steel slag on the formation of humic-like dark-colored polymers by the polycondensation of humic precursors. *Colloids and Surfaces A : Physicochemical and Engineering Aspects*, 418, 117-123, 2013.

[12] N. Fujisawa, M. Fukushima, M. Yamamoto, H. Iwai, T. Komai, Y. Kawabe and D. Liu. Structural alteration of humic acid fractions in a steel slag-compost fertilizer during fertilization. Analysis by pyrolysis/methylation-gas chromatography/mass spectrometry. *Journal of Analytical and Applied Pyrolysis*, 95, 126-133, 2012.

[13] R.A. Royer, W.D. Burgos, A.S. Fisher, B. Jeon, R.F. Unz and B.A. Dempsey. Enhancement of hematite bioreduction by natural organic matter. Environmental Science Technology, 36, 2897-2904, 2002.

[14] S. Bose, M.F. Hochella Jr., Y.A. Gorby, D.W. Kennedy, D.E. AcCready, A.S. Madden and B.H. Lower. Bioreduction of hematite nanoparticles by the dissimilatory iron reducing bacterium *Shewanella oneidensis* MR-1, *Geochimica et Cosmochimica Acta*, 73, 962-976, 2009.

[15] M. Fukushima, K. Yamamoto, O. Ohtsuka, T. Aramaki, T. Komai, S. Ueda and S. Horiya. Effect of the maturity of wood-waste compost on the structural features of humic acids. *Bioresource Technology*, 100, 791-797, 2009.

[16] E.A. Ghazy, M.G. Mahmoud, M.S. Asker, M.N. Mahmoud, M.M. Abo Elsoud and M.E. Abdel Sami. Cultivation and detection of sulfate reducing bacteria (SRB) in sea water. *Journal of American Science*, 7(2), 604-608, 2011.

[17] H. Iwai, M. Fukushima and M. Yamamoto. Determination of labile Fe(II) species complexed with seawater extractable organic matter under seawater conditions based on the kinetics of ligand-exchange reactions with ferrozine. *Analytical Science, The Japan Society for Analytical Chemistry*, 29, 723-728, 2013.

[18] APHA Annual Meeting Continuing Education Program, the 19th edition of Standard Methods for the Examination of Water and Wastewater, September 1995. (http://ajph.aphapublications.org/doi/pdf/10.2105/AJPH.85.8_Pt_2.P.164)

[19] B. Stilinovic and J. Hrenovic. Plate method for counting proteolytic sulphide-producing bacteria. *Acta Botanica Croatica*, 68(1), 57-66, 2009.

[20] T.A. Vishnivetskaya, S. Katariou and J.M Tiedje. The *Exiguobacterium* genus : biodiversity and biogeography. *Extremophiles*, 13, 541-555, 2009.

[21] N. Bharti, D. Yadav, D. Barnawal, D. Maji and A. Kalra. *Exiguobacterium oxidotolerans*, a halotolerant plant growth promoting rhizobacteria, improves yield and content of secondary metabolites in *Bacopa monnieri* (L.) Pennell under primary and secondary salt stress. *World Journal of Microbial Biotechnology*, 29, 379-387, 2013.

[22] I. Yumoto, M. Hishinuma-Narisawa, K. Hirota, T. Shingyo, F. Takebe, Y. Nodasaka, H. Matsuyama and I. Hara. *Exiguobacterium oxidotolerans* sp. Nov., a novel alkaliphile exhibiting high catalase activity. *International Journal of Systematic and Evolutionary Microbiology*, 54, 2013-2017, 2004.

[23] N.M. Kulshreshtha, A. Kumar, G. Bisht, S. Pasha and R. Kumar. Usefulness of organic acid produced by *Exiguobacterium sp.*12/1 on neutralization of alkaline water. *The Scientific World Journal*, ID 345101, Vol. 2012.

[24] F. Takebe, I. Hara, H. Matsuyama and I. Yumoto. Effect of H2O2 under low- and high-aeration-level conditions on growth and catalase activity in *Exiguobacterium oxidotolerans* T-2-2. *Journal of Bioscience and bioengineering*, 104, 464-469, 2007.

[25] B.C. Okeke. Bioremoval of hexavalent chromium from water by a salt tolerant bacterium, *Exiguobacterium* sp. GS1. *Journal of Industrial Microbial Biotechnology*, 35, 1571-1579, 2008.

[26] P. Pattanapipitpaisal, A.N. Mabbett, J.A. Finlay, A.J. Beswick, M. Paterson-Beedle, A. Essa, J. Wright, M.R. Tolley, U. Badar, N. Ahmed, J.L. Hobman, N.L. Brown and L.E. Macaskie. Reduction of Cr(VI) and bioaccumulation of chromium by gram positive and gram negative microorganisms not previously exposed to Cr-stress. *Environmental Technology*, 23(7), 731-745, 2002.

[27] W.G. Sunda, D.R. Turner and K.A Hunter (eds.). The biogeochemistry of iron in seawater, chapter 3. *Wiley New York*, 2001.

[28] C.S. Lobban and P.J. Harrison. Seaweed Ecology and Physiology. *Cambridge University Press*, Cambridge, 1994.

[29] K. Naito, I Imai and H. Nakahara. Complexation of iron by microbial siderophores and effects of iron chelates on the growth of marine microalgae causing red tides. *Phycological Research*, 56, 58-67, 2008.

[30] R. Schneider, A Hartmann and V. Braun. Transport of the iron ionophore ferrichrome in *Escherichia coli* K-12 and *Salmonella typhimurium* LT2. *FEMS Microbial Lett*, 11, 115-119, 1981.

[31] C.S. Hassler and M.R. Twiss. Bioavailability of iron sensed by a phytoplanktonic Fe-bioreporter. *Environmental Science and Technology*, 40, 2544-2551, 2006.

[32] Y. Suzuki, K. Kuma and K. Matsunaga. Bioavailable iron species in seawater measured by macroalga (*Laminaria japonica*) uptake. *Marine Biology*, 123, 173-178, 1995.

[33] H. Iwai, M. Fukushima and T. Motomura. Effect of iron complexes with seawater extractable organic matter on oogenesis in gametophytes of a brown macroalga (*Saccharia japonica*). *Journal of Applied Phycology*, 27, 1583-1591, 2015.

[34] L. Cromieres, V. Moulin, B. Fourest and E. Giffaut. Physico-chemical characterization of the colloidal hematite/water interface : experimentation and modelling. *Colloids and Surfaces A : Physicochemical and Engineering Aspects*, 202, 101-115, 2002.

[35] A.R. Shashikala and A.M. Raichur. Role of interfacial phenomena in determining adsorption of *Bacillus polymyxa* onto hematite and quartz. *Colloids and Surfaces B : Biointerfaces*, 24, 11-20, 2002.

[36] K. Maeda, A.J. Robinson, K.B. Henbest, E.J. Dell and C.R. Temmel. Protein surface interactions probed by magnetic field effects on chemical reactions. *Journal of American Chemical Society*, 132, 1466-1467, 2010.

[37] D. Oulkadi, C. Balland-Bolou-Bi, L.J. Michot, M. Grybos, P.Billard, C. Mustin and S. Banon. Bioweathering of nontronite colloids in hybrid silica gel : implications for iron mobilization. *Journal of Applied Microbiology*, 116, 325-334, 2014.

[38] E.E. Roden, D. Sobolev, B. Glazer, G.W. Luther. Potential for microscale bacerial Fe redox cycling at the aerobic -anaerobic interface. *Journal of Geomicrobiology*, 21, 379-391, 2004.

[39] J. Coates. Interpretation of infrared spectra, A practical approach. *Encyclopedia of Analytical Chemistry*, John Wiley & Sons Ltd, 10815-10837, 2000.

[40] M. Cagnasso, V. Boero, M.A. Franchini and J. Chorover. ATR-FTIR studies of phopholipid vesicle interactions with α-FeOOH and α-Fe_2O_3 surfaces. *Colloids and Surfaces B : Biointerfaces*,76, 456-467, 2010.

[41] E.J Elzinga and D.L Sparks. Phosphate adsorption onto hematite: An in situ ATR-FTIR investigation of the effects of pH and loading level on the mode of phosphate surface complexation. *Journal of Colloid and Surface Science*,308, 53-70, 2007.

CHAPTER 3 BACTERIAL LEACHING OF IRON FROM HEMATITE: DIRECT OR INDIRECT INTERACTION

3.1 Introduction

In chapter 2, the elution mechanism was demonstrated, however, the possible mechanism of the iron elution via bacterial activity is still unclear. To clarify this mechanism, we proposed two systems on iron elution especially focusing on the contact condition of hematite and bacteria. The first system is based on the study in chapter 2, where *E. oxidotolerans* directly interact with the hematite surface. This system is illustrated in Fig.3-1(a), in which *E. oxidotolerans* directly gives electron to Fe(III)-oxide to reduce Fe(III) into soluble Fe(II) form. Fig.3-1(b) illustrated the second system, indirect interaction. In this system, bacterial metabolite, oxalic acid, should pass through dialysis membrane and give electron to the Fe(III)-oxide. In this scenario, Fe(III) dissolution occur mainly because of interaction between organic acid and hematite (Care et al., 2015). Lee reported the reaction showing oxalic acid forms the complexation with hematite to convert to eluted form (Lee et al.,2007). This reaction would occur via the oxidation of oxalic acid give the electron to Fe(III)-oxide which would reduce and form as Fe(II)-oxalate. Therefore, dissolution reaction could be summarized as below:

$$H^+ + Fe_2O_3 + 5HC_2O^-_4 \longrightarrow 2Fe(C_2O_4)_2^{2-} + 3H_2O + 2CO_2$$

However, they also reported iron oxide dissolution via oxalate complexation observed at the optimum pH 2.5-3.0 (Lee et al., 2007). In the present study, we focus on the dissolution in alkaline condition. This hypothesis should be investigated. We reported the examination and discussion in this chapter.

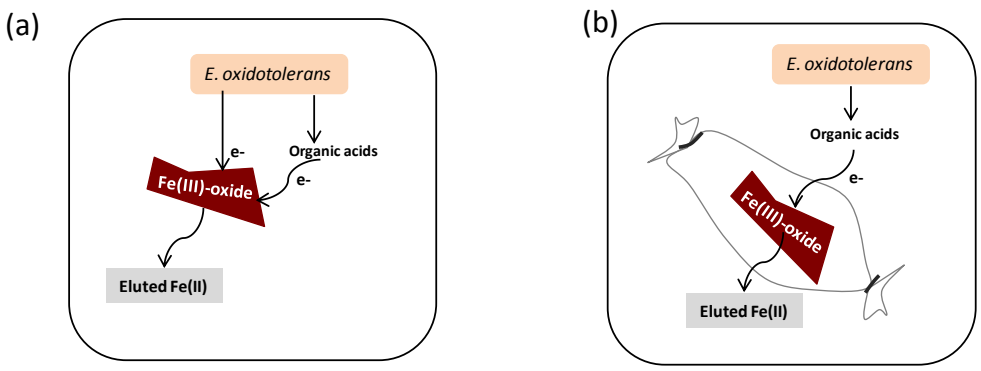

Fig. 3-1 Experimental systems and hypothesized mechanism of iron elution; (a) Direct and (b) Indirect interaction

3.2 Objectives

In previous chapter, we reported that bacteria activities might play an important role on hematite elution in seawater condition. In this chapter, we investigated interaction between bacteria cells and hematite surface, one is direct interaction system, and another is indirect interaction, where bacteria and hematite are separated by dialysis tube.

3.3 Materials and Methods

3.3.1 Preparation of bacteria culture

Artificial seawater was prepared by dissolving the following reagents in 1 L of distilled water: NaCl 28 g; $MgSO_4 \cdot 7H_2O$ 7.0 g; $MgCl_2 \cdot 6H_2O$ 4.0 g; $CaCl_2 \cdot 2H_2O$ 1.47 g; and KCl 0.7 g. The modified Postgate's B medium was prepared by dissolving the following components in a 1 L mixture of distilled water/artificial seawater (1:1, v/v): NaCl 26 g; KH_2PO_4 0.5 g; NH_4Cl 1.0 g; Na_2SO_4 1.0 g; $CaCl_2 .2H_2O$ 0.1g; $MgSO_4 \cdot 7H_2O$ 2.0 g; sodium lactate (60 - 70%) 5 mL; yeast extract 1.0 g; L-ascorbic acid 0.1 g and $FeSO_4 \cdot 7H_2O$ 0.5 g; the pH was 8.0±0.2. The medium was sterilized by autoclaving at 121°C for 20 min[7]. Plate Count Agar (PCA) medium was prepared dissolving the

following components in 1 L of distilled water: peptone bacteriological 5.0 g; protease peptone 5.0 g; L-cysteine 0.25 g; NaCl 5.0 g; ammonium iron (III) citrate 1.0 g; K_2HPO_4 0.3 g; and agar 15.0 g. The pH of the PCA medium was adjusted to 7.4 ± 0.2, and was sterilized by autoclave (121°C, 20 min) before use. Glycerol stocks of *E. oxidotolerans* were enriched with Postgate's B medium at 20.0±0.5 °C in an incubator shaking at 120 rpm for 5 days to obtain cell density at 10^8 cells mL^{-1}. Then 50 µL aliquot was plated into PCA agar plate for colony isolation. After 5 days of incubation, orange-pale colonies were selected to enrich in Postgate's B medium as main culture for the elution test. The preparation of bacteria culture followed from our previous study in chapter 2.

3.3.2 Direct or indirect elution of Fe ions from hematite by bacteria

The 30 mL of Postgate's B media were transferred to 50 mL centrifugal tube. The 150 µL of culture solution has been added to the tube, followed by addition of 0.15 g of hematite powder for direct elution. In indirect elution system, hematite powder was introduced into a dialysis tube (MWCO: 12000 - 14000 Da, Japan Medical Science, Japan) instead of direct expose to bacteria cells. The investigation was done for 10 days. To confirm the effect of metabolites on the dissolution of hematite, similar experiment with direct elution was conducted using mixture of organic acids, contained oxalic, acetic, citric and lactic acids, with hematite. The amounts of organic acids mixture were decided from the highest concentration of organic acids production which was detected at the same day of incubation as the detection of the highest eluted iron concentration, from chapter 2 (Table 3-1). Hematite elution with only medium was investigated as negative control. Four cases were investigated as shown in Table 3-2 and were incubated at 20±0.5 °C in an incubator at 160 rpm for 10 days. The dynamics of the oxidation-reduction potential (ORP) of the media were measured with an ORP meter (TOA-DKK, Japan) during the 10 days of incubation.

Table 3-1 Organic acids concentration for investigation of organic acid to hematite dissolution

Organic acid	Concentration (mg L^{-1})
Oxalic acid	11300
Citric acid	11
Lactic acid	230
Acetic acid	75

Figure 3-2 show the elution system, comparison between direct elution(a) and indirect elution(b).

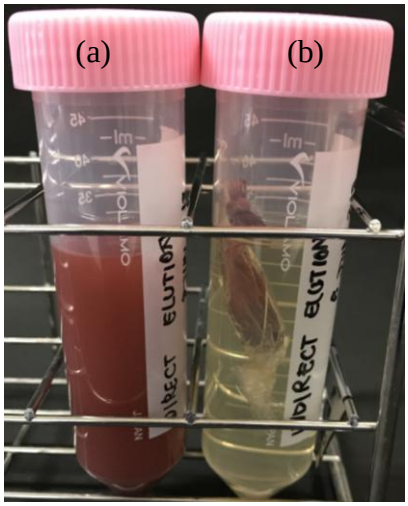

Fig. 3-2 The iron elution test (a) direct elution and (b) indirect elution

Table 3-2 The reaction mixture composition

Composition	Direct	Indirect	Organic acid addition	Hematite only
Postgate's B (mL)	30	30	30	30
E. oxidotolerans (mL)	0.15	0.15	Mixture of organic acid as show in Table3-1	
Hematite (g)	0.15	0.15	0.15	0.15

3.3.3 Quantification of iron by ICP and ferrozine analysis

After 0, 1, 3, 5, 7 and 10 days of incubation, a 1.2 mL aliquot of culture suspension was transferred to a 2 mL centrifugal tube and then centrifuged at 6500 rpm for 10 min. After centrifuge, it was filtered with a 0.45µm membrane filter. A 1 mL aliquot of the filtrate was transferred to a polyethylene tube and diluted to 10 mL with 0.01 M HCl to preserve Fe in the solution. The total iron concentration was analyzed with an ICPE-9000 type ICP-AES (Shimadzu, Japan) (Nishimoto et al., 2013).

The concentrations of Fe(II) species in the media were colorimetrically determined with ferrozine as an indicator of Fe(II). A 0.05 mL aliquot of 0.05 mM ferrozine was added to a 1 mL aliquot of media was centrifuged and filtered (0.45 µm). After 30 min of incubation, the concentration of Fe(II) species was determined based on the concentration of Fe(II)-ferrozine complexes by measuring the absorbance at 562 nm (Iwai et al., 2013).

3.3.4 Ion Chromatography analysis for organic acid production

1 mL aliquot of culture solution was transferred to the centrifugal tube then centrifuged at 6500 rpm for 10 minutes. The supernatant of aliquot was filtered through 0.45 µM membrane filter and then transferred to the HPLC vial. Mixture of oxalic, lactic and acetic acid (at 1, 2, and 3 ppm) were used as standard organic acids. The concentration of organic acids were analyzed by IC20-type Ion Chromatography (Thermo Fisher Scientific, USA) equipped with Dionex^{TM} IonPac®ICE-AS6 column (Thermo Fisher Scientific, USA). The regenerant was 1.5 mM Tetrabutyl ammonium hydroxide (TBAOH) and eluent was 1mM of Heptafluorobutyric acid. The flow rate was set at 0.80 mL min^{-1}, background conductivity was in the range of 45 - 50 µS, backpressure at 550-600 psi.

3.3.5 Analysis of treated hematite

Hematite slurry cultured for 30 days of incubation was transferred into a dialysis tube and dialyzed against ultrapure water. After dialyzed, the slurry was freeze-dried to obtain powdered sample. The samples were sputtered with Pt ion at ion current 10 mA by JFC-110E ion sputtering machine (JEOL, Japan) for 60 second before observation.

The Fourier transform infrared (FTIR) spectroscopy, 6200HFV (Jasco, Japan) equipped with attenuated total reflectance (ATR) extension ATR-pro one (Jasco, Japan) with view-through diamond prism to observe the hematite surface alteration. Spectra were obtained via spectra manager program (Jasco, Japan).

The Scanning electron microscope with energy dispersive X-ray Spectroscopy (SEM-EDS, JSM-IT 200 InTouchScope™, JEOL, Japan) was used to observe the elemental composition of C, N, O and Fe on the hematite surface.

3.4 Results and discussion

3.4.1 Characterization of incubation medium comparison between direct and indirect elution

(a) Elution of Fe

Figure 3-3 shows the total iron concentration in culture solution in all the four cases. The total iron concentration the concentration was below detection limit at the beginning of the incubation and increased to 30.57 mg L^{-1} at the end of incubation in direct elution (Fig.3-3a). On the contrary, negligible iron concentration was monitored for indirect elution, organic acids addition and negative control. The Fe^{2+} concentration was almost similar to that of total iron concentration (Fig.3-3b). The direct elution gave the increase of Fe^{2+} concentration with a finally of 7.389 mg L^{-1}. The significant difference in iron concentration between direct and other systems suggest that direct interaction of the

bacteria cell with hematite affects iron elution. The contact surface area between bacteria and hematite probably assist increasing microbial reduction and generation high amount of eluted Fe(II) (Roden et al., 1996). The eluted Fe(II) could possibly serve as metabolites for the bacteria consequently assist in bacterial metabolism to produce more metabolites into the system (Lovley et al., 1988 and Arnold et al., 1988).

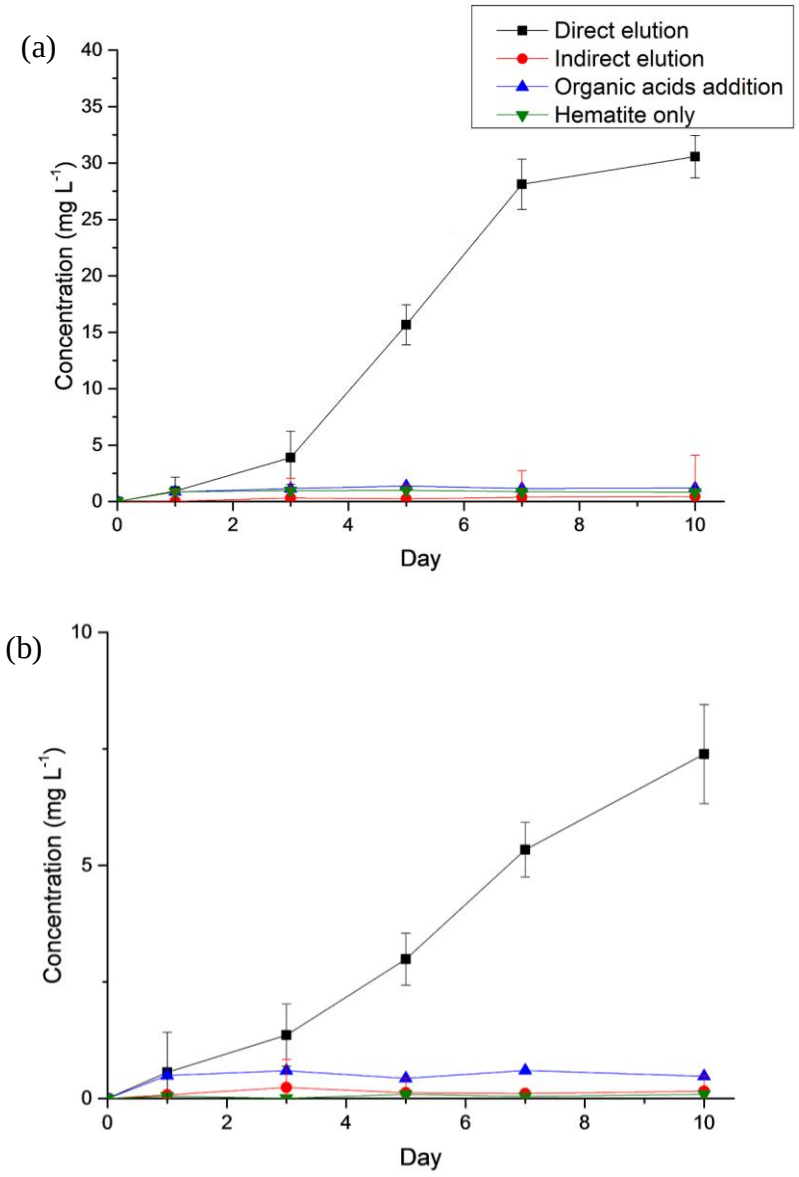

Figure 3-3 Iron elution comparison between direct and indirect elution; (a) Total iron and (b) Ferrous ion

3.4.2 Physicochemical analysis of culture solution

Physicochemical properties of cultured solution were daily monitored for pH and ORP. The pH decrease might have affected amount of iron elution (Fig.3-4(a). During the 10 days of incubation, pH values in direct and indirect system decreased in two days from pH around 7.4 at the beginning. The decrease of both direct and indirect elution should be probably because bacteria activity produces the organic acids which lowered the pH value in the system. In the organic acids addition system, pH was the lowest of all samples at around 6.8-7 and remained constant throughout the experiment. The hematite only system shows the highest pH value at 7.8 and remained constant throughout the experiment too.

Fig.3-4(b) shows the ORPs value. The ORP of direct elution showed more significant decrease compared to that of indirect elution. Figure 3b showed that in organic acids addition system, ORP was lower than that in direct and indirect elution test at the beginning of incubation. The difference of the ORPs between direct and indirect interaction might due to the higher activity of bacteria in the direct interaction. In direct interaction, bacteria might give electron to hematite to reduce into eluted Fe(II) form this phenomenon would lead to lower amount of ORP value. The ORP was almost stable during the monitoring time in organic acids additional system. The negative control, ORP was the highest at the oxidative phase and remained almost stable. The ORPs monitoring showed that microorganism activities might influence the decrease of ORPs in both direct and indirect elution. The reduction in both chemical profiles supported the iron elution data. The decrease of pH and ORP were preferable to the dissolution of iron by *E. oxidotolerans*, especially in direct interaction which ORP reached to the -300mV (Apichaya et al., 2018).

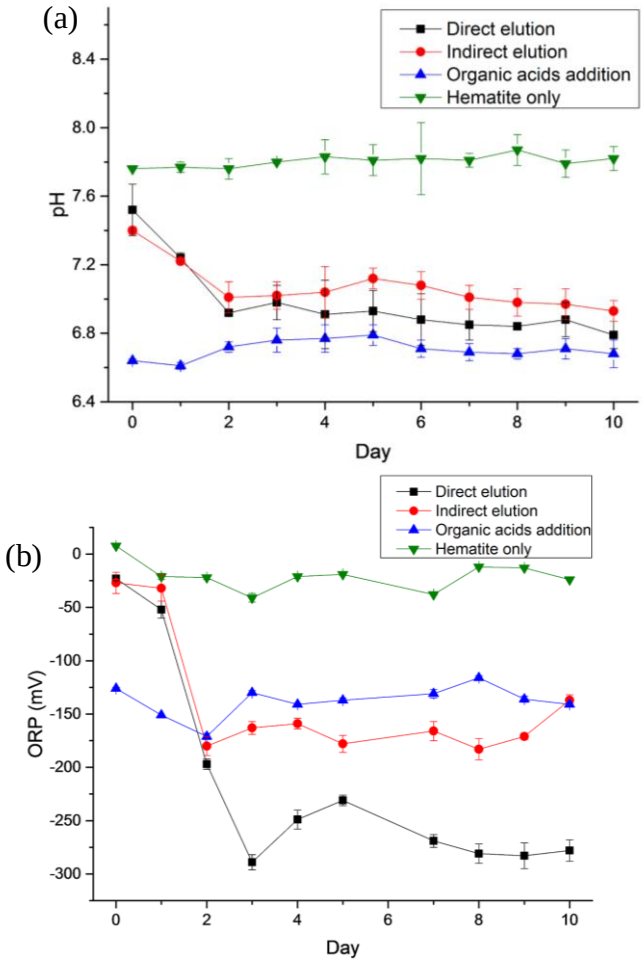

Figure 3-4 Characteristic of culture solution; (a) pH and (b) ORPs

3.4.3 Organic acids production

Organic acids production was monitored during 10-day of incubation (Fig. 3-5). As we reported in chapter 2, oxalic acid and lactic acid are initially included in the Postgate's B medium. Figure 3-5(a) to 3-5(c) show oxalic, acetic and lactic acid production, respectively. However, bacteria in the direct elution produced higher amount of oxalic acid and reached the highest at 2199.47 mg L^{-1} while indirect interaction gave the concentration of 1986.76 mg L^{-1} (Fig. 3-5(a)). Figure 3-5b shows the concentration of acetic acid at the end of incubation at 4.67 and 2.05 mg L^{-1} for direct and indirect interaction respectively. The acetic acid production is relatively low, which is consistent with our previous study in chapter 2. Oulkadi et al., reported that both oxalic acid and acetic acid might provide the electron to reduce Fe(III) into Fe(II) (Oulkadi et al., 2014). However, the trace amount of

acetic acid detected in both systems could not affect Fe elution. Figure 3-5(c) also shows the higher lactic acid production in direct sample of 149.85 mg L^{-1} and lower production in indirect sample of 115.95 mg L^{-1}. At the beginning stage of incubation, lactic acid concentration was detected at relatively high concentration because sodium lactate is the component in medium solution. This is the reason why we could observe the high amount of lactic acid at the beginning of both systems.

The different amount of oxalic acid production between direct and indirect interaction might depend on the expose of bacteria cells to hematite surface. There are some evidences show that iron oxide containing condition could facilitate bacteria growth and metabolism (Roden et al., 1996, Hersman et al., 2001, Appenzeller et al., 2005, Lentini et al., 2012 and Weber et al., 2006). The trace amount of eluted Fe(II) could act as nutrient to the bacteria. This might be the reason for increase the production of bacterial metabolites (Roden et al., 1996 and Appenzeller et al., 2005). Oxalic acid also a key role to dissolve iron oxides in alkaline condition (Al-Mobarak et al., 2008, Borghi et al., 1996, Blesa et al., 1987 and Panias et al., 1996, Oulkadi et al., 2014). When the system contained both eluted Fe(II) and oxalic acid, the eluted Fe(II) act as metabolite to the bacteria. The bacteria would have high activity to produce organic acid (e.g., oxalic acid). The oxalic acid that highly produced could help to stabilize Fe(II) to remain as eluted Fe(II) in the system. This also might be one of the reasons that in direct interaction showed high amount of eluted Fe(II).

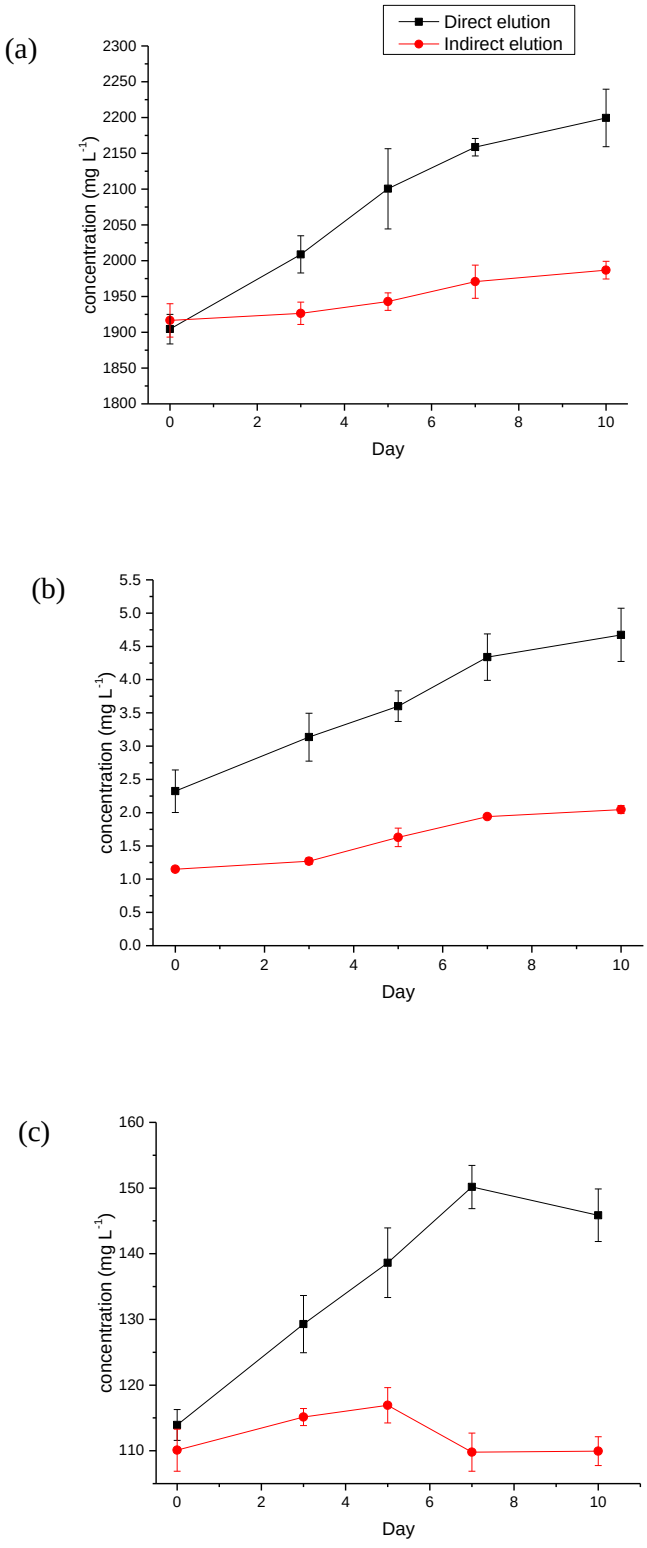

Fig. 3.5 The organic acid production during 10-day incubation; (a) oxalic acid, (b) acetic acid and (c) lactic acid.

3.4.4 Hematite surface analysis

(a) FE-SEM

The hematite surface observation after 10 days elution for direct and indirect interaction show in Fig.3-6a and 3-6b, respectively. Hematite particle aggregation was observed in indirect interaction test more than loose formation in the direct interaction. The dispersion of hematite in direct interaction might occur due to direct interaction of bacteria cell to the hematite surface which required the electron transfer via the cytochrome system (Schroder, 2007, Pankratova et al., 2018, Kato et al., 2012, Rosso et al., 2003 and Kato et al., 2015).

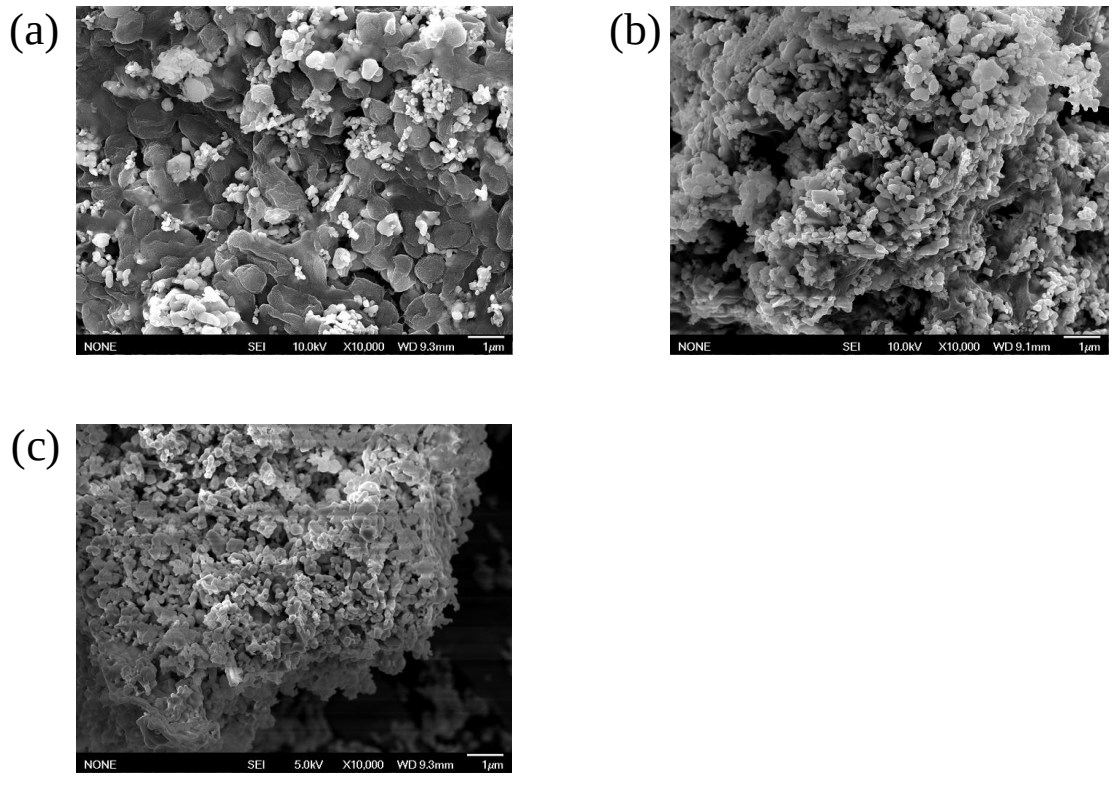

Fig. 3-6 FE-SEM image of (a) direct elution, (b) indirect elution, and (c) untreated hematite

(b) ATR-FTIR

Comparison of ATR-FTIR spectra of hematite between direct and indirect interaction show in Figure 3-7. In direct interaction specific peak appeared around 1220-1250 (cm^{-1}), indicating PO_2^- asymmetric stretching vibration and P-OH bending vibration (Blesa et al., 1987). The attributed peak for Fe-P-O complexation appeared around the group frequency at 1033-1085 (cm^{-1}) (Cagnasso et al., 2010 and Elzinga et al., 2007). This could indicate for bacteria cell attached to hematite. The formation of iron-phosphate might be one of the evidences to detect the elution of iron in the direct interaction system (Elzinga et al., 2007, Arai et al., 2001 and Spiteri et al., 2008). The appearance of amino acid functional group around 1590-1680 (cm^{-1}) for primary amine (NH bend) and group frequency around 1550 (cm^{-1}) for secondary amine (NH-bend) (Cagnasso et al., 2010, Elzinga et al., 2007, Arai et al., 2001 and Coates, 2000), also detected only in direct interaction. These two amino acids related peaks suggested to the bacteria cell adsorb/attach to the hematite surface corresponded to bacteria cell interaction with iron (Coates, 2000). No clear peak was observed in indirect interaction.

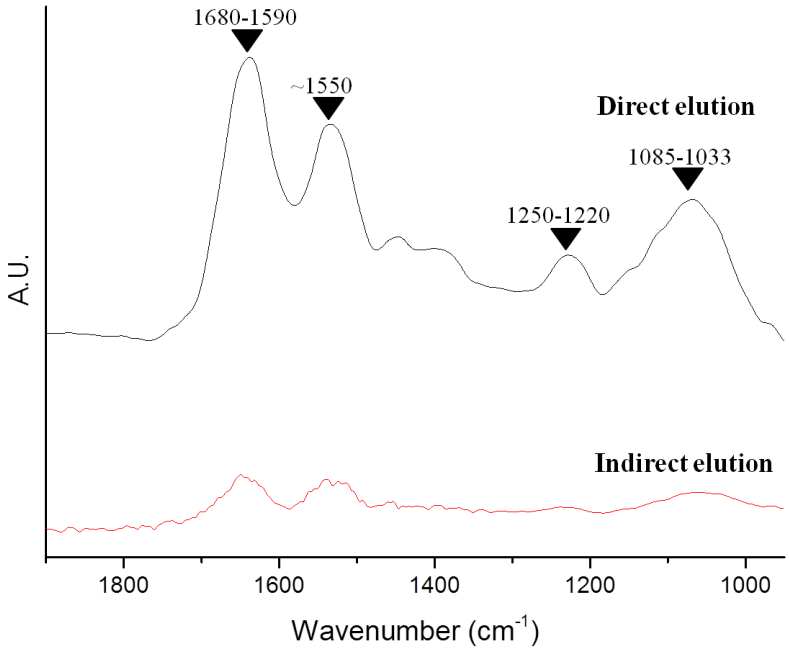

Figure 3-7 ATR-FTIR chromatogram of hematite comparison between two interaction systems

(c) SEM-EDS

SEM-EDS was observed for the elemental composition at the hematite surface after treated with culture solution show in Table 3-3. In direct interaction, iron mass percentage relatively low compared to other systems. Composition of Nitrogen indicated for amino acid group from bacteria cells was observed only in direct interaction. Composition of carbon also higher in the direct interaction which might referred to production of metabolites during the culture period. Composition of phosphorus indicated phosphate groups from bacteria cell can detected in direct interaction. This composition should have come from bacteria cell attached to hematite surface. However, indirect and organic acid addition systems also show trace amount of phosphorus, these detection might come from the composition of Postgate's B medium which might not fully dialysed from the dislysis process during the material preparation. From the elemental composition data as a supportive to FTIR spectrum, we could confirmed that bacteria cell attached to the hematite surface in direct interaction system.

Table 3-3 The elemental composition from elemental mapping, comparison between four interaction systems

Mass %	Direct	Indirect	Organic acid addition	Hematite
C	45.68±3.67	23.55±1.97	40.35±2.96	15.63±2.70
N	10.58±7.13	n.d	n.d	n.d
O	2.48±2.70	2.58±1.94	4.64±4.10	1.15±2.58
P	4.12±3.74	1.03±3.89	0.92±2.45	n.d
Fe	37.84±27.28	66.87±27.01	54.02±36.11	83.22±67.79

*n.d = not detected

Figure 3-8(a-d) show the elemental mapping position for elements in each samples on the treated hematite surface. For direct interaction (Fig.3-8(a)), shows some amounts of phosphorus(P) and nitrogen(N) indicated for bacteria cell/amino acid at the hematite surface. For other three analysis

system (Fig.3.8(b)-(d)), also revealed the relative amounts between elemental composition data (Table 3-3) and the elemental colored mapping data(Fig.3-8)). We could confirmed that This SEM-EDS observation is one of the evidences show bacteria interaction to the hematite surface.

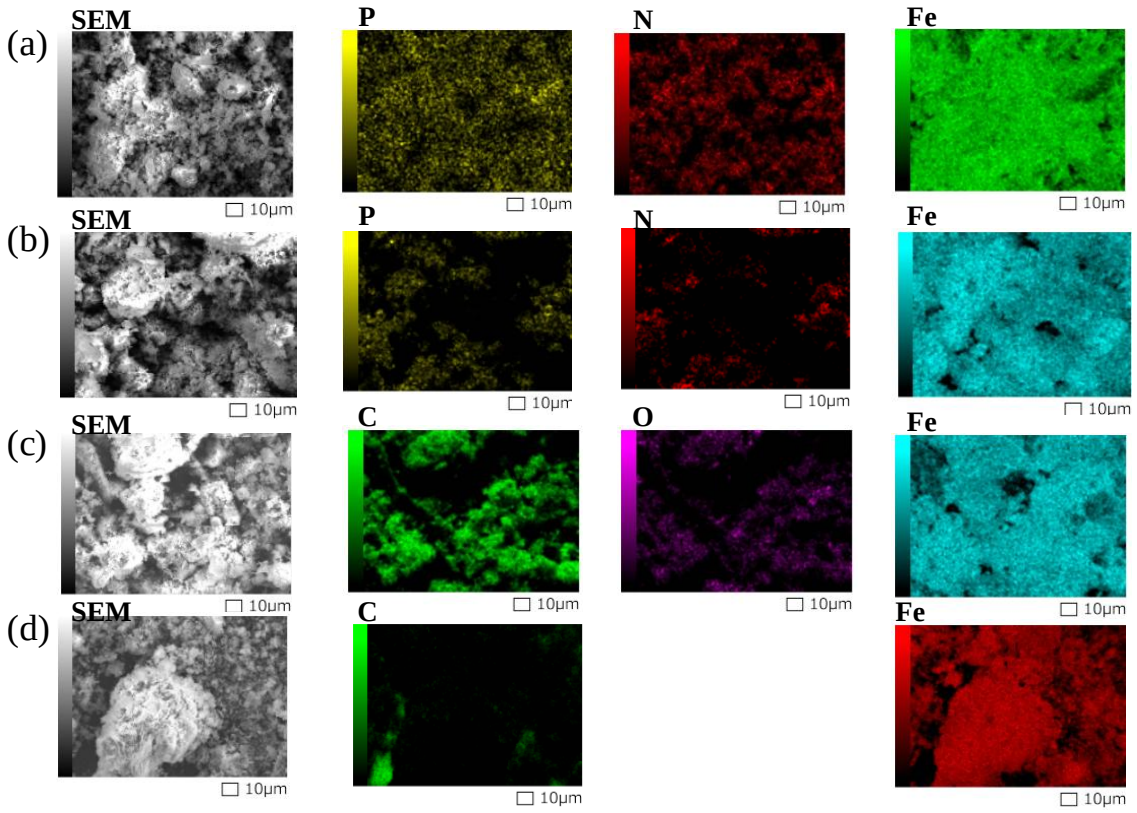

Fig. 3-8 the elemental mapping of hematite surface after incubation (a) direct interaction, (b) indirect interaction, (c) organic acid addition, and (d) hematite only

3.4.5 Possible mechanism of bacterial influence in iron elution in seawater

The amount of iron concentration during the incubation showed significantly different between two interaction systems. Direct interaction between hematite and cell surface could have had a major contribution to iron elution rather than indirect hematite surface interaction. The effect of direct interaction-reduction between hematite and microbial cells via electron transfer has been reported (Kato et al., 2012, Rosso et al., 2003 and Lovley, 2017). The microbial electron transfer

between bacteria cell and solid materials has been reported and could called as extracellular electron transfer (EET) (Schroder, 2007, Pankratova et al., 2018, Kato et al., 2012, Rosso et al., 2003, Kato, 2015, Lovley, 2017 and Kostka et al., 1995). EET is a type of microbial metabolic process which required electron transfer between microbial cells and extracellular solid material (Kato, 2015 and Kerisit et al., 2007). The Model organism has been investigated in direct EET which microorganisms attach to solid surfaces and then directly transfer electrons (Kato, 2015, Castelle et al., 2008, Shi et al., 2007 and Weber et al., 2006). The c-type cytochrome could have played an important role in direct EET. The electron transferred from inner to outer membrane via electron hopping through multiple redox-active proteins (cytochrome) that connected microbial respiratory chains and external surfaces (Kato, 2015). The possible mechanism in direct interaction might occurred via bacteria cell attached and directly gave electron to hematite surface which acted as terminal electron acceptor in the system (Fig.3-9). The higher oxalic acid and Fe(II) concentration would also cooperated in the higher amount of iron dissolution in direct interaction. Based on this study, when bacteria cell could not directly contact to hematite surface, the reduction of hematite into eluted Fe(II) might occurred in lower rate and concentration. Therefore, the reduction of Fe oxide in indirect system would depend solely on the metabolites of bacteria which produced lowered than that in direct elution. The bacterial activities also reduced when the bacteria cannot utilize Fe(III)/Fe(II) as one of metabolisms sources (Roden et al., 1996, Lentini et al., 2012, Kato et al., 2012 and Rosso et al., 2003).

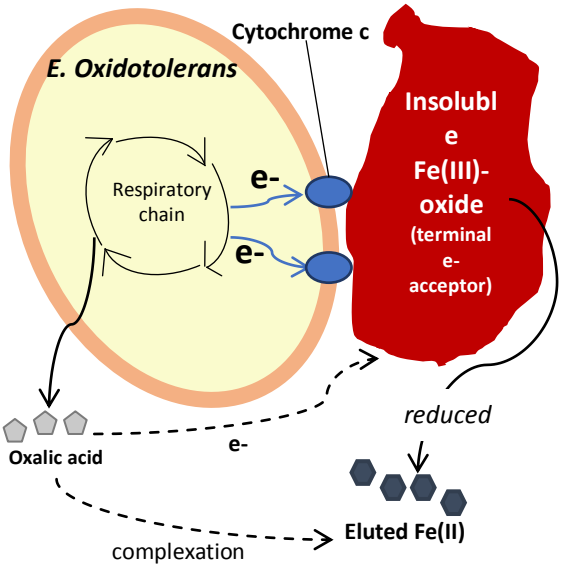

Fig.3-9 Hypothesis of Fe(II) elution in the direct system : *E. oxidotolerans* give electron from the e-shuttle transport in the respiratory system to Fe(III)-oxide(hematite) which reduced to eluted-Fe(II)

3.5 Conclusions

The interaction between bacteria cell to hematite surface shows the majority cooperation in the elution of hematite from Fe(III) oxide to Fe(II) in alkaline condition. The iron elution was detected only in direct interaction. The monitoring of oxalic acid production also presented in higher concentration in direct interaction compare to indirect interaction. In addition, the chemical profile which preferable to iron elution was observed mainly in the direct interaction system. Surface analysis also showed the alteration and scattering of hematite particles only in direct interaction. Especially, the evidence for bacteria attached to the hematite surface. From all the evidence, we proposed the hypothesis which demonstrated in Fig.3-8 that direct interaction between bacteria cell to surface of hematite performed a major role in the reduction of hematite to eluted- Fe(II).

Reference

[1] K. Matsunaga, T. Kawaguchi, Y. Suzuki, and G. Nigi, The role of terrestrial humic substances on the shift of kelp community to crustose coralline algae community of the southern Hokkaido Island in the Japan Sea, J. Exp. Mar. Biol. Ecol. 241, 193-205, 1999.

[2] T. Motomura and Y. Sakai, Regulation of gametogenesisi of *Laminaria* and *Desmrestia* (Pheaophyta) by iron and boron, Jpn. J. Phycol. 32, 209-215, 1984.

[3] Y. Suzuki, K. Kuma, I. Kudo, and K. Matsunaga, Iron requirement of the brown macroalgae Laminaria japonica, Undaria pinnatifida (Phaeophyta) and the crustose coralline alga Lithophyllum yessoense (Rhodophyta), and their competition in the northern Japan Sea, Phycologia 34, 201-205, 1995.

[4] H. Iwai, M. Fukushima and T. Motomura. Effect of iron complexes with seawater extractable organic matter on oogenesis in gametophytes of a brown macroalga (*Saccharia japonica*). *Journal of Applied Phycology*, 27, 1583-1591, 2015.

[5] M. Boye, C.M.G. van der Berg, J.T.M. de Jong, H. Leach, P. Croot and H.J.W. de Baar. Organic complexation of iron in the Southern ocean. *Deep Sea Research Part I*, 48, 1477-1497, 2001.

[6] A.L. Rose, T.D. Waite. Role of superoxide in the photochemical reduction of iron in seawater. *Geochimica et Cosmochimica Acta*, 70, 3869-3882, 2006.

[7] A. Care, P.L. Bergquist and A. Sunna. Solid-binding peptides: smart tools for nanobiotechnology. *Trends in Biotechnology*, Vol.33 No.5, 259-268, 2015

[8] S.O. Lee, T. Tran, B.H. Jung, S.J. Kim and M.J. Kim. Dissolution of iron oxide using oxalic acid, Hydrometallurgy, 87, 91 – 99, 2007.

[9] E.E. Roden and J.M. Zachara. Microbial Reduction of Crystalline Iron(III) Oxides: Influence of Oxide Surface Area and Potential for Cell Growth. Environmental Science Technology, 30, 1618-1628, 1996.

[10] D.R. Lovley and E.J.P. Phillips. Novel Mode of Microbial Energy Metabolism: Organic Carbon Oxidation Coupled to Dissimilatory Reduction of Iron or Manganese, Applied and environmental microbiology, 54, 1472-1480, 1988.

[11] R.G. Arnold T.J. DiChristina and M.R. Hoffmann, Biotechnol. Bioeng, 32, 1081-1096, 1988.

[12] L.E. Hersman, J.H. Forsythe, L.O. Ticknor and P.A. Maurice, Growth of *Pseudomonas mendocina* on Fe(III) (Hydr)Oxides , Appl. Environ Microbiol, 67, 4448-4453, 2001.

[13] B.M.R. Appenzeller, C. Yanez, F. Jorand and J. Block, Advantage Provided by Iron for *Escherichia coli* Growth and Cultivability in Drinking Water, Appl. Environ. Microbiol, 71, 5621-5623, 2005.

[14] C.J. Lentini, S.D. Wankel and C.M. Hansel, Enriched iron(III)-reducing bacterial communities are shaped by carbon substrate and iron oxide mineralogy, Front Microbiol, 3, 1-19, 2012.

[15] K.A. Weber, L.A. Achenbach and J.D. Coates, Microorganisms pumping iron: anaerobic microbial iron oxidation and reduction, Nat. Rev. Microbiol, 4, 752-764, 2006.

[16] N.A. Al-Mobarak, Chemical and Electrochemical Investigations of L- Arginine as Corrosion Inhibitor for Steel in Hydrochloric Acid Solutions, Int. J. Electrochem. Sci, 3, 666-675, 2008.

[17] E.B. Borghi, S.P.Ali, P.J., Morando and M.A. Blesa, Cleaning of Stainless Steel Surfaces and Oxide Dissolution by Malonic and Oxalic acids, J. of Nuclear Materials, 229, 115-123, 1996.

[18] M.A. Blesa, H.A. Marinovich, E.C. Baumgartner and A.J.G Maroto, Mechanism of Dissolution of Magnetite by Oxalic Acid-Ferrous Ion Solutions, Inorg. Chem., 26, 3713-3717, 1987.

[19] D. Panias, M. Taxiarchou, I. Paspaliaris and A. Kontopoulus, Mechanisms of dissolution of iron oxides in oxalic acid solutions, Hydrometallurgy, 42, 257-265, 1996.

[20] M. Cagnasso, V. Boero, M.A. Franchini and J. Chorover. ATR-FTIR studies of phopholipid vesicle interactions with α-FeOOH and α-Fe_2O_3 surfaces. *Colloids and Surfaces B : Biointerfaces*,76, 456-467, 2010.

[21] E.J Elzinga and D.L Sparks. Phosphate adsorption onto hematite: An in situ ATR-FTIR investigation of the effects of pH and loading level on the mode of phosphate surface complexation. *Journal of Colloid and Surface Science*,308, 53-70, 2007.

[22] Y. Arai and D.L Sparks, ATR–FTIR Spectroscopic Investigation on Phosphate Adsorption Mechanisms at the Ferrihydrite–Water Interface, J. Colloid Interfac. Sci, 241, 317–326, 2001.

[23] C. Spiteri, Surface complexation effects on phosphate adsorption to ferric iron oxyhydroxides along pH and salinity gradients in estuaries and coastal aquifers, Geochim. Cosmochim. Acta.,72, 3431–3445, 2008.

[24] J. Coates. Interpretation of infrared spectra, A practical approach. *Encyclopedia of Analytical Chemistry*, John Wiley & Sons Ltd, 10815-10837, 2000.

[25] U. Schroder, Anodic electron transfer mechanisms in microbial fuel cells and their energy efficiency, Phys. Chem. Chem. Phys., 9, 2619-2629, 2007.

[26] G. Pankratova, D. Leech, L. Gorton and L. Hederstedt, Extracellular Electron Transfer by the Gram-Positive Bacterium *Enterococcus faecalis*, Biochemistry. 57, 4597-4603, 2018.

[27] Kato, S., Hashimoto, K. & Watanabe, K. Methanogenesis facilitated by electric syntrophy via (semi)conductive iron-oxide minerals. Environ. Microbiol. 14, 1646–1654, 2012

[28] K.M. Rosso, J.M. Zachara, J.K. Fredrickson, Y.A. Gorby and S.C. Smith, Nonlocal bacterial electron transfer to hematite surfaces, Geochim. Cosmochim. Acta.,67, 1081-1087, 2003.

[29] S. Kato, Biotechnological Aspects of Microbial Extracellular Electron TransferMicrobes Environ., 30, 133-139, 2015.

[30] D.R. Lovley, Syntrophy Goes Electric: Direct Interspecies Electron Transfer, Annu. Rev. Microbiol, 71, 643-664, 2017.

[31] J.E. Kostka and K.H. Nealson, Environ. Sci. Technol, 29 (1995), 2535-2540. J.E. Kostka and K.H. Nealson, Dissolution and Reduction of Magnetite by Bacteria, Environ. Sci. Technol, 29, 2535-2540, 1995.

[32] S. Kerisit, K.M. Rosso, M. Dupuis and M Valiev, Molecular Computational Investigation of Electron-Transfer Kinetics Across Cytochrome-Iron Oxide Interfaces, J. Phys. Chem, 111, 11363–11375, 2007.

[33] C. Castelle, M. Guiral, G. F. Ledgham, G. Leroy, M.Brugna and M.T. Giudici-Ortconi, J. Biol. Chem, 283, 25803-25811, 2008.

[34] L. Shi, H. Dong, G. Reguera, H. Beyenal A. Li J. Liu, H.Q. Yu and J.K. Fredrikson. Extracellular electron transfer mechanisms between microorganisms and minerals. Nature review, Microbiology, 14, 651-662, 2016.

[35] K.A. Weber, L.A. Achenbach and J.D. Coates, Microorganisms pumping iron: anaerobic microbial iron oxidation and reduction, Nat. Rev. Microbiol, 4, 752-764, 2006.

CHAPTER 4 PERFORMANCE IMPROVEMENT FOR BACTERIA ABSORPTION ONTO HEMATITE SURFACE

4.1 Introduction

In chapter 3, we examined bacteria cell interaction onto the hematite surface using wild-type bacteria. Based on the result in chapter 3, direct interaction between bacteria and hematite surface played a significant role in electron transfer to reduce insoluble-Fe(III) to eluted-Fe(II). Efficient and active adsorption of bacteria cells to hematite surface might lead to improvement in iron dissolution. The results from this investigation lead us to study bacteria as a tool in our study for Fe elution which is environmentally sustainable. Initially, we investigate the role of bacteria in eluting iron into seawater. This condition contained some difficulty to overcome. Our previous study revealed the importance and the possibility that bacterial interaction to hematite surface impacted on a large amount of eluted iron in seawater condition. This finding lead us to using this bacterial as a biological- tool.

Since bacteria cells should be important for their interaction to the iron oxide surface, molecular level scale investigation should be able to observe this phenomenon. Richter et al.(2012) reported the important role of the close contact between bacteria cell to the iron oxide surface, the direct electron transfer can occur via the outer membrane of bacteria to the extracellular ferric oxide minerals. Figure 4-1 show the electron transfer pathways from the respiratory chain of bacteria carried out via the outer membrane of *S. oneidensis* to reduce ferric to ferrous (Richter et al., 2012). This phenomenon should relatively occur in the electron transfer pathway of our isolated bacteria *E. oxidotolerans* T-2-2 to reduce iron oxide in to elution form in the iron elution test.

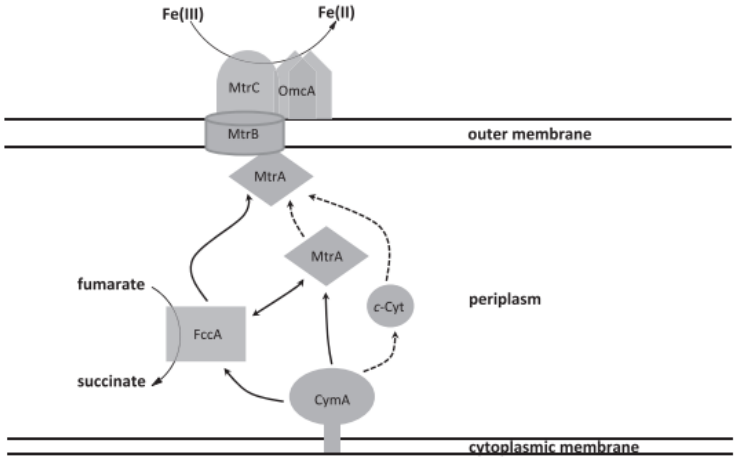

Fig. 4-1 Proteins involved in the extended respiratory chain in *Shewanella oneidensis*. Proven electron transfer pathways are shown with solid arrows, speculative pathways with dashed arrows. Other periplasmic c-type cytochromes that might have a role in electron transfer are displayed as ovals, c-Cyt, c-type cytochromes (Richter et al., 2012).

In order to understand the interaction between biological surface and hematite, we investigate the potential use of solid-binding peptides (SBPs). The solid binding peptides has been on the spotlight for over a decade (Care et al., 2015). Such kinds of specific peptide can be used potentially improve or control many biocompatible materials which could be more environmentally friendly when its applied to the environmental system (Avvakumova et al., 2014, Sengupta et al., 2008). The SBPs are the short amino acid sequences that contain specific binding affinity for each material e.g. metals, metal oxides, minerals carbon materials of semiconductors (Care et al., 2016). The basic application in term of biotechnology SBPs has been introduced via genetic modification of microorganisms that contain the SBPs sequences. One of the appealing functions of SBPs is the ability for direct immobilize to the enzyme without any interferance to enzyme function (Johnson et

al., 2008; Kacar er al., 2009; Yang et al., 2011 and Cetinel et al., 2013). Yang et al., 2011 reported the usage of gold-binding peptide (GBP) direct assemble onto organophosphorus hydrolase (OPH). The performance of this modified enzyme contained higher sensitivity and activity compare to unmodified one. The discussed advantage motivated this study to investigate the properties of SBPs attachment to enhance the efficiency of bacterial function. In our study, Iron-binding peptide (IBP) was used to enhance the binding efficiency of bacteria cell to hematite surface to improve the elution of iron. The use of bacteria containing IBP should be useful in varieties field in the future.

To achieve the goal of this study *Esherichia coli* was used as a host by displaying the target peptide on the outer membrane protein of bacterial cell. The outer membrane of *E. coli* allows the target peptides to be displayed. The outer membrane protein A (OmpA) was selected as a carrier protein for the solid binding motif. (Tsai et al., 2015). The target iron-binding sequence was introduced to the OmpA loop three (L3) to carry the expression of binding peptide on the bacteria cell surface (Smith et al., 2007). Smith et al., (2007) reported the structure topological model of OmpA as shown in Fig. 4-2. In this chapter we selected 2 types of metal binding peptides; iron oxide-binding peptide (Brown 1992) and hematite-binding peptide (Zare-Eelanjegh et al., 2016) for the adsorption study. The adsorption efficiency to hematite surface was investigated in both two types of peptide sequences. This investigation could reveal the characteristic of IBP to the hematite surface. The conducted analysis we reported in this chapter could be useful in the future application for the engagement between bacteria and iron in the environmental system.

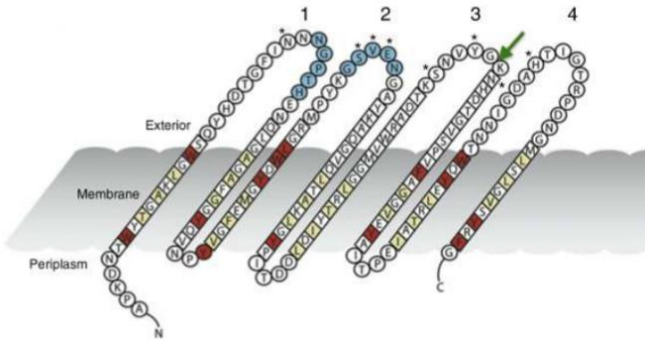

Fig. 4-2 Outer membrane protein A structure (Smith et al., 2007).

4.2 Objectives

In this chapter we investigated *E. coli* containing the iron-binding peptide expressed at the outer membrane protein A(OmpA) of the bacteria cells. This investigation aims to observe the behavior of the iron binding peptide chain expressed on *E. coli* cell surface effect to the adsorbing at the hematite surface. The study of two-peptide sequences were carried out to decide one that had high adsorption efficiency.

This chapter investigated the molecular mechanism between bacteria and hematite. The investigation was conducted using *E. coli* as model microorganisms containing IBP and evaluate its effect on iron elution.

4.3 Materials and Equipment

4.3.1 Materials

(a) Plasmid vector and host bacteria

pET-22b(+) vector was used as expression vector to carried target gene fragment. The host strain for plasmid amplification was *Escherichia coli* DH5α and *E. coli* BL21(DE3) was used as host in protein expression.

(b) Restriction enzymes and reagents for PCR

Restriction enzymes XhoI, NdeI and Cutsmart enzyme (Takara Bio Inc., Japan) were used linearized the pET22b vector. The overlap PCR was conducted into 2 steps. Both of PCR step used Primestar max DNA polymerase in the reaction. KAPA2G polymerase were used in colony PCR with T7 primer (forward and reverse).

(c) Solid materials for adsorption observation

Iron oxide, Titanium, Copper, Wolfram and Zirconium plate were cut down into 1×1 cm for absorption analysis. The surface of all materials has been smoothened.

(d) Gel electrophoresis and SDS-PAGE analysis

The agarose gel was prepared in 1xTAE buffer. The gel has been prepared into 2 concentrations, 1.5% for <1000 basepairs and 1% for >1000 basepairs. Midori green dye was used as staining agent for PCR products in a ratio of 10:1 ratio. The reference DNA ladder was also stained with Midori green at 5:1 ratio.

DNA and plasmid purification were conducted using a FastGene gel/PCR extraction kit (NIPPON Genetics Co.Ltd.) and FastGene Plasmid extraction kit (NIPPON Genetics Co.Ltd.), respectively.

(e) Adsorption investigation

The adsorption buffer used was Tris buffer (20mM) at pH 6.0, 7.0, 7.6, 8.0 and 9.0, acetate buffer (0.1M, pH 5.0). *E. coli* BL21(DE3) inserted with pET-22b(+) contained OmpA-IBP(1 and 2, separately) was used for the adsorption investigation. In this study, we named this bacterium as *E. coli* with pET-22b(+)-OmpA-IBP. For all negative control, *E. coli* contained pET-22b(+) was used.

4.4 Methodology

4.4.1 Primer design for iron-binding peptide gene (IBP)

Iron oxide binding peptide and hematite binding peptide sequence data show in Table 4-1 (Care et al., 2015, Zare-Eelanjegh et al., 2016). In this study, iron oxide binding peptide1 (IBP1) stand for iron oxide binding peptide and iron oxide binding peptide2 (IBP2) stand for hematite binding peptide.

Table 4-1 Iron oxide binding peptide sequence

Iron oxide binding peptide	Sequence	MW (Da)	Reference
IBP1	RRTVKHHVN	1146.32	Care et al., 2015
IBP2	STVQTISPSNH	1170.24	Zare-Eelanjegh et al., 2016

The primers were designed for infusion technique. We combined OmpA gene with IBP gene fragment. OmpA-IBP insert primer for both IBP1 and IBP2 has been designed as show in Table 4-2.

Table 4-2 Primer sequence for iron oxide binding peptide

Insert primer	Sequences (5'-3')
IBP1-Fw	CGCCGTACCGTGAAACACCATGTTAACGTTTATGGTAAAAACCACGA
IBP1-Rv	GTTAACATGGTGTTTCACGGTACGGCGGTTGGATTTAGTGTCTGCAC
IBP2-Fw	TCGACCGTGCAGACGATTAGCCCGAGTAACCATGTTTATGGTAAAAACCACGA
IBP2-Rv	ATGGTTACTCGGGCTAATCGTCTGCACGGTCGAGTTTATGGTAAAAACCACGA

4.4.2 Transformation of iron-binding peptide vector onto protein expression bacteria

Fusion gene technique was applied to construct the target gene (Nakashima et al., 2014). The plasmid pET-22b(+) was prepared by digesting with two restriction enzymes; XhoI and NdeI. The restriction enzyme treatment was as follows; pET-22b(+) 20 µL, XhoI enzyme 1.5µL, NdeI enzyme 1.5µL, CutSmart 5µL and distilled water 22µL then incubated at 37 °C for 15 minutes to obtain linear plasmid. The insert gene was constructed using overlap PCR technique. The schematic representation for the OmpA-IBP gene construction shows in Fig. 4-3. OmpA gene was prepared as negative control sample, the methodology from *E. coli* DH5α transformation to the protein expression was the same. The agarose gel contained target fragment was extracted the obtained the DNA fragment. After extracting the targeted gene the DNA fragment was then in-fused with linearized pET-22b(+) plasmid. The in-fusion composition as follows; linearized pET-22b(+) 5 µL,

in-fusion product (OmpA-IBP) 2µL, in-fusion enzyme 2µL and distilled water 1µL then incubated at 50 °C for 15 min. The in-fusion products were immediately transformed into *E. coli* DH5α cell with proportion; DH5α 30 µL: OmpA-IBP 1µL. The mixture was placed on to ice shock at 0 °C for 30 min then heat shock at 42 °C for 1 min and then on ice for 5 min. The final transformation products were grown at 37 °C in LB-AMP agar medium with 100 mg L^{-1} of ampicillin for 16-18 hours. The single colony appeared was selected to confirm the transformation by colony-PCR. After colony-PCR confirmation, selected colony was growth at 37 °C in 5 mL of LB liquid medium with 100 mg L^{-1} of ampicillin at 160 rpm. After 16-18 hours the culture liquid was extracted for the plasmid obtained OmpA-IBP target gene.

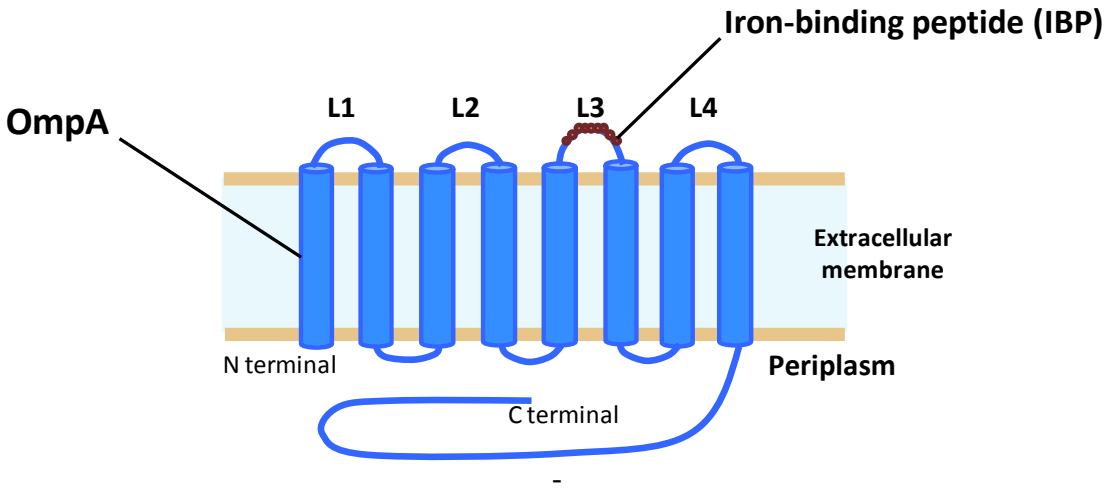

Fig. 4-3 Schematic representation the gene construction used in this study. The Iron oxide binding-peptide (IBP) is fused with outer membrane protein (OmpA).

4.4.3 Iron-binding protein expression test

The extracted plasmids were transformed into *E. coli* BL21(DE3) as same as transformation into *E. coli* DH5α and confirmed by PCR. After 16-18 hours of incubation 50μL of pre-culture was introduced into 5 mL of LB containing ampicillin medium at 37 °C. The absorbance at 600 nm was monitored until reach at 0.4, the protein expression was induced by adding the isopropyl β-D-1thiogalactopyranoside (IPTG) at final concentration of 1 mmol L^{-1} to the culture and then culture temperature was changed from 37 °C to 15 °C. The monitoring of protein production was done by collecting *E. coli* cell samples (centrifugation at 12,000 rpm, 2 min) at 0, 4, 12, 24 and 48 hours. The samples were then sonicated for 1 minute (on/off intervals at 20s/20s). The 10μL sonicated sample was mixed into SDS treatment buffer and heated at 95 °C for 5 minutes before being analyzed by SDS-poly-acrylamide gel electrophoresis (SDS-PAGE). The molecular weight of target protein is shown in table 4-3.

Table 4-3 Molecular weight of each iron-binding peptide fragment

Peptide fragment	Molecular weight (kDa)
OmpA-IBP1	38.35
OmpA-IBP2	38.37

4.4.4 Adsorption test of iron-binding protein

In order to conduct adsorption tests, *E. coli* with pET-22b(+)-OmpA-IBP1 and IBP2 were grown in LB liquid medium amended with ampicillin. To induce protein expression, IPTG was

added at final concentration of 1 mmol L^{-1}. Once IPTG was added the culture medium was incubated at 15 °C, 160 rpm for 24 hours. The bacteria cell that contained the expressed protein fragment was then collected by centrifugation at 10,000 rpm for 10 minutes. The cells pellet was then suspended in Tris buffer (20mM, pH 7.6). 1 mL of cell suspension was added to 20 mL of Tris buffer and incubated for 1 hour with mixing every 15 minutes. Cell pellet was collected by centrifugation at 10,000 rpm for 10 minutes. Hematite plate was introduced into the suspension containing 20 mL of Tris buffer. The adsorption was conducted at 25 °C, 100 rpm, for 24 hours (Zare-Eelanjegh et al., 2016). Tris buffer was used to wash the plates sample 3 times.

In order to observe the live/dead cells, a dye kit L7007 (LIVE/DEAD® Baclight™, Invitrogen, USA) was used to stain the bacteria cell onto the materials surfaces. Fluorescence microscopy was used to observe the adsorption. The negative control was non-genetically modified *E. coli* with pET-22b(+).

The effect of pH variation to adsorption of peptide to hematite surface was investigated. Tris buffer was used to adjust the pH during the adsorption test to 6.0, 7.0, 7.6, 8.0 and 9.0 on each hematite sample. At pH 5.0 was investigated using acetate buffer (0.1M).

Solid materials selectivity test was investigated for the adsorption using *E. coli* with pET-22b(+)-OmpA-IBP2 with same protocol for preparation and adsorption as done in hematite plate.

4.4.5 Desorption test of iron-binding protein on increase pH

The adsorption was conducted at 25 °C, 100 rpm, after 24 hours then the supernatant was removed (Zare-Eelanjegh et al., 2016). Tris buffer (20 mM, pH 7.6) was used to wash the sample 3 times. After washing with the buffer, desorption test was performed by immersing the plate in Tris buffer at pH 8.0 and 9.0 for 24 hours. Dye components kit L7007 for LIVE/DEAD® Baclight™

(Invitrogen, USA) was used to stain the bacteria cell on the materials surface. Fluorescence microscopy was used to observe the bacteria cell adsorbed to hematite surface.

4.4.6 Iron elution test using *E. coli* contained pET-22b(+)-OmpA-IBP

E. coli containing pET-22b(+)-OmpA-IBP2 was grown in LB liquid medium with ampicillin. IPTG was added at final concentration 1 mmol L^{-1} to induce protein expression and, then culture was incubated at 15 °C, 160 rpm for 24 hours. The 10 mL of LB liquid medium with ampicillin were transferred to 20 mL centrifugal tube, then 1 mL of culture solution of *E. coli* containing pET-22b(+)-OmpA-IBP2 was added to the tube followed by addition of 0.05 g of hematite powder. The control experiment only had *E. coli* contained pET-22b(+) with the same amount of hematite. After 0, 3, 6, 12, 24, 36 and 48 hours of incubation a 1.2 mL aliquot of culture was transferred to a 2 mL centrifugal tube and then centrifuged at 6500 rpm for 10 min. After centrifuge, supernatant was filtered with a 0.45μm membrane filter, a 1 mL aliquot of the filtrate was transferred to a polyethylene tube and diluted to 10 mL with 0.01 M HCl to preserve Fe in the solution (Nishimoto et al., 2013). The total iron concentration was analyzed with an ICPE-9000 type ICP-AES (Shimadzu, Japan).

The concentrations of Fe(II) species in the media were colorimetrically determined with ferrozine as an indicator of Fe(II). A 0.05 mL aliquot of 0.05 mM ferrozine was added to a 1 mL aliquot of media was centrifuged and filtered (0.45 μm). After 30 min of incubation, the concentration of Fe(II) species was determined based on the concentration of Fe(II)-ferrozine complexes by measuring the absorbance at 562 nm (Iwai et al., 2013).

The precipitation test was observed to confirm the adsorption of *E. coli* with pET-22b(+)-OmpA-IBP2 to hematite particle. The preparation of adsorption to hematite particle followed the

same method as with the hematite plate. The precipitation test was conducted after the adsorption was completed. The adsorption mixture (*E. coli* with pET-22b(+)-OmpA-IBP2 with 0.5 g of hematite powder in 5 mL of tris buffer) was used to observe precipitation. Four precipitation test cases were conducted; (i) *E. coli* contained pET-22b(+)-OmpA-IBP2 adsorb with hematite, (ii) *E. coli* contained pET-22b(+)-OmpA adsorb with hematite, (iii) *E. coli* contained pET-22b(+) adsorb with hematite, and (iv) hematite only, all of the systems were conducted in tris buffer. Cases (2) - (4) were negative control.

4.5 Results and discussion

4.5.1 Overlap (infusion) PCR result

The result shows the products obtained from gene construction. 1st time PCR for amplification of OmpA-IBP at the N and C-terminal was obtained in Fig. 4-4 at 450 bp and 710 bp respectively. The 2nd time PCR has been successfully amplified to obtain the gene fragment of OmpA-IBP (Fig.4-5).

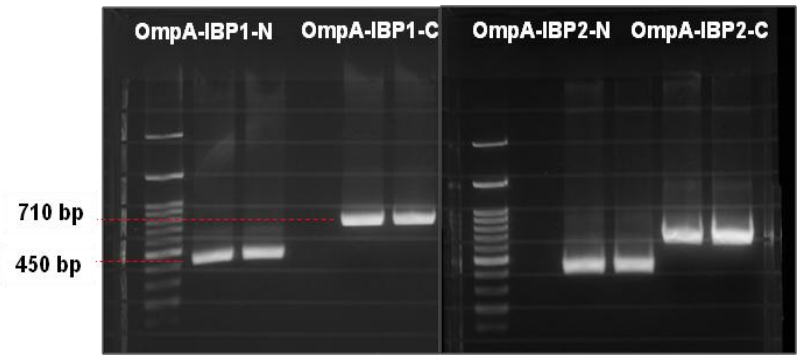

Fig. 4-4 Amplified fragment for OmpA-IBP1 and OmpA-IBP2 at N and C terminus, respectively.

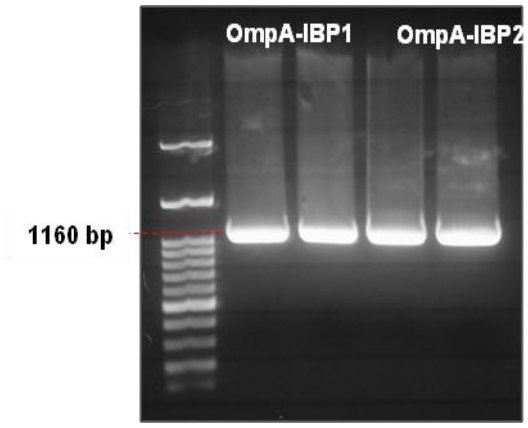

Fig. 4-5 Amplified of final fragment for OmpA-IBP1 and OmpA-IBP2.

4.5.2 Transformation of plasmid and colony PCR confirmation

To confirm that the fragments were successfully transferred into *E. coli* DH5α, colony PCR was conducted. As can be seen in Fig. 4-6, the PCR confirms that the transformation was successful. Lane 1-4 indicated with a red rectangle box were for OmpA-IBP1 whereas lane 5-7 were for OmpA-IBP2. The plasmids from these colonies were then transformed into *E. coli* BL21(DE3) for protein (iron binding peptide) expression.

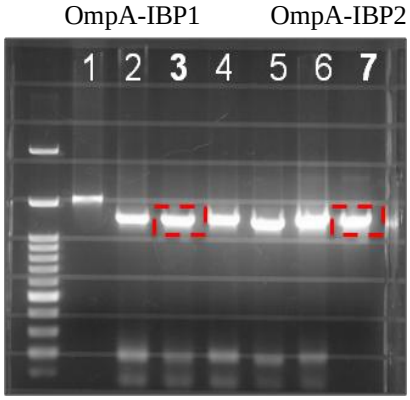

Fig. 4-6 Confirmation of *E. coli* DH5α colonies contained OmpA-IBP1 and OmpA-IBP2.

Figure 4-7 show the successful transformation of purified plasmid into *E. coli* BL21(DE3). The selected colonies for protein expression investigation also show in the red rectangular for both OmpA-IBP1 and OmpA-IBP2.

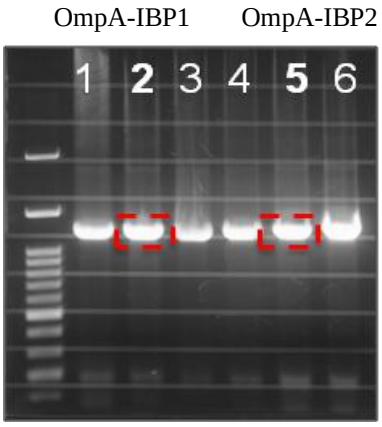

Fig. 4-7 Confirmation of *E. coli* with pET-22b(+)-OmpA-IBP1 and *E. coli* with pET-22b(+)-OmpA-IBP.

4.5.3 Iron-binding protein expression

Protein expression for each type of binding peptide (*E. coli* contained pET-22b(+)-OmpA-IBP1 and *E. coli* contained pET-22b(+)-OmpA-IBP2) has been monitored for 48 hours. The SDS-PAGE result show protein express was observed at 6 hours of incubation and the amount of expression increase as the incubation time increase.

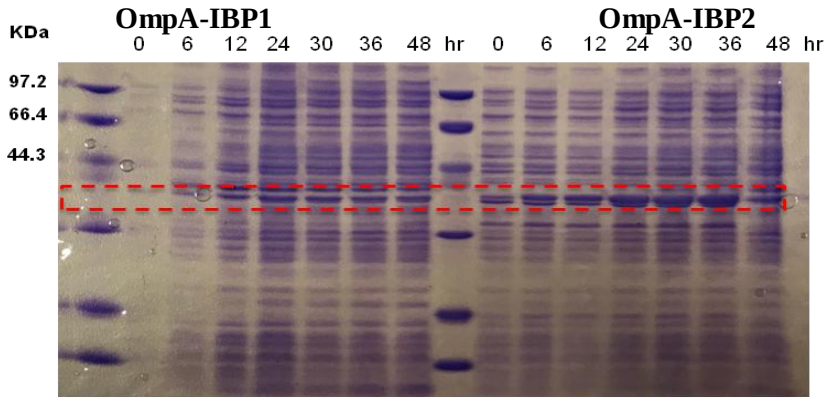

Fig. 4-8 SDS-PAGE analysis to confirm expression of iron-binding peptides

4.5.4 Adsorption observation

The adsorption test to hematite surface was compared between IBP1 and IBP2 protein shown in Fig. 4-9(a)-(c). Fig. 4-9(a) show that the adsorption efficiency of *E. coli* with pET-22b(+)-OmpA-IBP1 to hematite surface was low. The number of the bacterial cells observed by green fluorescence appeared on the observation area. In comparison, *E. coli* with pET-22b(+)-OmpA-IBP2 (Fig. 4-9(b)) adsorption to hematite surface, higher number of bacteria cells attached to the surface. This result could suggest that *E. coli* with pET-22b(+)-OmpA-IBP2 has more efficiency in binding to hematite surface than that in IBP1. For *E. coli* with pET-22b(+)-OmpA without any iron binding peptide gene (Fig.4-9(c)) show no adsorption of bacteria cell to hematite surface. This result confirms that IBP is important in the attachment of bacterial cell to hematite. Because of the high adsorption capability of *E. coli* with pET-22b(+)-OmpA-IBP2 it was further evaluated for the effect of pH on adsorption as well as material selectivity.

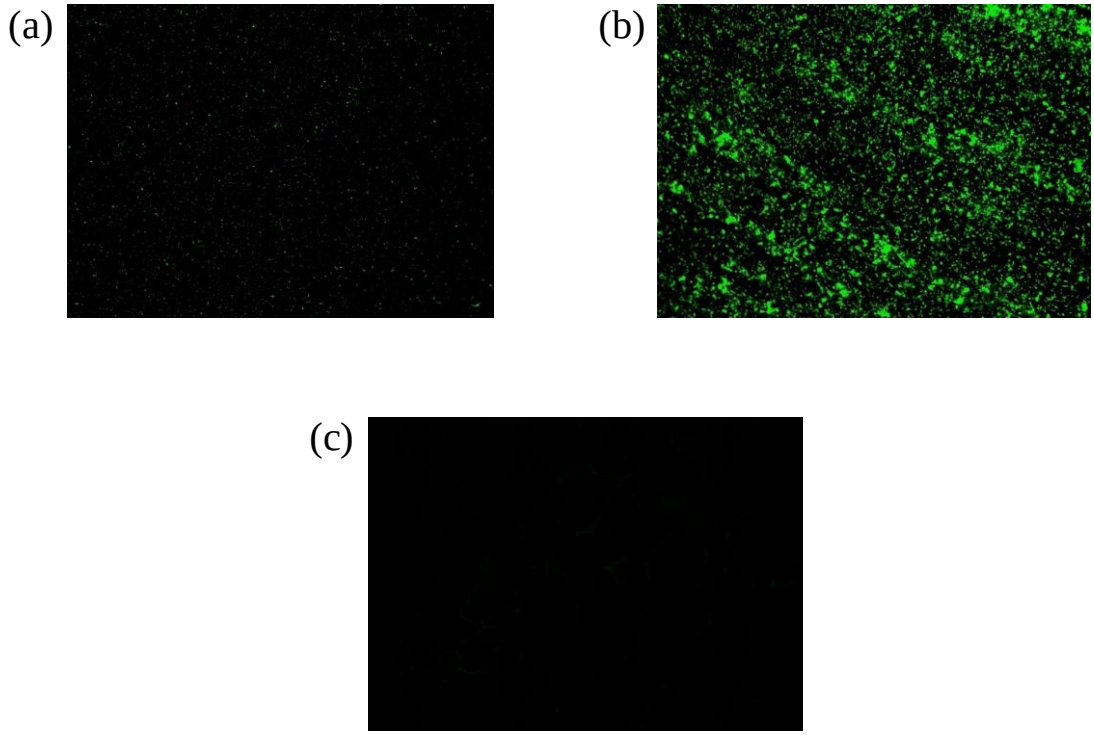

Fig. 4-9 The adsorption observation of hematite using variation of iron-binding peptide (IBP), (a) *E. coli* with pET-22b(+)-OmpA-IBP1, (b) *E. coli* with pET-22b(+)-OmpA-IBP2 and (c) f *E. coli* with pET-22b(+)-OmpA

4.5.5 Effect of pH variation to adsorption

Figure 4-10(a)-(f) show the adsorption of IBP2 to hematite surface at different of pH of 5.0, 6.0, 7.0, 8.0 and 9.0 and compared to pH 7.6 which had already been investigated in section 4.5.4. Fig 4-10(a) and (b) show the adsorption test at pH 5.0 and 6.0. As can be observed, bacteria cells adsorbed onto the hematite surface. This result in acidic condition could be due to the adsorption of bacterial cells to the metal surface as the positive charge at the cell surface is attracted to negative charge of the metal surface. Fig. 4-10(c) shows the adsorption of *E. coli* containing pET-22b(+)-

OmpA-IBP2 attached to hematite surface at pH 7.0. It was observed that the highest efficiency of adsorption to the hematite surface at pH 7.6 (Fig.4-10(d)). From this we concluded that this pH value is the optimum condition for the adsorption. Lower number of bacteria cells were observed at pH 8.0 and almost none at pH 9.0 as shown in Fig. 4-10(e) and (f), respectively. This result could be suggested that IBP2 has more efficiency in binding to hematite surface at pH around 7-7.6. The possible reason for non-adsorb of bacteria at higher pH could be due to the negatively charge of bacteria cell surface repelled from the hematite surface. This result should lead to the further investigating the optimum of pH for the future application using this adsorption property.

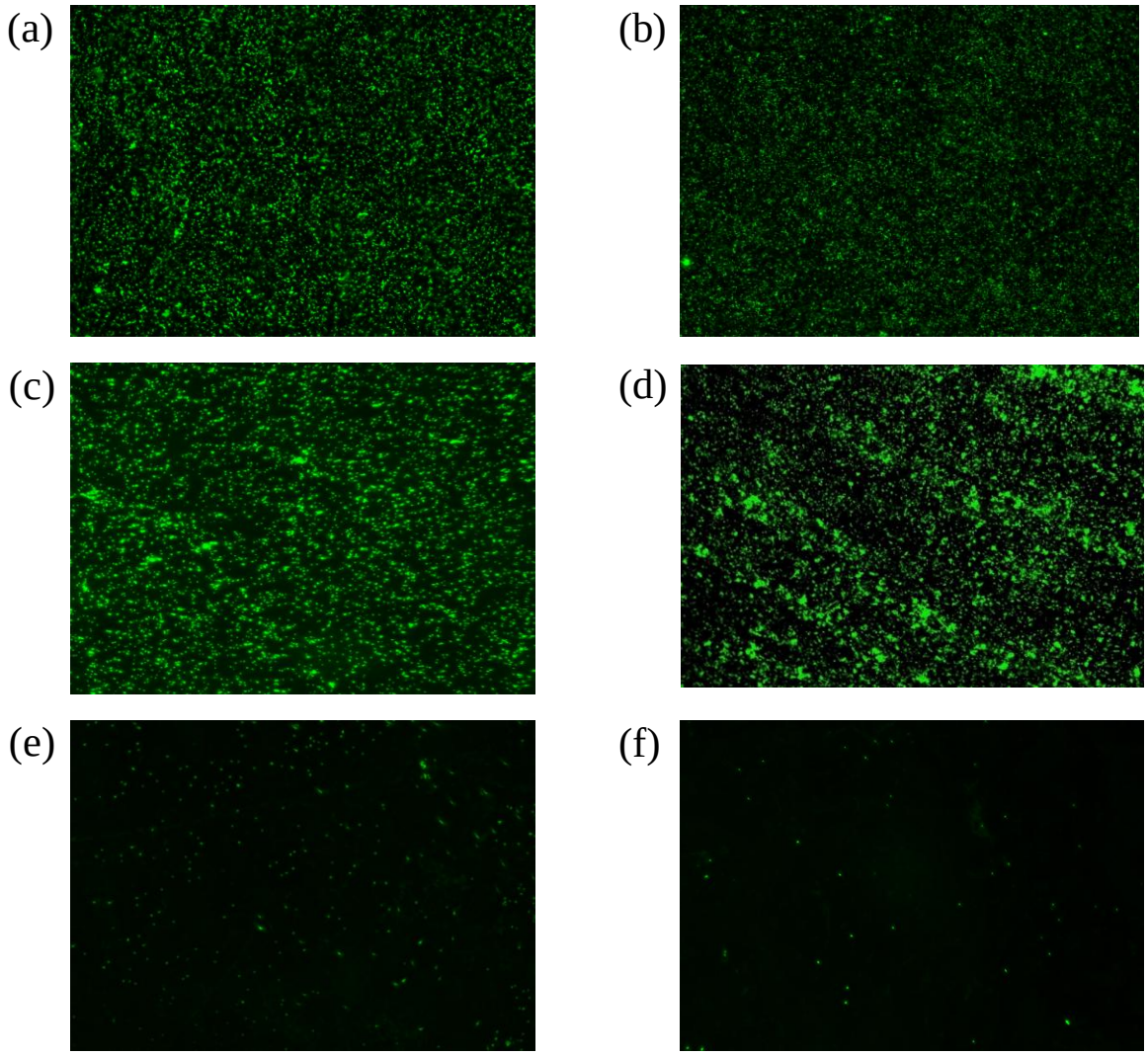

Fig. 4-10 Effect of pH variation of buffer to adsorption between *E. coli* with pET-22b(+)-OmpA-IBP2 and hematite (a) pH5.0, (b) pH6.0, (c) pH7.0, (d) pH7.6, (e) pH8.0, and (f) pH 9.0

4.5.6 Materials selectivity test

To test the adsorption of the protein on other material hematite plate was replaced by copper, titanium, wolfram and zirconium to test the selectivity of IBP to the metal surface. Similar conditions were test on these materials just like the ones that were conducted on the hematite. Figure 4-11(a)-(d) show the adsorption of *E. coli* with pET-22b(+)-OmpA-IBP2 binding test to copper, titanium, zirconium and wolfram, respectively. The negative control using *E. coli* containing only pET-22b(+) was also observed with four others same materials (Fig.4-11(a)-(d) right position). The adsorption to copper surface was observed (Fig.4-11(a)), relatively high amount compares to hematite and other materials. The negative control could not detect the adsorption of bacteria on the copper surface. This suggested that IBP2 has a potential to bind to the copper surface. Fig. 4-11(b) shows the titanium adsorption test. The adsorption on titanium surface cannot detected in both *E. coli* with pET-22b(+)-OmpA-IBP2 and negative control. As same observation situation with wolfram (Fig.4-11(d)), the adsorption of bacteria could not be observed. The small amount of *E. coli* with pET-22b(+)-OmpA-IBP2 was observed on the zirconium surface (Fig.4-11(c)) compared to none bacteria attached to zirconium surface in negative control. The material selectivity could imply that the IBP2 has an ability to bind to others metal materials such as copper and zirconium. We suggest that varieties of metal materials should be observed in future study.

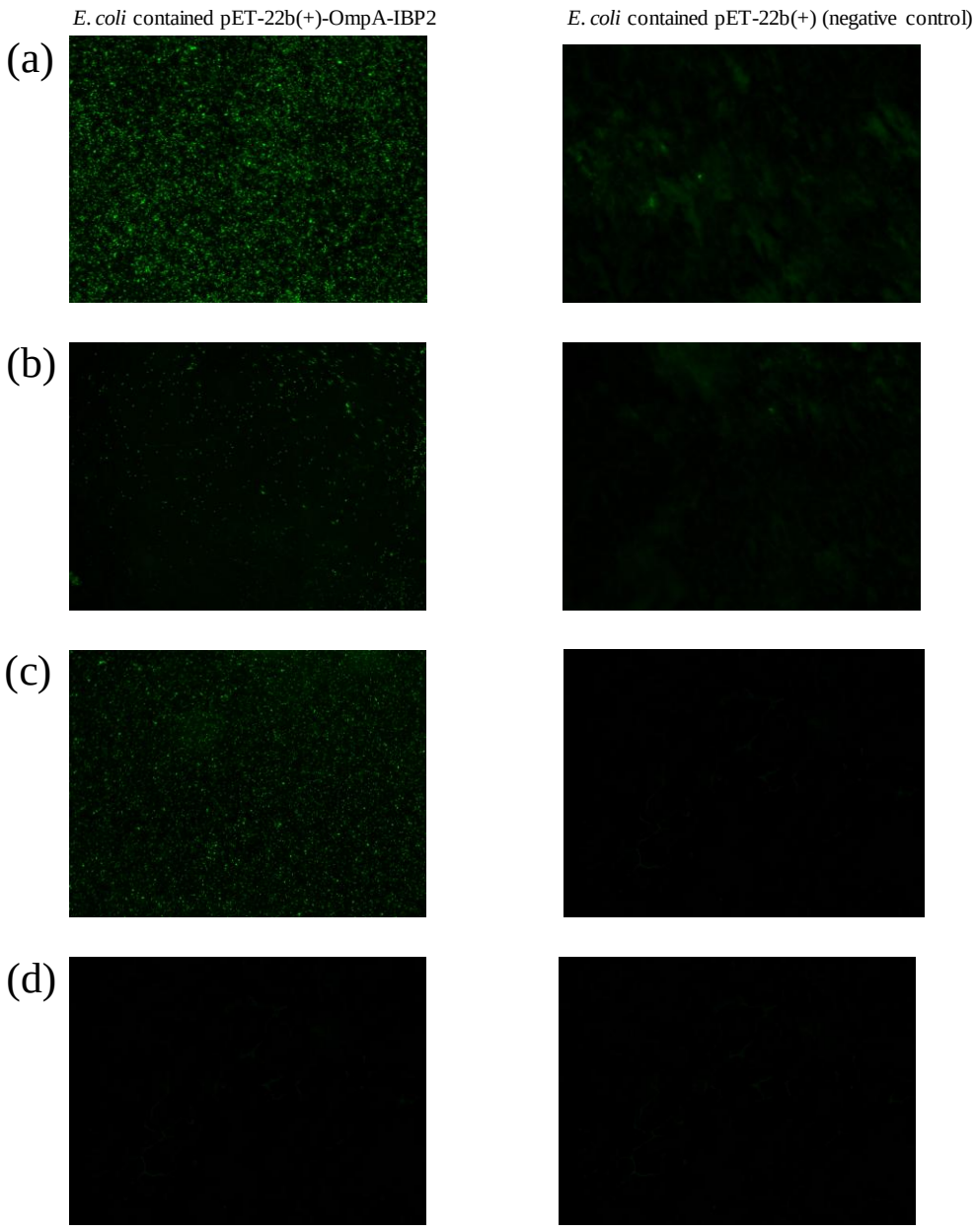

Figure 4-11 the adsorption of *E. coli* contained pET-22b(+)-OmpA-IBP2 binding test to (a)copper, (b)titanium, (c)zirconium, and (d)wolfram, the right position shows the negative control using *E. coli* with pET-22b(+)

4.5.7 Desorption test

Desorption test are shown in Figure 4-12 (a) and (b). After adsorption of *E. coli* containing pET-22b(+)-OmpA-IBP2 with hematite plate in Tris buffer at pH 7.6 was used. The adsorption of bacteria was observed again under fluorescence microscopy. However, desorption of the bacteria could not be observed at both pH 8.0 and 9.0. This result suggested that *E. coli* containing pET-22b(+)-OmpA-IBP2 had high affinity to attach to the hematite surface after several washings. These results shown that after bacterial cells adsorbed onto the hematite surface, pH could not affect the binding efficiency. One of the advantages of this desorption test could be the possible use *E. coli* containing pET-22b(+)-OmpA-IBP2 is that it would attach to hematite and can assist in eluting iron into seawater condition. This experiment can be further investigated at pH 8.0 which is similar to the seawater condition.

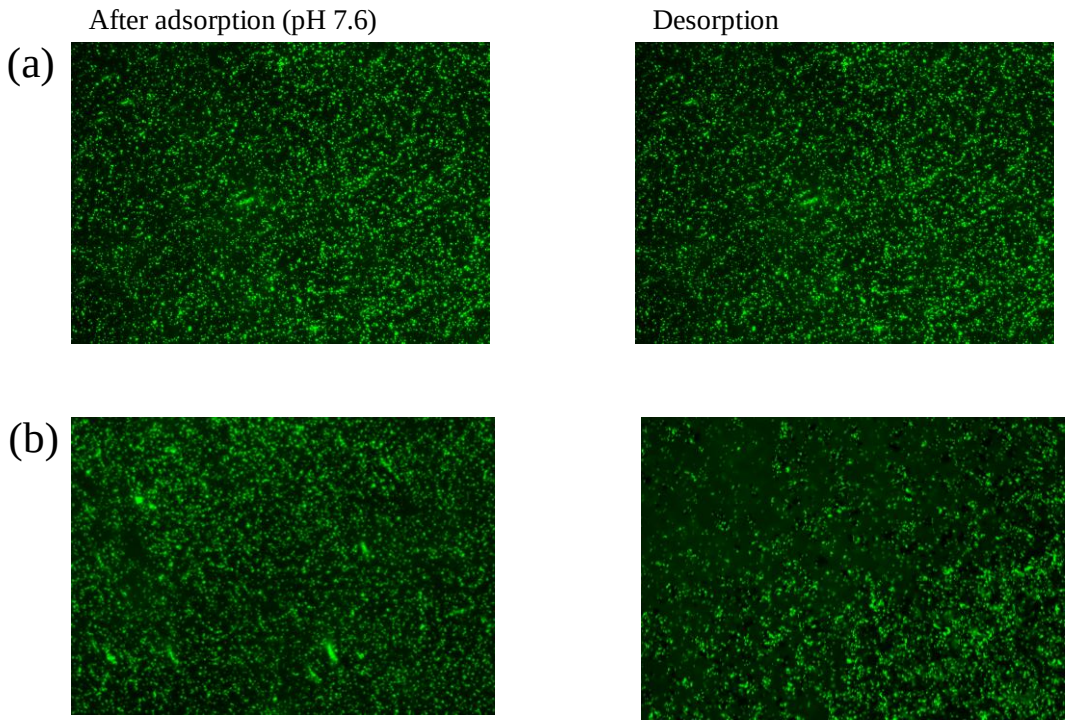

Figure 4-12 the desorption test of *E. coli* contained pET-22b(+)-OmpA-IBP2 binding at pH7.6 then change to (a) pH8.0 and (b) pH9.0

4.5.8 *E. coli* contained pET-22b(+)-OmpA-IBP2 effect to iron elution

The *E. coli* containing pET-22b(+)-OmpA-IBP2 was used to investigate the ability to elute iron at two different adsorption conditions of pH 7.0 and 7.6. When bacteria cell attaches or have a very close contact to hematite surface the electron transfer should occur as discuss in subsection 3.4.5. Fig. 4-13(a) shows the total iron concentration during a 48-h incubation period. The bacteria with IBP increased the iron elution. The amount of eluted Fe at pH 7.0 was detected at 3 h incubation and reach stability with highest concentration of 4.43 mg L^{-1}, for the bacteria containing

pET-22b(+)-OmpA-IBP2 at pH7.0. At pH 7.6, slightly lower amount of both total iron concentration and ferrous iron was eluted. Adsorption at pH 7.6 showed higher efficiency to hematite surface however the elution of iron was lower compared to pH 7.0. For bacteria without IBP, no elution iron was detected at both pH 7.0 and 7.6. This result might be useful for further application using genetically modification bacteria as some tools to elute iron into seawater as the data obtain review that this phenomenon is plausible.

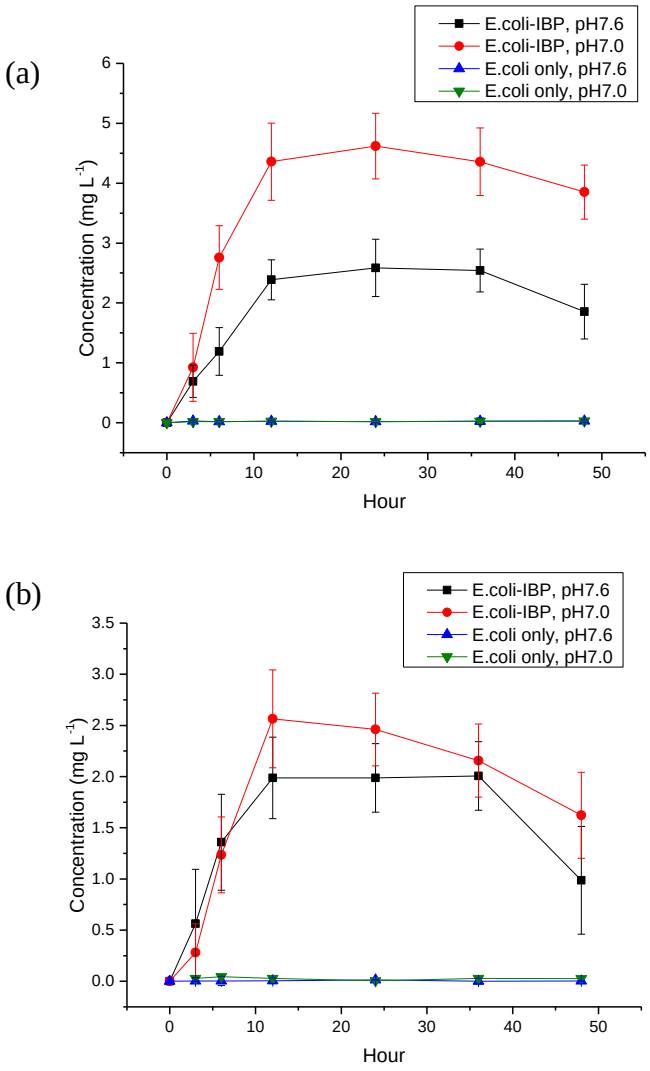

Figure 4-13 Iron elution of *E. coli* contained pET-22b(+)-OmpA-IBP2 (a) Total iron and (b) Ferrous iron

4.5.9 *E. coli* contained pET-22b(+)-OmpA-IBP2 precipitation test

The *E. coli* containing pET-22b(+)-OmpA-IBP2 precipitation test is shown in Fig. 4-14. Figure 4-14(a) cases were in a homogenous pattern. Noticeable difference was observed after 2 hours (Fig. 4-14(c)), in which the *E. coli* containing pET-22b(+)-OmpA-IBP2 shows the fastest precipitation rate compare to other systems. At 4 hours (Fig.4-14(d)), all of the cases containing bacteria showed almost complete precipitation. At the end of all 7 h of precipitation test, it was observed that hematite only could precipitate slowest compared to the adsorbed hematite (Fig. 4-14(f)). These results suggest that *E. coli* containing pET-22b(+)-OmpA-IBP2 adsorbed to the hematite powder due to the fastest rate of the precipitation.

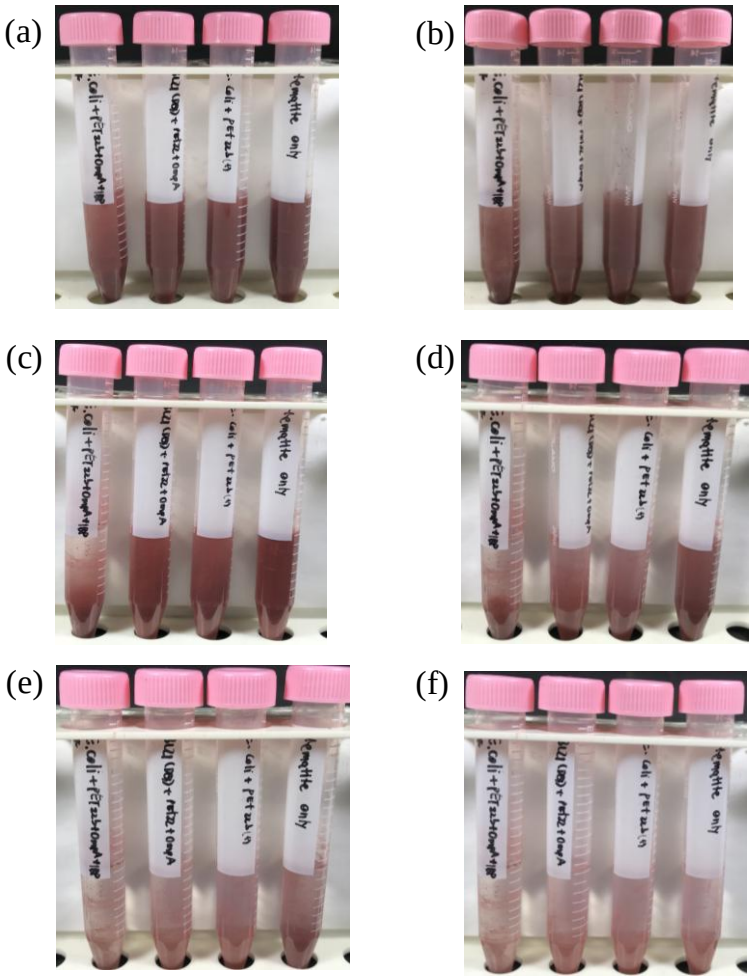

Figure 4-14 Precipitation observation test of *E. coli* containing pET-22b(+)-OmpA-IBP2 adsorb with hematite compare with control at different of time intervals (a) at 0 hour, (b) 1 hour, (c) 2 hours, (d) 4 hours, (e) 5 hours, and (f) 7 hours

4.6 Conclusion

The iron binding peptides (IBP) inserted in OmpA were successfully expressed in *E. coli*. The IBPs showed the different adsorption behavior confirmed by fluorescence spectroscopy. We found the higher adsorption ability to hematite surface in *E. coli* expressing OmpA-IBP2. The suitable pH for the adsorption was determined to be at pH 7.6. Additionally, the *E. coli* expressing OmpA-IBP2 could adsorb not only to hematite, but also copper and zirconium. The small-scale laboratory test revealed *E. coli* expressing OmpA-IBP2 could elute Fe(II) from hematite particle. The precipitation test also confirm that bacteria possibly could attach to the hematite particle due to the rate of precipitation. Further investigation should be necessary for the possible application of metal-binding *E. coli*.

References

[1] K. Richter, M. Schicklberger and J. Gescher. Dissimilatory reduction of extracellular electron acceptors in anaerobic respiration. *Applied and Environmental Microbiology*, 78, 913-921, 2012.

[2] A. Care, P.L. Bergquist and A. Sunna. Solid-binding peptides: smart tools for nanobiotechnology. *Trends in Biotechnology*, Vol.33 No.5, 259-268, 2015

[3] S. Avvakumova, M. Colombo, P. Tortora and D. Prosperi. Biotechnology approaches toward nanoparticle biofunctionalization. *Trends in Biotechnology*, Vol.32 No.1, 11-20, 2014.

[4] A. Sengupta, C.K. Thai, M.S R. Sastry, J.F. Matthaei, D.T. Schwartz, E.J. Davis and F. Baneyx. A Genetic Approach for controlling the binding and orientation of proteins on nanoparticles. *Langmuir*, 24(5), 2000-2008, 2018

[5] A.K. Johnson, A.M. Zawadazka, L.A. Deobald, R.L. Crawford and A.J. Paszczynski. Novel method for immobilization of enzymes to magnetic nanoparticles. *Journal of Nanoparticle Research*, Vol.10 Issue.6, 1009-1025, 2008.

[6] T. Kacar, M.T. Zin, C. So, B. Wilson, H. Ma, N. Gul-Karaguler, A. K.-Y. Jen, M. Sarikaya and C. Tamerler. Directed self-immobilization of alkaline phosphatase on micro-patterned substrates via genetically fused metal-binding peptide. *Biotechnology and Bioengineering*, 103, 696-705, 2009.

[7] M. Yang, BG. Choi, T.J. Park, N.S. Heo, W.H. Hong and S.Y. Lee. Site-specific immobilization of gold binding polypeptide on gold nanoparticle-coated graphene sheet for biosensor application. *Nanoscale*, 3(7), 2950-2956, 2011

[8] S. Cetinel, H.B. Caliskan, D.T. Yucesoy, A.S. Donatan, E.Yuca, M.Urgen, N.G. Karaguler and C. Tamerler. Addressable self-immobilization of lactate dehydrogenase across multiple length scales. *Biotechnology Journal*, Vol.8 issue 2, 262-272, 2013.

[9] R.R. Naik, L.L. Brott, S.J. Clarson and M.O. Stone. Silica-precipitaing peptides isolated from a combinatorial phage display peptide library. *Journal of Nanoscience and Nanotechnology*, 2(1), 95-100, 2002.

[10] D-Y. Tsai, Y-J. Tsai, C-H. Yen, C-Y. Ouyang and Y-C. Yeh. Bacterial surface display of metal binding peptides as whole-cell biocatalysts for 4-nitroaniline reduction. *RSC advance*, 5, 87998-88001, 2015.

[11] S. Brown. Engineered iron oxide-adhesion mutants of the Escherichia coli phage lambda receptor. *Proceeding of the National Academy of Science U.S.A*, 89, 8651-8655, 1992.

[12] E. Zare-Eelanjegh, D.K. Bora, P. Rupper, K. Schrantz, L. Thony-Meywr, K. Maniura-Weber, M. Richter and G. Faccio. Affinity-driven immobilization of proteins to hematite nanoparticles. *Applied Materials and Interfaces*, 8, 20432-20439, 2016.

[13] K. Nakashima, K. Endo, N. Shibasaki-Kitakawa and T. Yonemoto. A fusion enzyme consisting of bacterial expansin and endoglucanase for the degradation of highly crystalline cellulose. *RSC Advances*, 4, 43815, 2014.

CHAPTER 5 CONCLUSION

This thesis focused on the application of iron oxide to various environmental problems using biotechnology to solve the problem of barren grounds in coastal areas. The challenging point is to clarify the mechanism of bacteria by which iron dissolution occurs with the absorption properties of the bacteria related to future application in the future study.

Novel microorganism was isolated from Fe-fertilizer incubated in coastal seawater and was identified as *Exiguobacterium oxidotolerans* by 16S rDNA analysis. The iron elution of the bacteria was demonstrated based on the increase of dissolved iron by incubation with hematite under a seawater-like condition. The value of ORP was changed from ca. 0 mV to ca. –400 mV by inoculation of the bacteria, which causes reductive elution of Fe. The concentration of eluted iron was significantly affected by Anthraquinone-2,7-disulfonate (AQDS), which was used as a model for organic matter in the system. The eluted iron concentration was higher in AQDS containing sample at 38 mg L^{-1} compared to the sample containing only *E. oxidotolerans* with hematite which was detected only 22.3 mg L^{-1}. The relatively high concentration of organic acids (Oxalic acid, 11,300 mg L^{-1}) was found in samples containing *E. oxidotolerans* and hematite. The hematite surface was analyzed by using X-ray photoelectron spectroscopy (XPS), field emission scanning electron microscope (FE-SEM) and attenuated total reflectance Fourier transform infrared (ATR-FTIR) after 30-days exposure to bacterial culture. The surface alteration were observed in the treated hematite which indicated evidence of iron elution into the culture medium. Based on the results, it was understood that *E. oxidotolerans* is capable of reductive elution of iron from Fe_2O_3 into seawater. AQDS, which can play as an electron acceptor/donor between microbe and insoluble Fe_2O_3 particles, enhanced the effect of iron bio-leaching.

In Chapter 3, the interaction between bacteria cell and hematite surface was investigated to clarify the mechanism in iron elution. We proposed two possible mechanisms of iron elution focusing on the contact condition between bacteria and hematite surface, and investigated two systems of iron elution: direct elution system and indirect elution, where bacteria and hematite are separated by dialysis tube. The elution test was conducted for 10 days, and iron elution, metabolite production (oxalic acids), ORP and pH were monitored. The effect of organic acids which are usually produced by *E. oxidotolerans* was also examined in indirect elution system by adding external organic acids (i.e. chemical reagents). Adequate iron elution was detected only in direct elution system (30.57 mg L^{-1}). Hematite surface observation using FE-SEM, ATR-FTIR and SEM-EDS also revealed the surface alteration and particles dispersion in direct elution system. Our study could conclude direct interaction of bacteria cell with hematite would mainly facilitate iron elution, probably due to the electron transfer via cell membrane to hematite, resulting in reductive elution of hematite.

In Chapter 4, the adsorption ability of bacteria cell to hematite surface were investigated using genetically-modified bacteria. Based on the result in chapter 3, direct interaction between bacteria and hematite surface played an important part in electron transfer to reduce insoluble-Fe(III) to eluted-Fe(II). Efficient and active adsorption of bacteria cells to hematite surface might lead to improvement in iron dissolution. *E. coli* displaying iron-binding peptide on its cell surface has been prepared to enhance the adsorption ability. The two types of iron-binding peptide (IBP1 and IBP2) were selected to evaluate the adsorption efficiency to the hematite. We introduced IBPs into outer membrane protein (OmpA) by using fusion genes IBPs-OmpA in this work. Construction of expression vector, transformation of the cell, and protein expression in *E. coli* have been successful. The adsorption of *E. coli* expressing IBP1 or IBP2 has been conducted using fluorescent microscope after staining the cells by LIVE/DEAD staining kit. IBP2-displaying cell was revealed

to show higher adsorption efficiency at pH 7-7.6. The bacteria cells could bind to hematite surface at pH 5 and 6. However, bacteria cells could not bind to hematite surface at pH8 and 9. The desorption test revealed the binding peptide ability to the hematite surface could not be detached after once adsorb. IBP2 could adsorb to other surfaces hematite, the material selectivity test showed that copper and zirconium could attach to IBP2 in the same condition as hematite. The IBP2-displaying cell also showed the ability to elute iron form the hematite in small amount of both total iron and ferrous iron. Furthermore, the IBPs-displaying cells facilitated the settling of hematite particles in a solution, probably due to the aggregation of the particle via hematite-binding cells. These results suggested that genetically modified bacteria could be used in further application.